

# NCHRP

## REPORT 573

NATIONAL  
COOPERATIVE  
HIGHWAY  
RESEARCH  
PROGRAM

### **Superpave Mix Design: Verifying Gyration Levels in the $N_{\text{design}}$ Table**

TRANSPORTATION RESEARCH BOARD  
*OF THE NATIONAL ACADEMIES*

## **TRANSPORTATION RESEARCH BOARD 2007 EXECUTIVE COMMITTEE\***

### **OFFICERS**

CHAIR: **Linda S. Watson**, CEO, LYNX—Central Florida Regional Transportation Authority, Orlando

VICE CHAIR: **Debra L. Miller**, Secretary, Kansas DOT, Topeka

EXECUTIVE DIRECTOR: **Robert E. Skinner, Jr.**, Transportation Research Board

### **MEMBERS**

**J. Barry Barker**, Executive Director, Transit Authority of River City, Louisville, KY

**Michael W. Behrens**, Executive Director, Texas DOT, Austin

**Allen D. Biehler**, Secretary, Pennsylvania DOT, Harrisburg

**John D. Bowe**, President, Americas Region, APL Limited, Oakland, CA

**Larry L. Brown, Sr.**, Executive Director, Mississippi DOT, Jackson

**Deborah H. Butler**, Vice President, Customer Service, Norfolk Southern Corporation and Subsidiaries, Atlanta, GA

**Anne P. Canby**, President, Surface Transportation Policy Partnership, Washington, DC

**Nicholas J. Garber**, Henry L. Kinnier Professor, Department of Civil Engineering, University of Virginia, Charlottesville

**Angela Gittens**, Vice President, Airport Business Services, HNTB Corporation, Miami, FL

**Susan Hanson**, Landry University Professor of Geography, Graduate School of Geography, Clark University, Worcester, MA

**Adib K. Kanafani**, Cahill Professor of Civil Engineering, University of California, Berkeley

**Harold E. Linnenkohl**, Commissioner, Georgia DOT, Atlanta

**Michael D. Meyer**, Professor, School of Civil and Environmental Engineering, Georgia Institute of Technology, Atlanta

**Michael R. Morris**, Director of Transportation, North Central Texas Council of Governments, Arlington

**John R. Njord**, Executive Director, Utah DOT, Salt Lake City

**Pete K. Rahn**, Director, Missouri DOT, Jefferson City

**Sandra Rosenbloom**, Professor of Planning, University of Arizona, Tucson

**Tracy L. Rosser**, Vice President, Corporate Traffic, Wal-Mart Stores, Inc., Bentonville, AR

**Rosa Clausell Rountree**, Executive Director, Georgia State Road and Tollway Authority, Atlanta

**Henry G. (Gerry) Schwartz, Jr.**, Senior Professor, Washington University, St. Louis, MO

**C. Michael Walton**, Ernest H. Cockrell Centennial Chair in Engineering, University of Texas, Austin

**Steve Williams**, Chairman and CEO, Maverick Transportation, Inc., Little Rock, AR

### **EX OFFICIO MEMBERS**

**Thad Allen** (Adm., U.S. Coast Guard), Commandant, U.S. Coast Guard, Washington, DC

**Thomas J. Barrett** (Vice Adm., U.S. Coast Guard, ret.), Pipeline and Hazardous Materials Safety Administrator, U.S.DOT

**Marion C. Blakey**, Federal Aviation Administrator, U.S.DOT

**Joseph H. Boardman**, Federal Railroad Administrator, U.S.DOT

**John A. Bobo, Jr.**, Acting Administrator, Research and Innovative Technology Administration, U.S.DOT

**Rebecca M. Brewster**, President and COO, American Transportation Research Institute, Smyrna, GA

**George Bugliarello**, Chancellor, Polytechnic University of New York, Brooklyn, and Foreign Secretary, National Academy of Engineering, Washington, DC

**J. Richard Capka**, Federal Highway Administrator, U.S.DOT

**Sean T. Connaughton**, Maritime Administrator, U.S.DOT

**Edward R. Hamberger**, President and CEO, Association of American Railroads, Washington, DC

**John H. Hill**, Federal Motor Carrier Safety Administrator, U.S.DOT

**John C. Horsley**, Executive Director, American Association of State Highway and Transportation Officials, Washington, DC

**J. Edward Johnson**, Director, Applied Science Directorate, National Aeronautics and Space Administration, John C. Stennis Space Center, MS

**William W. Millar**, President, American Public Transportation Association, Washington, DC

**Nicole R. Nason**, National Highway Traffic Safety Administrator, U.S.DOT

**Jeffrey N. Shane**, Under Secretary for Policy, U.S.DOT

**James S. Simpson**, Federal Transit Administrator, U.S.DOT

**Carl A. Strock** (Lt. Gen., U.S. Army), Chief of Engineers and Commanding General, U.S. Army Corps of Engineers, Washington, DC

---

\*Membership as of March 2007.

---

---

**NCHRP REPORT 573**

---

---

**Superpave Mix Design:  
Verifying Gyration Levels  
in the  $N_{\text{design}}$  Table**

**Brian D. Prowell**

**E. Ray Brown**

NATIONAL CENTER FOR ASPHALT TECHNOLOGY  
Auburn, AL

*Subject Areas*

Materials and Construction

---

Research sponsored by the American Association of State Highway and Transportation Officials  
in cooperation with the Federal Highway Administration

---

**TRANSPORTATION RESEARCH BOARD**

WASHINGTON, D.C.

2007

[www.TRB.org](http://www.TRB.org)

## **NATIONAL COOPERATIVE HIGHWAY RESEARCH PROGRAM**

Systematic, well-designed research provides the most effective approach to the solution of many problems facing highway administrators and engineers. Often, highway problems are of local interest and can best be studied by highway departments individually or in cooperation with their state universities and others. However, the accelerating growth of highway transportation develops increasingly complex problems of wide interest to highway authorities. These problems are best studied through a coordinated program of cooperative research.

In recognition of these needs, the highway administrators of the American Association of State Highway and Transportation Officials initiated in 1962 an objective national highway research program employing modern scientific techniques. This program is supported on a continuing basis by funds from participating member states of the Association and it receives the full cooperation and support of the Federal Highway Administration, United States Department of Transportation.

The Transportation Research Board of the National Academies was requested by the Association to administer the research program because of the Board's recognized objectivity and understanding of modern research practices. The Board is uniquely suited for this purpose as it maintains an extensive committee structure from which authorities on any highway transportation subject may be drawn; it possesses avenues of communications and cooperation with federal, state and local governmental agencies, universities, and industry; its relationship to the National Research Council is an insurance of objectivity; it maintains a full-time research correlation staff of specialists in highway transportation matters to bring the findings of research directly to those who are in a position to use them.

The program is developed on the basis of research needs identified by chief administrators of the highway and transportation departments and by committees of AASHTO. Each year, specific areas of research needs to be included in the program are proposed to the National Research Council and the Board by the American Association of State Highway and Transportation Officials. Research projects to fulfill these needs are defined by the Board, and qualified research agencies are selected from those that have submitted proposals. Administration and surveillance of research contracts are the responsibilities of the National Research Council and the Transportation Research Board.

The needs for highway research are many, and the National Cooperative Highway Research Program can make significant contributions to the solution of highway transportation problems of mutual concern to many responsible groups. The program, however, is intended to complement rather than to substitute for or duplicate other highway research programs.

## **NCHRP REPORT 573**

Project 9-9(1)  
ISSN 0077-5614  
ISBN 978-0-309-09877-9  
Library of Congress Control Number 2007901205

© 2007 Transportation Research Board

### **COPYRIGHT PERMISSION**

Authors herein are responsible for the authenticity of their materials and for obtaining written permissions from publishers or persons who own the copyright to any previously published or copyrighted material used herein.

Cooperative Research Programs (CRP) grants permission to reproduce material in this publication for classroom and not-for-profit purposes. Permission is given with the understanding that none of the material will be used to imply TRB, AASHTO, FAA, FHWA, FMCSA, FTA, or Transit Development Corporation endorsement of a particular product, method, or practice. It is expected that those reproducing the material in this document for educational and not-for-profit uses will give appropriate acknowledgment of the source of any reprinted or reproduced material. For other uses of the material, request permission from CRP.

### **NOTICE**

The project that is the subject of this report was a part of the National Cooperative Highway Research Program conducted by the Transportation Research Board with the approval of the Governing Board of the National Research Council. Such approval reflects the Governing Board's judgment that the program concerned is of national importance and appropriate with respect to both the purposes and resources of the National Research Council.

The members of the technical committee selected to monitor this project and to review this report were chosen for recognized scholarly competence and with due consideration for the balance of disciplines appropriate to the project. The opinions and conclusions expressed or implied are those of the research agency that performed the research, and, while they have been accepted as appropriate by the technical committee, they are not necessarily those of the Transportation Research Board, the National Research Council, the American Association of State Highway and Transportation Officials, or the Federal Highway Administration, U.S. Department of Transportation.

Each report is reviewed and accepted for publication by the technical committee according to procedures established and monitored by the Transportation Research Board Executive Committee and the Governing Board of the National Research Council.

The Transportation Research Board of the National Academies, the National Research Council, the Federal Highway Administration, the American Association of State Highway and Transportation Officials, and the individual states participating in the National Cooperative Highway Research Program do not endorse products or manufacturers. Trade or manufacturers' names appear herein solely because they are considered essential to the object of this report.

*Published reports of the*

### **NATIONAL COOPERATIVE HIGHWAY RESEARCH PROGRAM**

*are available from:*

Transportation Research Board  
Business Office  
500 Fifth Street, NW  
Washington, DC 20001

*and can be ordered through the Internet at:*

<http://www.national-academies.org/trb/bookstore>

Printed in the United States of America

# THE NATIONAL ACADEMIES

*Advisers to the Nation on Science, Engineering, and Medicine*

The **National Academy of Sciences** is a private, nonprofit, self-perpetuating society of distinguished scholars engaged in scientific and engineering research, dedicated to the furtherance of science and technology and to their use for the general welfare. On the authority of the charter granted to it by the Congress in 1863, the Academy has a mandate that requires it to advise the federal government on scientific and technical matters. Dr. Ralph J. Cicerone is president of the National Academy of Sciences.

The **National Academy of Engineering** was established in 1964, under the charter of the National Academy of Sciences, as a parallel organization of outstanding engineers. It is autonomous in its administration and in the selection of its members, sharing with the National Academy of Sciences the responsibility for advising the federal government. The National Academy of Engineering also sponsors engineering programs aimed at meeting national needs, encourages education and research, and recognizes the superior achievements of engineers. Dr. William A. Wulf is president of the National Academy of Engineering.

The **Institute of Medicine** was established in 1970 by the National Academy of Sciences to secure the services of eminent members of appropriate professions in the examination of policy matters pertaining to the health of the public. The Institute acts under the responsibility given to the National Academy of Sciences by its congressional charter to be an adviser to the federal government and, on its own initiative, to identify issues of medical care, research, and education. Dr. Harvey V. Fineberg is president of the Institute of Medicine.

The **National Research Council** was organized by the National Academy of Sciences in 1916 to associate the broad community of science and technology with the Academy's purposes of furthering knowledge and advising the federal government. Functioning in accordance with general policies determined by the Academy, the Council has become the principal operating agency of both the National Academy of Sciences and the National Academy of Engineering in providing services to the government, the public, and the scientific and engineering communities. The Council is administered jointly by both the Academies and the Institute of Medicine. Dr. Ralph J. Cicerone and Dr. William A. Wulf are chair and vice chair, respectively, of the National Research Council.

The **Transportation Research Board** is a division of the National Research Council, which serves the National Academy of Sciences and the National Academy of Engineering. The Board's mission is to promote innovation and progress in transportation through research. In an objective and interdisciplinary setting, the Board facilitates the sharing of information on transportation practice and policy by researchers and practitioners; stimulates research and offers research management services that promote technical excellence; provides expert advice on transportation policy and programs; and disseminates research results broadly and encourages their implementation. The Board's varied activities annually engage more than 5,000 engineers, scientists, and other transportation researchers and practitioners from the public and private sectors and academia, all of whom contribute their expertise in the public interest. The program is supported by state transportation departments, federal agencies including the component administrations of the U.S. Department of Transportation, and other organizations and individuals interested in the development of transportation. [www.TRB.org](http://www.TRB.org)

[www.national-academies.org](http://www.national-academies.org)

# COOPERATIVE RESEARCH PROGRAMS

## **CRP STAFF FOR NCHRP REPORT 573**

**Christopher W. Jenks**, *Director, Cooperative Research Programs*  
**Crawford F. Jencks**, *Deputy Director, Cooperative Research Programs*  
**Edward T. Harrigan**, *Senior Program Officer*  
**Eileen P. Delaney**, *Director of Publications*  
**Beth Hatch**, *Editor*

## **NCHRP PROJECT 9-9(1) PANEL**

### **Field of Materials and Construction—Area of Bituminous Materials**

**Maghsoud Tahmoressi**, *PaveTex Engineering and Testing, Inc., Dripping Springs, TX* (Chair)  
**Timothy B. Aschenbrener**, *Colorado DOT*  
**John Bukowski**, *Federal Highway Administration*  
**Cecil L. Jones**, *North Carolina DOT*  
**Rita B. Leahy**, *Nichols Consulting Engineers, Chtd, Sacramento, CA*  
**Richard C. Meininger**, *Federal Highway Administration*  
**Larry L. Michael**, *Hagerstown, MD*  
**Shakir R. Shatnawi**, *California DOT*  
**Ronald A. Sines**, *P.J. Keating Co., Lunenburg, MA*  
**Dale S. Decker**, *Other Liaison, Bailey, CO*  
**David E. Newcomb**, *National Asphalt Pavement Association Liaison, Lanham, MD*  
**Frederick Hejl**, *TRB Liaison*

## **AUTHOR ACKNOWLEDGMENTS**

The research reported herein was performed under NCHRP Project 9-9(1) by the National Center for Asphalt Technology, Auburn University. E. Ray Brown, Director, was the principal investigator and Brian D. Prowell, Assistant Director, was the co-principal investigator, at the National Center for Asphalt Technology.

The authors thank all of the state agencies and contractors who assisted with this project. The authors thank Shane Buchanan, Mike Huner, Graham Hurley, Robert James, Jason Moore, and all of the staff of the National Center for Asphalt Technology who began this project and assisted in the early field data collection. The authors thank Dr. Saeed Maghsoodloo for his assistance with the statistical analyses.

# FOREWORD

By Edward T. Harrigan

Staff Officer

Transportation Research Board

This report presents the findings of a research project to validate the gyration levels in the  $N_{\text{design}}$  table (Table 1) in AASHTO R 35 by following the behavior under traffic of a series of field projects. Its main finding is that, based on ultimate pavement densities achieved on 40 field projects in 16 states across the United States, modest reductions in  $N_{\text{design}}$  are possible. Such reductions, if adopted, should lead to hot mix asphalt (HMA) mix designs that are more readily compacted in the field. The report will be of particular interest to materials engineers in state highway agencies, as well as to materials suppliers and paving contractor personnel responsible for the specification, design, and production of HMA.

---

The original  $N_{\text{design}}$  table associated with the use of the Superpave gyratory compactor in HMA mix design was based on testing conducted on cores from 15 field projects that had been in service for at least 12 years when they were sampled. The asphalt binder was extracted from the cores and the recovered aggregate remixed with virgin AC-20 asphalt cement. The remixed samples were compacted in a gyratory compactor, and the numbers of gyrations necessary to match the core densities were determined. The density at the time of construction was assumed to be 92 percent of  $G_{\text{mm}}$  for all of the projects. The data from the 15 projects were extrapolated to produce the original  $N_{\text{design}}$  table, consisting of 28 levels representing four climatic regions and seven traffic levels. In 1999, this original  $N_{\text{design}}$  table was consolidated to four levels based on laboratory work conducted for NCHRP and FHWA that determined the sensitivity of mix volumetric properties and mix stiffness to  $N_{\text{design}}$ . However, these results were not verified for field conditions.

Under NCHRP Project 9-9(1), "Verification of Gyration Levels in the  $N_{\text{design}}$  Table," the National Center for Asphalt Technology at Auburn University was assigned the goal of verifying through a series of field project evaluations that the gyration levels in the  $N_{\text{design}}$  table (Table 1) of AASHTO Standard Practice R 35, "Superpave Volumetric Design for Hot-Mix Asphalt (HMA)," are correct for the four stated 20-year design traffic levels (less than 0.3 million; 0.3 million to 3 million; 3 million to 30 million; and greater than 30 million ESALs). To accomplish this goal, the research team conducted an extensive field experiment that followed the in-situ pavement densification of 40 field projects from their time of construction to 4 years under traffic.

The projects were located in 16 states in the Rocky Mountain, South Central, North Central, and Southeast regions of the United States, and they represented a wide range of traffic levels, asphalt binder performance grades, and aggregate types and gradations. At each project, gyratory compacted specimens were prepared from as-produced loose mix at the  $N_{\text{design}}$  level required for the project by Table 1 of AASHTO R 35, and the specimen densities were compared with those developed during the HMA mix design. The pavements

were cored at the time of construction and at 3 months, 6 months, 1 year, 2 years, and 4 years after construction. Core densities were then measured and in-place air void contents were calculated. Thus, the densification of each project was followed over time until an ultimate in-place density was reached. These results were then compared with the original mix design data to assess how well the project  $N_{\text{design}}$  level matched the ultimate pavement densification achieved under traffic.

Based on analyses of the experimental results, the research team concluded that the present  $N_{\text{design}}$  levels in AASHTO R 35 are higher than needed to match the ultimate in-place pavement density at design traffic levels greater than 0.3 million ESALs. The team recommended specific changes to the  $N_{\text{design}}$  values in Table 1 of AASHTO R 35 for consideration by the AASHTO Highway Subcommittee on Materials. In addition, the team proposed further reductions in  $N_{\text{design}}$  when the mix design is prepared with an asphalt binder with a performance grade of PG 76-XX or greater. Such binders are typically modified, and HMA prepared with them can provide superior performance.

All 40 field projects proved to have excellent resistance to rutting. Based on this fact and on an evaluation of the original mix design data for each project, the team recommended removal of the  $N_{\text{initial}}$  and  $N_{\text{maximum}}$  requirements in Table 1 of AASHTO R 35 as superfluous to the design of well-performing HMA.

This final report includes a detailed description of the experimental program, a discussion of the research results and their analysis, a summary of findings, and recommendations for implementation of key findings. These findings have been referred to the FHWA Asphalt Mixture Expert Task Group and the AASHTO Highway Subcommittee on Materials for review and revision of the applicable recommended practice.

# CONTENTS

1	Summary
5	<b>Chapter 1</b> Introduction and Research Approach
5	1.1 Background
5	1.2 Research Problem Statement
6	1.3 Objective
6	1.4 Scope
7	<b>Chapter 2</b> Summary of Literature Review
7	2.1 Brief History of Mix Design
7	2.2 Field Densification of Asphalt Pavements
8	2.3 Gyrotory Compaction
8	2.4 $N_{design}$
8	2.4.1 SHRP $N_{design}$ Experiment
8	2.4.2 Validation of $N_{design}$ After SHRP
10	2.5 Locking Point
11	2.6 Summary
12	<b>Chapter 3</b> Research Test Plan
14	<b>Chapter 4</b> Test Results and Analyses
14	4.1 Projects Selected
14	4.2 Test Results
16	4.2.1 Comparison of Mixture Data with Design Job Mix Formula
16	4.2.2 Estimation of Traffic
21	4.2.3 Pavement Densification
22	4.2.3.1 <i>As-Constructed Density</i>
24	4.2.3.2 <i>Densification with Time</i>
24	4.2.3.3 <i>Determination of Ultimate Density</i>
25	4.2.3.4 <i>Factors Affecting Pavement Densification</i>
28	4.2.3.5 <i>Pavement Densification at the 2000 NCAT Test Track</i>
30	4.2.4 Determination of $N_{design}$ to Match Ultimate In-Place Density
30	4.2.4.1 <i>Predicted <math>N_{design}</math> Versus 2-Year Traffic</i>
32	4.2.4.2 <i>Comparison of Laboratory Density at <math>N_{design}</math> and In-Place Density After 2 Years of Traffic</i>
33	4.2.4.3 <i>Predicted <math>N_{design}</math> Versus Accumulated Traffic for 2000 NCAT Test Track</i>
35	4.2.4.4 <i>Predicted <math>N_{design}</math> Versus 2-Year Traffic, Excluding Mixes Produced with PG 76-22</i>
38	4.2.4.5 <i>Predicted <math>N_{design}</math> Versus 2-Year Traffic for PG 76-22 Mixes</i>
38	4.2.4.6 <i>Predicted <math>N_{design}</math> Versus Traffic for All Sampling Intervals</i>
38	4.2.4.7 <i>Model Development to Account for Low As-Constructed Density</i>

45	4.2.5 Evaluation of Locking Point
49	4.2.6 Pavement Condition After 4 Years
49	4.2.7 Evaluation of $N_{\text{initial}}$
51	4.2.8 Evaluation of $N_{\text{maximum}}$
51	4.2.9 Summary and Discussion of Test Results
<b>56</b>	<b>Chapter 5 Conclusions and Recommendations</b>
56	5.1 Conclusions
57	5.2 Recommendations
<b>58</b>	<b>References</b>
<b>61</b>	<b>List of Acronyms</b>
<b>62</b>	<b>Appendixes</b>

## S U M M A R Y

The original Superpave  $N_{\text{design}}$  table was based on testing conducted on a single core from each of 15 different sites. The sites were selected to represent three climatic regions (cool, warm, and hot) and three traffic levels (low, medium, and high). Two replicates were desired for each of the nine cells, but only a single replicate was identified for each of the three cells representing the hot climate. The sites had been in service for at least 12 years when they were sampled. The asphalt was extracted from the cores and the recovered aggregate remixed with virgin AC-20. The remixed samples were compacted in a gyratory compactor, and the numbers of gyrations were determined to match the densities of the cores. The density at the time of construction was assumed to be 92 percent of  $G_{\text{mm}}$  for all of the projects. The data from the 15 cores were extrapolated to produce the original  $N_{\text{design}}$  table consisting of 28 levels representing four climatic regions and seven traffic levels.

In 1999, the Superpave  $N_{\text{design}}$  table was consolidated to four levels based on the sensitivity of mixture volumetric properties and mixture stiffness to  $N_{\text{design}}$ . The climatic regions were eliminated because differences in climate should be accounted for by the selection of the binder grade. Testing was conducted on a range of mixes and determined that a difference of approximately 30 gyrations resulted in a change in voids in mineral aggregate (VMA) of approximately 1 percent. Similarly, a change of approximately 25 gyrations resulted in a change in mixture stiffness, as measured by the Superpave shear tester frequency sweep at a constant height test, of 25 percent. However, these data were not verified for field conditions.

NCHRP Project 9-9(1) was conducted to verify the  $N_{\text{design}}$  levels in the field. Samples were collected, tested, and analyzed from 40 field projects at the time of construction. The projects were selected in 16 states. The projects represent a wide range of traffic levels, binder grades, aggregate types, and gradations. A mobile lab was taken to each of the project sites so that mix could be compacted in the field without reheating. Two gyratory compactors were used to compact samples in the field: a Pine Model AFG1a and a Troxler Model 4141. Each project was cored at the time of construction and at 3 months, 6 months, 1 year, 2 years, and 4 years after construction. Visual condition surveys were conducted in conjunction with the coring.

Analyses of the pavement densification data produced a number of important findings:

- 55 percent of the pavements tested had as-constructed densities less than 92 percent of  $G_{\text{mm}}$ .
- The majority of the pavement densification occurred in the first 3 months after construction.
- The month of construction significantly affected pavement densification. Pavements constructed in late spring or early summer tended to densify more than average, and pavements constructed in early spring or the fall tended to densify less than average.
- The ultimate densities of the pavements evaluated in this study were obtained after 2 years of traffic.
- A fair relationship was found between the as-constructed density of the pavement and the density after 2 years of traffic or ultimate density.

- Based on data collected at the 2000 National Center for Asphalt Technology (NCAT) Test Track, Superpave mixes containing modified binders (Performance Grade [PG] 76-22) densified 25 percent less and rutted 60 percent less than mixes containing neat (i.e., unmodified) PG 67-22. The modified mixes had an average reduction in air voids after 10 million equivalent single axle loads (ESALs) of 4.1 percent, while the unmodified mixes had an average reduction of 5.6 percent. The modified mixes had an average rut depth of 1.7 mm, while the unmodified mixes had an average rut depth of 4.1 mm.

One of the premises of hot mix asphalt design is that the density of the laboratory-compacted samples used to determine the optimum asphalt content should approximate the ultimate density of the pavement. If the ultimate density of the pavement is too low, the durability of the pavement will be reduced, and if the ultimate density of the pavement is too high (more than 98 percent  $G_{mm}$ ), the pavement will tend to bleed or rut. The ultimate in-place densities of the pavements evaluated in this study were approximately 1.5 percent less than the densities of the laboratory-compacted samples at the agency-specified  $N_{design}$ . This would indicate that the laboratory compaction effort is too high. Testing conducted by the Asphalt Institute as part of the  $N_{design}$  II experiment would suggest that the higher-than-designed in-place air voids would reduce pavement shear stiffness by approximately 23 percent.

The number of gyrations to match the ultimate in-place density was calculated for each project in this study. The calculated values for the two compactors used in this study differed by approximately 20 gyrations. This difference was attributed to differences in the dynamic internal angle. The predicted gyrations adjusted to a dynamic internal angle of 1.16 degrees showed good agreement between the two machines. The dynamic internal angle of all gyratory compactors should be set to 1.16 degrees.

A relationship was developed between predicted  $N_{design}$  and design traffic for the projects that were not constructed using PG 76-22. Although there was a great deal of scatter in the data, this scatter was expected. The predicted gyration levels were generally less than those currently specified. Predicted gyrations to match ultimate density for mixes 50 mm below the pavement surface were approximately 30 gyrations less than those for the surface mixes at the 2000 NCAT Test Track.

A model was developed relating the 2-year or ultimate pavement density (expressed as a percentage of the laboratory density of samples compacted to  $N_{design} = 100$  gyrations) to as-constructed density, high PG, and the log of the accumulated ESALs after 2 years. Using this model, the percentage of laboratory density was predicted for pavements compacted to 92 percent of  $G_{mm}$ , using both PG 64-22 and PG 76-22 and a range of traffic levels. The number of gyrations required to match a given percentage of laboratory density was approximately the same for each of the 40 projects, with a standard deviation of approximately eight gyrations. The average number of gyrations for each percentage of laboratory density was then regressed against the variables that were used to predict the percentages of laboratory density (as-constructed density, high PG, and 2-year ESALs) to determine a new model. Since the as-constructed density was held constant at 92 percent, this variable dropped out of the model. The new model could then use the anticipated high PG and design traffic to predict  $N_{design}$ . The  $N_{design}$  levels determined with this model for PG 64-22 were slightly higher than those determined to match the ultimate density of the pavement, particularly at the lower traffic levels. However, both analyses indicated lower gyration levels than those currently specified. The  $N_{design}$  levels for mixes using PG 76-22 are approximately 15 gyrations less than the  $N_{design}$  levels for mixes using PG 64-22. A reduction in  $N_{design}$  for modified mixes is supported by both testing conducted as part of the  $N_{design}$  II experiment by the Asphalt Institute and by data from the NCAT Test Track. The test track data indicated that modified mixes densified approximately 25 percent less under traffic. Mixture stiffness testing conducted during the  $N_{design}$  II experiment suggested that changing the binder grade from

PG 70-22 to PG 76-22 resulted in a change in shear stiffness equivalent to changing  $N_{\text{design}}$  by 30 gyrations. This methodology was selected to recommend new  $N_{\text{design}}$  levels. This method was preferable to the other methods, since the low as-constructed densities could be accounted for and the gyration levels could be adjusted for binder grades of PG 76-XX or stiffer.

The concept of the locking point—defined as the gyration at which the aggregate skeleton “locks” together and further compaction results in aggregate degradation and very little additional compaction—was evaluated as a potential alternative to  $N_{\text{design}}$ ; four methods of determining the locking point gyration were tested. The original method, developed by Bill Pine, is referred to as the 3-2-2 locking point. It uses the first gyration in a series of three gyrations of equal sample height that immediately followed two sets of two gyrations of equal sample heights, as shown in Figure S.1. This original method gave the best results of the four methods tested. The specimen density determined at this 3-2-2 locking point was correlated to the ultimate pavement density. The correlation was weak; 36 of the 40 3-2-2 locking point densities exceeded the ultimate pavement density. Thus, conservatively, the optimum asphalt content of an HMA mix could be selected to produce 96 percent of  $G_{\text{mm}}$  at the 3-2-2 locking point as an alternative to  $N_{\text{design}}$ . However, the variance in the locking point at various asphalt contents was not evaluated in this study.

All of the field projects in this study were very rut resistant. The maximum observed rutting for the field projects was 7.4 mm, with an average rut depth for all of the projects of 2.7 mm after 4 years of traffic.

The requirements for  $N_{\text{initial}}$  and  $N_{\text{maximum}}$  were also evaluated. One or more sample densities at the agency-specified  $N_{\text{initial}}$  failed the  $N_{\text{initial}}$  requirements (which are a function of design traffic) for 11 of 40 projects. The majority of the failures occurred with fine-graded mixes having design traffic levels in excess of 300,000 ESALs. The mix was reported as being tender for only one of the pavements that failed  $N_{\text{initial}}$ . Historically, contractors have been able to deal with tender mixes. Since all pavements were rut resistant,  $N_{\text{initial}}$  does not appear to indicate rutting potential. At the agency-specified  $N_{\text{maximum}}$ , the density of at least one sample from 25 of 40 projects exceeded 98 percent  $G_{\text{mm}}$ . Failures for 10 of these projects may have been due to extrapolation. However, as noted previously, all of the projects were extremely rut resistant. This indicates that the  $N_{\text{maximum}}$  requirements are not indicative of rutting potential and should be eliminated.

New  $N_{\text{design}}$  levels are recommended based on all of the analyses conducted.  $N_{\text{design}}$  levels are recommended for binders with high temperature grades less than PG 76 and binders with high temperature grades of PG 76 or greater. The recommended  $N_{\text{design}}$  levels closely follow the numbers determined from the model described previously. The results from the model are slightly more conservative (i.e., higher) than those determined to match the ultimate density. The  $N_{\text{design}}$  levels are based on having all gyratory compactors set to a dynamic internal angle of 1.16 degrees. Table S.1 shows the proposed  $N_{\text{design}}$  levels for an SGC dynamic internal angle (DIA) or  $1.16 \pm 0.02$  degrees.

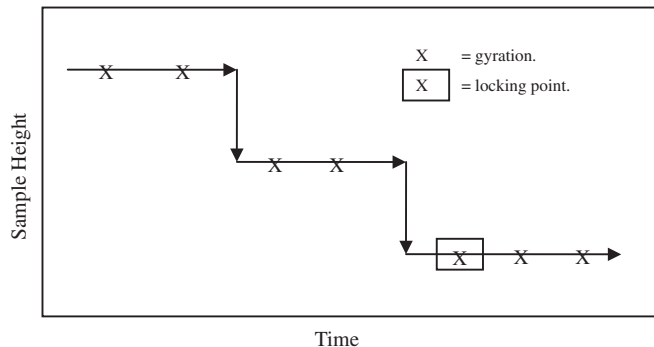


**Figure S.1. Locking Point 3-2-2.**

**Table S.1. Proposed  $N_{\text{design}}$  levels for an SGC DIA of  $1.16 \pm 0.02$  degrees.**

20-Year Design Traffic, ESALs	2-Year Design Traffic, ESALs	$N_{\text{design}}$ for binders < PG 76-XX	$N_{\text{design}}$ for binders $\geq$ PG 76-XX or mixes placed > 100 mm from surface
< 300,000	< 30,000	50	NA
300,000 to 3,000,000	30,000 to 230,000	65	50
3,000,000 to 10,000,000	230,000 to 925,000	80	65
10,000,000 to 30,000,000	925,000 to 2,500,000	80	65
> 30,000,000	> 2,500,000	100	80

Reducing  $N_{\text{design}}$  will tend to allow contractors to design mixes that can be more readily compacted in the field. This should improve in-place density. It may not, however, result in an increase in the optimum asphalt content. If the contractor were to use the same aggregate type and gradation, then VMA and the optimum asphalt content would increase with lower gyration levels. However, most contractors would tend to adjust their gradations to reduce VMA, leaving some cushion above the minimum value, to produce a more economical mix. This cushion may tend to be slightly larger with lower  $N_{\text{design}}$  values. If a larger increase in optimum asphalt content is desired, the reduction in  $N_{\text{design}}$  should be accompanied by a small increase in minimum VMA. An increase in minimum VMA of 0.5 percent accompanied by the proposed reductions in  $N_{\text{design}}$  would tend to improve the compactability of the mix in the field and increase the optimum asphalt content.

---

## CHAPTER 1

# Introduction and Research Approach

### 1.1 Background

The Superpave mix design system, a product of the Strategic Highway Research Program (SHRP), was released in 1994. The Superpave mix design system for hot mix asphalt (HMA) includes binder specifications, aggregate property specifications, design gradation ranges, a laboratory compaction procedure, specifications for volumetric properties, and an evaluation of moisture sensitivity. These specifications are to act in concert to provide a system of checks and balances to ensure that the resulting HMA is durable and rut resistant. Durability includes such performance parameters as resistance to low temperature and age-related cracking, resistance to raveling or other surface wear, and resistance to moisture damage. Rut resistance refers to resistance to permanent deformation resulting from shear flow of the HMA; it does not include permanent deformation or rutting of the subgrade due to insufficient pavement structure. The Superpave mix design system accounts for differing traffic and environmental conditions.

Central to the Superpave mix design system is the Superpave gyratory compactor (SGC). The SGC is used to compact trial HMA mixtures to a design number of gyrations in the laboratory in order to allow an evaluation of the volumetric properties of the compacted sample. The volumetric properties evaluated include air voids, voids in mineral aggregate (VMA), voids filled with asphalt (VFA), and ratio of dust to effective binder content. Two additional parameters are included to examine the rate of densification: density at an initial number of gyrations ( $N_{\text{initial}}$ ) and density at a maximum number of gyrations ( $N_{\text{maximum}}$ ). The laboratory design air void content is supposed to be related to the ultimate field density of the HMA.

The overall performance of an HMA pavement depends highly on the pavement structure and the construction quality. The pavement structure is evaluated in the pavement thickness

design procedure, which is a separate topic. The ability to construct the HMA pavement layers should be, as much as possible, considered in the mix design procedure. The purpose of this research was to verify the relationship between laboratory testing and field performance with regards to the SGC and, where needed, to provide alternative recommendations.

### 1.2 Research Problem Statement

When the Superpave mix design system was initially released in 1994, it included 28 different design gyration ( $N_{\text{design}}$ ) levels for the SGC, representing seven traffic levels for each of four climates (1). Traffic levels were represented by 18-kip equivalent single axle loads (ESALs) accumulated during a 20-year design life. Differing climates were represented by the average 7-day high air temperature for the project site.  $N_{\text{design}}$  increased as either design ESAL or high air temperature increased.

In 1999, the Federal Highway Administration (FHWA) Superpave Mixture Expert Task Group recommended a consolidation of the original 28  $N_{\text{design}}$  levels to four  $N_{\text{design}}$  levels. The consolidation eliminated differing  $N_{\text{design}}$  levels for differing climates and reduced the design traffic to five ranges, two of which use the same  $N_{\text{design}}$  level. This consolidation was primarily based on research conducted in two studies (2, 3). One of the studies did not address the magnitude of the  $N_{\text{design}}$  levels with respect to field performance, but rather differences in the gyration levels that resulted in significant differences in the resulting volumetric properties (2). The other study was based on variations in mixture stiffness as a function of  $N_{\text{design}}$  (3). The American Association of State Highway and Transportation Officials (AASHTO) adopted the recommended changes to the SGC compaction procedure of the Superpave mix design procedure in 2000 (4).

There is still concern that the current  $N_{\text{design}}$  levels do not maximize field performance. The optimum asphalt content

for a given blend of materials is selected at 4 percent air voids, based on laboratory samples compacted to  $N_{\text{design}}$ , assuming that the resulting mixture meets the other criteria of the Superpave mix design system. The asphalt content of HMA is critical to the mixture's performance: if there is too much asphalt, the mixture is likely to suffer excessive permanent deformation; if there is too little asphalt, field compaction may be difficult and the pavement may develop premature cracking, raveling, and/or other distresses related to lack of durability. The locking point concept has been proposed as an alternative to  $N_{\text{design}}$ . The locking point is believed to represent the point where the aggregate skeleton "locks" together and further compaction results in aggregate degradation and very little additional compaction.

### 1.3 Objective

The three objectives of this research were (1) to evaluate the field densification of pavements designed using the Superpave mix design system, (2) to verify or determine the

$N_{\text{design}}$  levels to optimize field performance, and (3) to evaluate the locking point concept.

### 1.4 Scope

This study included a literature search and extensive laboratory and field testing. Samples were collected, tested, and analyzed from 40 field projects at the time of construction. The field projects were selected in 16 states. The projects represent a wide range of traffic levels, binder grades, aggregate types, and gradations. Each project was visited at five time intervals after construction: 3 months, 6 months, 1 year, 2 years, and 4 years. Coring and distress surveys were conducted at each evaluation interval. In total, approximately 4,085 SGC samples and 5,670 cores were tested. Data obtained from the SGC samples and field cores, as well as traffic data provided by the agencies, were analyzed to provide recommendations for the  $N_{\text{design}}$  compaction levels and for the use of the locking point as an alternative to  $N_{\text{design}}$ .

---

## CHAPTER 2

# Summary of Literature Review

Chapter 2 presents a summary of the literature review designed to introduce the reader to the evolution of mix design, field densification under traffic,  $N_{\text{design}}$ , and the locking point. The complete literature review is presented in Appendix A.

### 2.1 Brief History of Mix Design

The first HMA (actually sand asphalt) was placed in the United States in 1876. Initially, optimum asphalt content was selected by experience. Several proprietary mixes were developed and widely used. As the popularity of HMA grew, there developed a need for standardized tests to assist with the design and control of HMA. This was partially because there were no longer enough experienced individuals to make decisions regarding the adequacy of a mix (5, 6).

One of the first tests applied to the determination of optimum asphalt content was the pat test, basically a visual assessment of the residual asphalt that has been pressed into a fresh sample of HMA, on a piece of manila paper (7). Hveem (5) recognized the relationship between aggregate gradation and optimum asphalt content: finer mixes generally required higher optimum asphalt contents because they have more surface area. In the 1930s, researchers began to look for a laboratory compaction procedure that would produce sample densities similar to the ultimate density of the in-place pavement. Pavements were observed to densify under traffic for a period of 2 to 3 years or more. Later, this search was expanded to include a laboratory compaction procedure that would produce samples with the same mechanical properties as field-compacted HMA (5, 8–12).

The most widely recognized study of this nature was that conducted by the U.S. Army Corps of Engineers during the development of the Marshall mix design procedure. More than 214 test sections representing 27 mixes were placed and tested with accelerated loading. Three wheel loads were used: 15,000 lb, 37,000 lb, and 60,000 lb; 3,500 passes were applied with the 15,000-lb load, and 1,500 passes were applied with

the remaining two loads. The filler content and asphalt content of each mixture were varied at three levels. Based on field performance, optimum asphalt content for each mixture was recommended. The laboratory compaction effort that produced an optimum asphalt content that best matched those determined in the field was 50 blows on each face (9, 10).

Hveem (5) placed less emphasis on sample air voids and more emphasis on stability, but recognized the importance of air voids as they relate to durability. Texas conducted studies with the Texas Gyrotory Compactor during the 1940s to verify that the laboratory compaction effort matched the ultimate pavement density. The density of cores taken 1 to 12 years after construction averaged 0.8 percent lower than the laboratory samples. The U.S. Army Corps of Engineers developed its Gyrotory Testing Machine (GTM) in response to even higher (up to 350 psi) tire pressures on military aircraft (8, 13, 14).

A general summary of the early design philosophies might be that HMA should be designed with the highest asphalt content (for durability) that does not result in premature stability or rutting problems. Marshall emphasized the importance of minimizing VMA by using the densest aggregate structure possible (6).

### 2.2 Field Densification of Asphalt Pavements

Numerous studies have been conducted to monitor the densification of in situ pavements (9, 15–29). Generally, pavements were believed to reach their ultimate density under traffic after 2 to 3 years, with most of the densification occurring in the first year. Some studies observed densification over a longer period of time (up to 10 years). Attempts were made to relate field densification to laboratory compaction, particularly with the Marshall method.

In the late 1970s and the 1980s, rutting problems became more prevalent in the United States. This prevalence is somewhat attributed to the use of radial tires and increased tire pressures on trucks. To address these concerns, \$50 million

was devoted to asphalt research in SHRP, which was authorized by the Surface Transportation and Uniform Relocation Assistance Act of 1987 (1). Superpave was a product of SHRP.

## 2.3 Gyrotory Compaction

The gyrotory compactor was selected for routine use in the Superpave mix design system because (1) it can produce samples with similar mechanical properties as field-compacted HMA, and (2) it is convenient (30–32). Further, the French indicated a relationship between the number of gyrations and the layer thickness and number of roller passes in the field. The operational characteristics of the French Gyrotory Compactor were adopted, with the exception that the speed of gyration was increased to 30 rpm (33).

## 2.4 $N_{\text{design}}$

### 2.4.1 SHRP $N_{\text{design}}$ Experiment

An experiment was conducted through SHRP to determine  $N_{\text{design}}$  (30, 34). The premise of the experiment was threefold: (1) there was a relationship between pavement densification and accumulated traffic, (2) there was a relationship between the densities of samples compacted in the SGC and in-place densities, and (3) there was a linear relationship between  $N_{\text{design}}$  and design traffic. Fifteen pavements, representing three climatic regions and three traffic levels, that had been in service for more than 12 years were cored (one core each). The density of the cores was measured and the asphalt extracted to recover the aggregate. The density at the time of construction was unknown and assumed to be 92 percent. No relationship was observed between pavement density and traffic for the lower lifts (more than 100 mm); therefore, these samples were not tested (34). The recovered aggregate was remixed with virgin asphalt and two samples compacted to 230 gyrations for each mix. The number of gyrations that matched the in-place density was backcalculated. A relationship was developed between design traffic ESALs and  $N_{\text{design}}$ . However, it was found that the angle of gyration of the SGC was 1.3 degrees, not the specified 1.0 degree. Therefore, the aggregates were again recovered, remixed, and compacted in the SGC, now set to an angle of gyration of 1 degree. From this experiment, a table of  $N_{\text{design}}$  levels for three climates and seven traffic levels was developed (30, 34). Later the SHRP researchers expanded this table to four climates (30). Late in SHRP's duration, the angle of gyration was changed to 1.25 degrees. The  $N_{\text{design}}$  levels were not altered at this time, even though angles had been demonstrated to affect  $N_{\text{design}}$  (30).

### 2.4.2 Validation of $N_{\text{design}}$ After SHRP

When Superpave was first released, researchers and agencies compared the results from the Superpave system using the SGC with the design systems they were familiar with, most frequently the Marshall system. The SGC was found to generally produce lower VMA and, therefore, lower optimum asphalt contents than the Marshall system did (29, 35–37).

Research indicated that significant differences did not exist between mix properties resulting from many of the  $N_{\text{design}}$  levels that were close together (2, 38, 39). Inconsistencies were observed between the density at  $N_{\text{design}}$  backcalculated from  $N_{\text{maximum}}$  (which was the method originally recommended in the Superpave system) and the density of samples compacted to  $N_{\text{design}}$  (39, 40).

Two significant studies were conducted to verify and refine  $N_{\text{design}}$ : NCHRP Project 9-9, conducted by NCAT of Auburn University (2), and the  $N_{\text{design}}$  II experiment, conducted by the Asphalt Institute and the University of Texas at Austin (3). NCHRP Project 9-9 focused on developing guidelines for gyrotory compaction. Specific areas of guidance included the following (2):

1. Consolidation of the  $N_{\text{design}}$  table,
2. Mix design procedures for large-stone and gap-graded mixes,
3. Potential for using the compaction temperature for short-term aging of samples for volumetric design,
4. Appropriate  $N_{\text{design}}$  as a function of depth, and
5. Validity of the  $N_{\text{initial}}$  and  $N_{\text{maximum}}$  criteria.

Buchanan (39) conducted much of the research that supported NCHRP Project 9-9. The first objective was evaluated by examining the effect of  $N_{\text{design}}$  on volumetric properties. An evaluation of the parameters of the SGC (gyration angle, vertical pressure, and gyration speed) was not included in this research.

An experimental matrix—including four aggregate sources, two gradations, and six  $N_{\text{design}}$  levels—was developed for the NCHRP 9-9(1) research. The four aggregate sources included New York Gravel, Georgia Granite, Alabama Limestone, and Nevada Gravel. Both gradations were 12.5 mm nominal maximum aggregate size (NMAS), but one was fine-graded and the other was coarse-graded; neither gradation passed through the restricted zone. The six gyration levels consisted of the lowest level (68) and highest level (172) in the original  $N_{\text{design}}$  table, three intermediate gyration levels (93, 113, and 139), and 40 gyrations. Based on previous work, it was felt that a lower level of gyrations may be required for low-volume roads. A single-binder, PG 64-22 sample was used in the experiment. Three asphalt contents were used to bracket  $N_{\text{design}}$ . The samples were compacted to  $N_{\text{design}}$  (not  $N_{\text{maximum}}$ ).

Separate samples were compacted to  $N_{\text{maximum}}$  for three  $N_{\text{design}}$  levels and compared with results from the Asphalt Pavement Analyzer. Some of the samples did not meet all of the volumetric requirements.

The data indicated that optimum asphalt content, VMA, and VFA all decreased with increasing  $N_{\text{design}}$ , and the coarse-graded mixes were more sensitive than the fine-graded mixes were. Analysis of variance (ANOVA) was performed to determine which of the experimental factors affected the VMA. All of the main factors (e.g.,  $N_{\text{design}}$ , aggregate source, and gradation) and their interactions were significant. Duncan's multiple-range comparison procedure was conducted to compare the measured VMA resulting from the differing  $N_{\text{design}}$  levels. The analyses were conducted separately for the coarse-graded and fine-graded mixes. For both gradations, the differing  $N_{\text{design}}$  levels used in this study resulted in significantly different VMA at the 5-percent significance level.

An evaluation was performed of the need for the differing gyration levels for the differing climatic zones in the  $N_{\text{design}}$  table. The argument was made that the average 7-day maximum temperature is less than 39°C for the majority of the United States. Further, where higher temperatures exist, a stiffer binder would likely be used. Using a Student's t-test, statistical comparisons were conducted between the resulting VMA calculated for each aggregate source and the gradation between the  $N_{\text{design}}$  climatic extremes for a given traffic level (e.g., 68 versus 82 gyrations, respectively, for less than 39°C and 43–45°C). No significant differences were observed for 41 of 56 comparisons. For the 15 comparisons that were significant, the average absolute difference in VMA was 0.57 percent. Based on these analyses, the differing  $N_{\text{design}}$  levels as a function of climate were eliminated from the  $N_{\text{design}}$  table, collapsing the table from 28 to 7 levels.

Since the coarse-graded mixes were more sensitive to  $N_{\text{design}}$  than the fine-graded mixes were, the VMA results for the coarse-graded mixes were evaluated to further consolidate the  $N_{\text{design}}$  table. The average difference in VMA between  $N_{\text{design}}$  levels was 0.32 percent for the coarse-graded mixes and 0.18 percent for the fine-graded mixes. A VMA range of 1 percent was selected for differing  $N_{\text{design}}$  levels. This would result in a

difference in optimum asphalt content of approximately 0.45 percent for the coarse-graded mixes. Thus, three levels of  $N_{\text{design}}$  were proposed: 70, 100, and 130 gyrations. A fourth  $N_{\text{design}}$  level, 50 gyrations, was proposed for low-volume roads.

None of the mixes included in this study failed to meet the  $N_{\text{maximum}}$  criterion. Further, it was determined that compacting samples to  $N_{\text{maximum}}$  and backcalculating the volumetric properties at  $N_{\text{design}}$  can result in errors of up to 0.8-percent air voids. Therefore, it was recommended that samples be compacted to  $N_{\text{design}}$  for the determination of volumetric properties. Separate samples could be compacted to  $N_{\text{maximum}}$  after the optimum asphalt content is determined. Table 2.1 presents the recommended revised  $N_{\text{design}}$  table (2, 39).

The  $N_{\text{design}}$  II experiment was the other major effort to verify  $N_{\text{design}}$ . Anderson et al. (3) conducted an evaluation of  $N_{\text{design}}$  based on the sensitivity of mixture stiffness to changes in  $N_{\text{design}}$ . This research had four tasks:

1. Examine the performance of in-place Superpave pavements designed with the original SHRP  $N_{\text{design}}$  table.
2. Select a performance test for rutting.
3. Determine the sensitivity of the performance test to changes in  $N_{\text{design}}$ .
4. Recommend a new  $N_{\text{design}}$  table.

Six Superpave mix designs were developed using two aggregate types—crushed limestone and crushed gravel—and three  $N_{\text{design}}$  levels—70, 100, and 130 gyrations. All of the mixes were 12.5 mm NMAS. The gradations of the three blends for each aggregate source were varied to produce a VMA slightly above the minimum (14.0 percent). This was done based on the assumption that because the binder is the most expensive component of HMA, the mix designers will alter the gradation to reduce VMA as  $N_{\text{design}}$  decreases. The resulting mixes had measured VMA ranging from 14.2 to 14.6 percent and optimum asphalt contents of either 4.6 or 4.7 percent. Samples were produced with a single unmodified PG 70-22.

The rutting properties of the mixes were evaluated using two tests performed in the Superpave Shear Tester (SST): frequency sweep at constant height (FSCH) and repeated shear at constant height (RSCH). FSCH is conducted by applying

**Table 2.1. Revised  $N_{\text{design}}$  table proposed by NCHRP Project 9-9 (2, 39).**

Design Traffic Level (million ESALs)	Gyrations Levels			% $G_{\text{mm}}$ at $N_{\text{initial}}$	% $G_{\text{mm}}$ at $N_{\text{maximum}}$
	$N_{\text{initial}}$	$N_{\text{design}}$	$N_{\text{maximum}}$		
< 0.1	6	50	74	< 91.5	< 98.0
0.1 to < 1.0	7	70	107	< 90.5	
1.0 to < 30.0	8	100	158	< 89.0	
> 30.0	9	130	212	< 89.0	

to the samples a small shear stress that results in a shear strain of less than 0.0005 kPa. Tests are conducted at 10 frequencies: 10, 5, 2, 1, 0.5, 0.2, 0.1, 0.05, 0.02, and 0.01 Hz. Highway traffic speeds are generally represented by the results at 10 Hz. The complex shear modulus ( $G^*$ ) is the ratio of the applied shear stress to the resulting shear strain. Higher  $G^*$  values at a given temperature indicate a stiffer mix. FSCH testing was conducted at two temperatures, 50°C and 60°C. RSCH is performed by applying a haversine shear stress of 69 kPa with a 0.1-second load and a 0.6-second rest period (1.4 Hz) for 5,000 cycles. The test result is reported as the accumulated permanent shear strain after 5,000 cycles. Testing was conducted at 60°C.

It was observed that  $G^*$  (10 Hz) was significantly higher for the limestone aggregate than for the gravel aggregate. Based on data reported in the paper, the limestone mixes were 65, 60, and 36 percent stiffer than the gravel mixes were when designed at 130, 100, and 70 gyrations, respectively. For a given aggregate, there were no significant differences between the stiffness of the mixes designed at 100 and 130 gyrations.  $G^*$  (10 Hz) was lower, 18 percent for the limestone mixes and 3 percent for the gravel mixes, for both aggregate mixtures designed with  $N_{\text{design}} = 70$  gyrations as compared to  $N_{\text{design}} = 100$  gyrations. There was a general trend of decreasing shear stiffness with decreasing  $N_{\text{design}}$ . It was believed that this trend is related to changes in the aggregate skeleton. For the RSCH test, the limestone aggregate was again identified as being more rut resistant. However, no significant differences were noted between the accumulated shear strain from the RSCH test for the mixes designed at different  $N_{\text{design}}$  levels.

The second part of the study was conducted to examine the sensitivity of VMA to  $N_{\text{design}}$ . In this phase, the mixes that were designed at one gyration level were compacted at the other gyrations levels without adjusting the asphalt content or gradation. This resulted in varying VMA and consequently air voids. Similar results to those observed in NCHRP Project 9-9 were noted in terms of change in VMA with change in  $N_{\text{design}}$ . Good correlations were found between air voids and  $G^*$ . The mixes were most sensitive in the range of 3- to 6-percent air voids, with an increase in air voids from 4 to 5 percent resulting in an average decrease in stiffness of 20 percent. Finally, the authors note that, according to experience, an increase in one high-temperature binder grade, say from PG 70 to PG 76, will result in the same increase in mix  $G^*$  as a change of 30 gyrations.

In 1999, at a meeting of the FHWA Superpave Mixtures Expert Task Group, Dr. Ray Brown and Mr. Mike Anderson presented the results of their respective studies on  $N_{\text{design}}$ . Based on that meeting, a new  $N_{\text{design}}$  table was recommended and adopted by AASHTO in 2001. The revised  $N_{\text{design}}$  table from AASHTO PP28 is shown in Table 2.2 (41). In 2004, AASHTO PP28 was adopted as AASHTO M323 (4).

Colorado DOT conducted a study that indicated that in-place air voids after 5 to 6 years of traffic were higher than those obtained at  $N_{\text{design}}$  using the SGC. Lower design gyrations or design air void contents were recommended (42). A study for Georgia DOT indicated that the design VMA of 12.5-mm NMA Superpave mixes was approximately 2 percent less than Marshall-designed mixes with corresponding aggregate sources (43). Studies attempting to relate the density at the end of service life to the density at  $N_{\text{design}}$  gyrations have been criticized (44). Partially, this criticism is because compaction in the field at the time of construction and under traffic tends to be a constant stress mode where as compaction in the SGC is a constant strain mode. Further, because mixtures are compacted in the SGC at an equiviscous compaction temperature, the SGC does not account for differences in binder stiffness, which have a profound effect in the field (44).

## 2.5 Locking Point

Illinois DOT developed an alternative to  $N_{\text{design}}$  termed the “locking point” concept to prevent the overcompaction of, and subsequent aggregate degradation in, the SGC (45). The locking point—defined as the gyration at which the aggregate skeleton “locks” together and further compaction results in aggregate degradation and very little additional compaction—was likened to the growth curve conducted to determine the maximum number of roller passes in the field before the increase in in-place density leveled off or decreased. It was noted that mixes are not compacted with the same number of passes in the field because each mix is different. Rolling was stopped at the peak density before excessive aggregate degradation occurred.

The locking point concept was developed from comparisons made between three years of Marshall and Superpave data and field growth curves (45). Initially, the Illinois locking point was defined as the first gyration in a set of three gyrations of the same height that was preceded by one set of

**Table 2.2. Superpave gyratory compaction effort (41).**

Design ESALs (millions)	Compaction Parameter		
	$N_{\text{initial}}$	$N_{\text{design}}$	$N_{\text{maximum}}$
< 0.3	6	50	75
0.3 to < 3	7	75	115
3 to < 30	8	100	160
≥ 30	9	125	205

two gyrations of the same height (each 0.1 mm taller than the set of three gyrations), as illustrated in Figure 2.1. The locking point was believed to indicate the development of some degree of coarse aggregate interlock and be related to the density achieved in the field growth curves. The standard deviation of the number gyrations equal to the locking point was less than the standard deviation of the number of gyrations to obtain 4-percent air voids.

Vavrik and Carpenter (46) refined the definition of the locking point to be the first gyration in the first occurrence of three gyrations of the same height preceded by two sets of two gyrations with the same height (each 0.1 mm taller than the set of three gyrations), as illustrated in Figure 2.2 and Table 2.3.

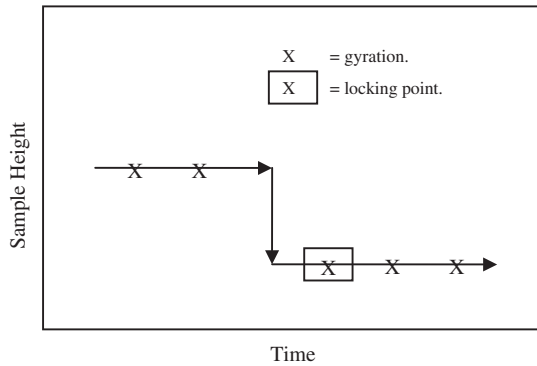


**Figure 2.1. Initial Illinois locking point definition (45).**

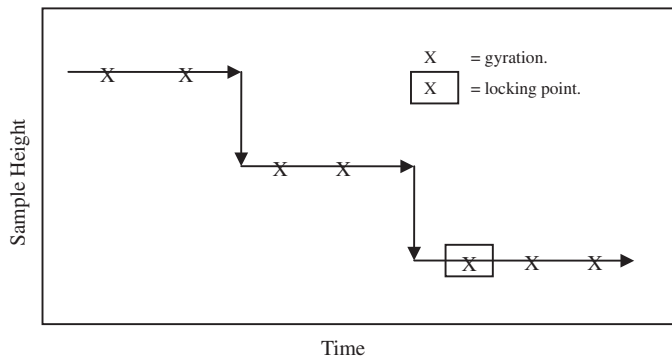


**Figure 2.2. Revised Illinois locking point definition—3-2-2 locking point (46).**

## 2.6 Summary

The literature indicates that there is still concern that the  $N_{\text{design}}$  levels have not been optimized to maximize field performance. The original  $N_{\text{design}}$  table was based on a limited data set for which the as-constructed densities were not available. The  $N_{\text{design}}$  table was consolidated based on a laboratory study designed to evaluate the sensitivity of volumetric properties to  $N_{\text{design}}$ . There is a need to verify the current  $N_{\text{design}}$  values and relate them to field densification and performance.

**Table 2.3. Sample gyratory height data illustrating locking point determination (46).**

Gyration	Height (mm)
61	111.9
62	111.9
63	111.8
64	111.8
65	111.7
66	111.7
67	111.6
68	111.6
69	111.5
70	111.5
71	<i>111.4</i>
72	<i>111.4</i>
73	<i>111.3</i>
74	<i>111.3</i>
75	<b>111.2</b>
76	<i>111.2</i>
77	<i>111.2</i>
78	111.1
79	111.1
80	111.0
81	111.0
82	110.9
83	110.9
84	110.8
85	110.8
86	110.8
87	110.7
88	110.7
89	110.7
90	110.6

The italicized heights were used to determine the locking point, and the boldfaced height is the locking point.

## CHAPTER 3

# Research Test Plan

In 1999, following the research of NCHRP Project 9-9, the  $N_{\text{design}}$  table was revised and consolidated from 28 to 4 levels. However, this consolidation was based on the sensitivity to  $N_{\text{design}}$  of both (1) volumetric properties and (2) a performance test for rutting; it was not tied to field performance. There is still concern that the  $N_{\text{design}}$  levels, in some cases, may be too high. Two states have adopted a single gyration level to design mixes; one of these levels has been successfully used for more than 4 years (47, 48). Therefore, there is a need to validate the  $N_{\text{design}}$  levels with respect to field performance.

In order to validate the  $N_{\text{design}}$  levels, an extensive field research project—NCHRP Project 9-9(1)—was conducted to relate  $N_{\text{design}}$  to the in-place densification of pavements under various traffic loadings while monitoring field performance. The approach selected for this project was similar to the approach used by Brown and Mallick (29). Experimental variables for the project included  $N_{\text{design}}$  level, lift thickness relative to NMAS, gradation, and PG. The experimental variables were selected on the basis of their suspected impact on initial field compaction, densification under traffic, rutting performance, or a combination thereof. The original experimental plan is shown in Table 3.1. Forty projects were required to fill the experimental plan. The projects were geographically distributed across the United States, as shown in Figure 3.1. Attempts were made to identify projects in the southwestern and northeastern United States. However, projects in the southwest were typically overlaid with open-graded friction course and, therefore, were not suitable for the study. Also, projects could not be identified in the northeast that could be sampled during the required timeframe. In 2000, 22 projects were visited and samples were obtained and tested. In 2001, the remaining 18 projects were visited and samples were obtained and tested. All of the mixes sampled were surface mixes.

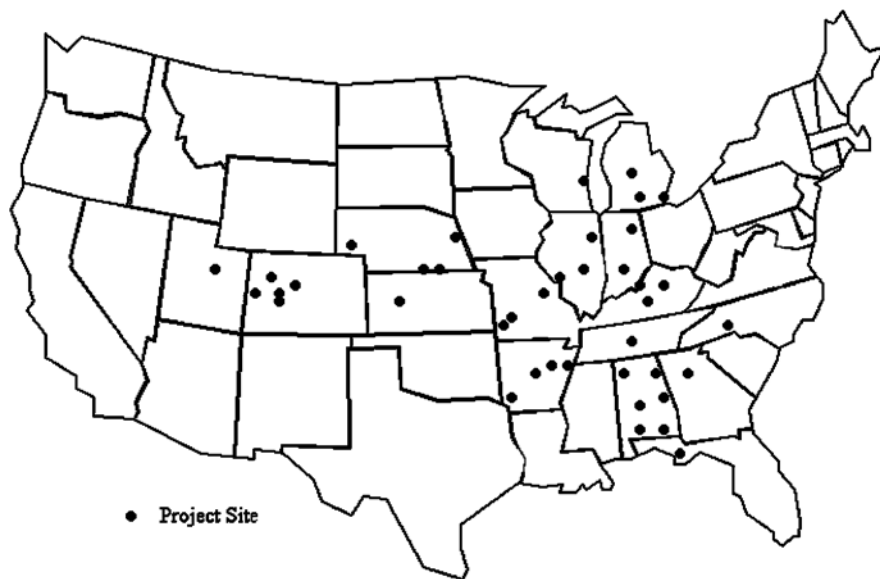
For each project, the following testing and evaluation procedure was conducted:

1. Samples of loose mix were taken from a truck at the asphalt plant; the corresponding location where the remainder of the mix was placed on the roadway was marked. Where possible, three samples were taken from each project, but in some cases only two could be obtained.
2. Three replicate specimens (i.e., gyratory samples) were compacted to two different gyration levels, 100 and 160, without reheating, using two different SGCs in a mobile laboratory. Twelve SGC specimens per production sample, or 24 to 36 specimens per project, were compacted.
3. Samples were split and boxed for determination of maximum specific gravity ( $G_{\text{mm}}$ ), asphalt content, and gradation.
4. Three cores were taken from the right wheel path of the area marked on the roadway where the mix corresponding to a given sample was laid. Thus, there were six cores (for two samples) or nine cores (for three samples) per project at the time of construction.
5. Gyratory specimens, cores, and loose mix were brought back to NCAT for testing to determine  $G_{\text{mm}}$ , asphalt content, and gradation.
6. The following tests were run at the NCAT laboratory:
  - a. Specific gravity of compacted sample ( $G_{\text{mb}}$ ) by AASHTO T166,
  - b.  $G_{\text{mm}}$  by AASHTO T209,
  - c. Asphalt content determination by AASHTO T164, and
  - d. Washed gradation analysis by AASHTO T30.
7. The sites were revisited at approximately 3 months, 6 months, 1 year, and 2 years after construction. During each visit, the following steps were taken:
  - a. Three additional cores were taken corresponding to each sample location at each project.
  - b. The pavement condition was visually assessed.
  - c. Rut depth measurements were taken adjacent to each core location with a 6-ft string line.
  - d. The cores were shipped back to NCAT for determination of specific gravity as described above.

Mix design and traffic information were also collected for each project. Because Brown and Mallick (29) had indicated a difference between the compacted SGC sample density of

**Table 3.1. Original test plan for NCHRP Project 9-9(1).**

Gyrations Level	Fine- or Coarse-Graded	Lift Thickness/Nominal Maximum Aggregate Size								
		2			3			4		
		High-Temperature Performance Grade								
		Normal	+1	+2	Normal	+1	+2	Normal	+1	+2
50	F	X			X			X		
	C	X			X			X		
75	F	X			X			X		
	C	X			X			X		
100	F	X			X	X	X	X	X	X
	C	X			X	X	X	X	X	X
125	F	X			X	X	X	X	X	X
	C	X			X	X	X	X	X	X

**Figure 3.1. Location of NCHRP Project 9-9(1) field studies.**

reheated and laboratory prepared mix, a mobile laboratory was used at each site so that the SGC samples could be compacted without reheating. Because previous research had indicated differences in compaction between different brands and models of SGCs (49, 50), the study used two different SGCs: a Pine Model AFG1a and a Troxler Model 4141. Although previous research had identified errors with the backcalculation procedure (39, 40), it was deemed impossible to compact samples to all possible  $N_{\text{design}}$  levels. Two levels, 100 gyrations and 160 gyrations, were selected to minimize

the number of gyrations for which the sample density needed to be backcalculated.

After 2 years, the project was extended to allow additional coring 4 years after the pavements were laid. This extension was done to ensure that the pavements had reached their ultimate density. The same procedure as described in Step 7 above was used at the 4-year interval. The collected traffic, in-place density, and SGC-compacted sample density information was used to evaluate the relationship between  $N_{\text{design}}$  and field performance.

## CHAPTER 4

## Test Results and Analyses

## 4.1 Projects Selected

A summary of the projects selected for the study is shown in Table 4.1. The data in Table 4.1 are grouped by  $N_{\text{design}}$  level, corresponding to 50, 75, 100, and 125 gyrations. Within each category, the data are sorted by high-temperature binder grade bumps and actual  $N_{\text{design}}$  level. The distribution of factors in Table 4.1 provides some interesting insights on the use of Superpave at the time the projects were sampled. Several states were still using the original  $N_{\text{design}}$  levels. These projects were grouped with the closest current  $N_{\text{design}}$  level. Only one project was identified with an  $N_{\text{design}}$  of 50 gyrations, 12 projects were identified with an  $N_{\text{design}}$  of 75 gyrations (68–86), 18 projects were identified with an  $N_{\text{design}}$  of 100 gyrations (90–109), and 9 projects were identified with an  $N_{\text{design}}$  of 125 gyrations. Although only one project with an  $N_{\text{design}}$  of 50 gyrations was sampled, it will be shown later that the distribution of design traffic meets the intent of the experimental design.

Three different NMASs were sampled: 9.5 mm (from 11 projects), 12.5 mm (from 26 projects), and 19.0 mm (from 3 projects). The average lift thickness was determined from the average of the core thickness measurements at the time of construction. Fine- and coarse-graded mixes were separated by the percentage of the aggregate passing the 2.36-mm sieve. Fine-graded mixes are defined as having a higher percentage of the aggregate passing the 2.36-mm sieve than the maximum density line. Coarse-graded mixes are defined as having a lower percentage of the aggregate passing the 2.36-mm sieve than the maximum density line. Figure 4.1 illustrates the distribution of lift thickness to NMAS ratio for the fine- and coarse-graded mixes.

From Figure 4.1, it can be seen that there is a trend for thicker lifts for coarse-graded mixes. Although the distribution of lift thickness to NMAS ratio does not exactly match the experimental design, it does indicate a representative distribution of field practice. Most of the 75-gyrations mixes were fine-graded, while two-thirds of the 100-gyrations mixes were

coarse-graded and all but one of the 125-gyrations mixes were coarse-graded. Therefore, it appears that higher-gyrations mixes are more likely to be coarse-graded.

The climatic binder grade for each project was determined using LTPPBind Version 2.1 (51). The high-temperature grade bumps were determined by comparing the climatic binder grade with the grade used on the project. As expected, high-temperature binder bumps were predominantly found with higher  $N_{\text{design}}$  levels. Only two 100-gyrations projects were identified that did not include a binder bump, and all of the 125-gyrations projects included at least one high-temperature binder bump. Therefore, for design traffic levels greater than 3 million ESALs, the majority of state agencies that were included in this data set are using high-temperature binder grades that are stiffer than the recommended climatic grade based on the long-term pavement performance (LTPP) weather station data. Binder bumps are recommended for slow-moving traffic (less than 70 km/hr [44 mph]) and for 20-year design traffic volumes greater than 30 million ESALs (4).

## 4.2 Test Results

There are several important hypotheses for this project:

- Pavement densification is related to traffic.
- The laboratory design density should match the ultimate density in the field.
- Therefore, the laboratory compaction effort should be related to traffic.

Data from the 2000 NCAT Test Track (52) support other hypotheses:

- Binder grade, particularly modified binders, affect the rate of densification.
- Densification (which was the majority of the “rutting” that occurred at the 2000 NCAT Test Track) occurred when the air temperature exceeded approximately 28°C.

Table 4.1. Summary of projects selected.

Project ID	Roadway	NMA5	Avg. Thick., mm	Lift/NMA5	Fine- or Coarse-Graded	Neat or Mod.	LTPP Grade		Grade Used			N <sub>design</sub>
							High	Low	High	Low	High Temp. Bump	
KY-1	CR 1796	9.5	31.2	3	C	N	64	28	64	22	0	50
NE-1	Hwy 8	12.5	39.8	3	F	N	64	28	64	22	0	68
KY-3	CR 1779	9.5	27.1	3	F	N	64	28	64	22	0	75
MI-2	Hwy 50	9.5	39.9	4	F	N	58	28	58	28	0	75
MI-3	Hwy 52	9.5	32.4	3	F	N	58	28	58	28	0	75
UT-1	Hwy 150	12.5	38.7	3	F	M	64	22	64	34	0	75
NE-3	Hwy 8	12.5	51.2	4	F	N	64	28	64	22	0	76
CO-2	Hwy 82	12.5	53.3	4	F	M	64	28	64	28	0	86
CO-5	Hwy 82	12.5	44.3	4	F	M	64	28	64	28	0	86
AL-5	Hwy 167	12.5	33.7	3	C	N	64	16	67	22	0.5	75
FL-1	Davis Hwy	9.5	34.3	4	C	N	64	10	67	22	0.5	86
CO-1	Hwy 9	19.0	49.6	3	F	N	52	34	58	28	1	68
CO-4	Hwy 13	12.5	47.6	4	F	N	58	34	64	28	1	86
NE-2	Hwy 77	19.0	48.7	3	F	N	64	28	64	22	0	96
MO-2	Hwy 65	12.5	78.8	6	C	N	64	22	64	22	0	100
AL-6	Andrews Rd	19.0	33.0	2	F	N	64	16	67	22	0.5	95
AL-2	Hwy 168	12.5	43.1	3	C	N	64	22	67	22	0.5	100
AL-4	Hwy 84	12.5	54.1	4	C	N	64	16	67	22	0.5	100
AL-1	Hwy 157	12.5	43.2	3	C	N	64	16	67	22	0.5	106
IL-1	I-57	9.5	40.5	4	C	M	64	28	70	22	1	90
IL-2	I-64	9.5	44.5	5	C	M	64	22	70	22	1	90
IN-1	Hwy 136	12.5	44.1	4	C	N	58	28	64	22	1	100
KS-1	I-70	9.5	22.3	2	F	M	64	28	70	28	1	100
TN-1	Hwy 171	12.5	34.8	3	F	M	64	22	70	22	1	100
IL-3	I-70	9.5	45.7	5	C	M	64	28	70	22	1	105
NE-4	I-80	12.5	55.2	4	F	M	64	28	70	28	1	109
AL-3	Hwy 80	12.5	38.0	3	C	M	64	10	76	22	2	100
GA-1	Hwy 13	12.5	44.1	4	F	M	64	16	76	22	2	100
KY-2	I-64	9.5	33.9	4	C	M	64	28	76	22	2	100
WI-1	I-94	12.5	36.3	3	C	M	58	28	70	28	2	100
CO-3	I-70	12.5	50.6	4	C	M	64	22	76	28	2	109
IN-2	I-69	12.5	37.1	3	C	N	58	28	64	22	1	125
MI-1	I-75	9.5	35.6	4	C	N	58	28	64	22	1	125
MO-1	I-70	12.5	51.1	4	C	M	64	22	70	22	1	125
MO-3	I-44	12.5	48.4	4	C	M	64	22	70	22	1	125
AR-1	I-40	12.5	53.5	4	C	M	64	16	76	22	2	125
AR-2	I-55	12.5	51.0	4	C	M	64	16	76	22	2	125
AR-3	I-40	12.5	52.8	4	C	M	64	16	76	22	2	125
AR-4	I-30	12.5	56.8	5	C	M	64	16	76	22	2	125
NC-1	I-85	12.5	45.8	4	F	M	64	16	76	22	2	125

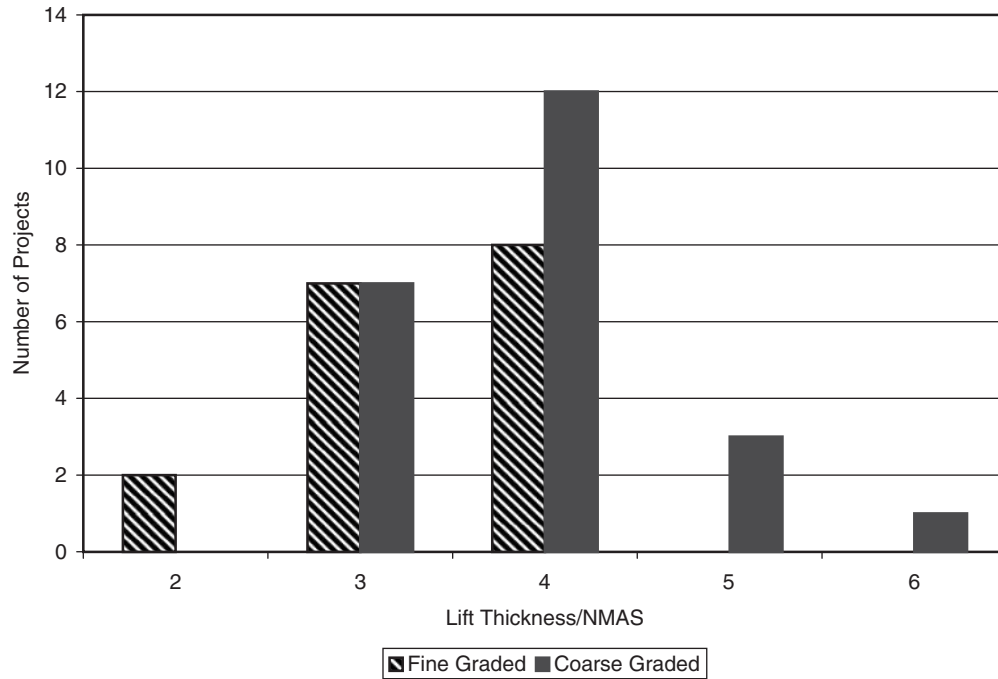


**Figure 4.1. Frequency distribution of lift thickness to NMAS by gradation.**

To address the hypotheses, test results are provided as they relate to the following:

- Evaluation of the validity of the data,
- Estimation of traffic at various sampling intervals,
- Evaluation of densification under traffic,
- Verification of  $N_{\text{design}}$ , and
- Evaluation of the locking point concept.

#### 4.2.1 Comparison of Mixture Data with Design Job Mix Formula

Table 4.2 presents the job mix formula (JMF) gradation and asphalt content for each of the 40 projects. No JMF was available for project MI-1, which was constructed as a warranty project. Three solvent extractions were performed for each sample taken at each project according to AASHTO T164, resulting in six or nine extractions per project depending on whether two or three samples were taken. Washed gradations were performed on the recovered aggregate according to AASHTO T30. The results from the six or nine extractions, representing two or three samples, respectively, were averaged for comparison with the JMF. Figure 4.2 shows the design versus average field gradations for the percentage passing the 2.36-mm sieve. The 2.36-mm sieve is one of the control sieves for Superpave mixes. Lines have been added to the figure representing  $\pm 4.5$  percent from the job mix formula, chosen to represent typical allowed variability for the average of three samples. Five

projects—KY-2, MI-2, NE-2, NE-3, and UT-1—exceeded the 4.5-percent tolerance on the 2.36-mm sieve. Figure 4.3 shows the design versus average field gradations for the percentage passing the 0.075-mm sieve. Lines have been added to the figure representing  $\pm 1.1$  percent of the job mix formula, a typical tolerance for three samples for the percentage passing the 0.075-mm sieve. The average percentage passing the 0.075-mm sieve for 15 projects exceeded the 1.1-percent tolerance. Three projects exceeded the tolerance by a large amount: CO-5, MO-2, and UT-1. Generally, dust content is expected to increase during production. However, only 7 of the 15 projects exceeding the 1.1-percent tolerance exceeded it on the high side. Figure 4.4 shows the design versus average recovered asphalt contents for the field samples. Lines were added to the figure representing  $\pm 0.33$  percent asphalt from the job mix formula, a typical tolerance for the average of three samples. With two exceptions, the 15 projects that fell outside of this range were all on the low side. Solvent extractions were performed, which may produce lower asphalt contents (incomplete recovery) compared with the ignition furnace that many agencies now use. Liquid asphalt is also the most expensive component in HMA; contractors may tend to use liquid asphalt in the least amount allowable by the specifications.

#### 4.2.2 Estimation of Traffic

Initially, traffic at the various sampling intervals was estimated by dividing the design ESALs reported by the

**Table 4.2. Design job mix formula for gradation and optimum asphalt content (AC).**

Project ID	Sieve Size										Design AC
	19 mm	12.5 mm	9.5 mm	4.75 mm	2.36 mm	1.18 mm	0.6 mm	0.3 mm	0.15 mm	0.075 mm	
	Percent Passing										
AL-1	100	96	79	45	32	25	19	11	6	3.4	4.90
AL-2	100	99	86	47	30	20	15	9	5	3.4	5.30
AL-3	100	90	75	47	34	22	14	7	4	3.0	5.00
AL-4	100	93	78	47	34	25	19	12	6	4.3	3.65
AL-5	100	99	87	57	36	25	18	12	7	4.2	5.00
AL-6	99	87	78	66	49	38	25	14	7	4.6	5.25
AR-1	100	96	78	45	31	21	15	11	7	4.8	5.10
AR-2	100	93	83	40	29	22	16	13	9	5.4	4.90
AR-3	100	94	83	46	30	20	15	12	8	5.6	5.50
AR-4	100	95	84	55	37	25	18	11	7	4.6	5.50
CO-1	99	89	78	59	44	31	22	15	11	7.4	6.10
CO-2	100	96	85	60	45	34	24	17	11	7.6	5.50
CO-3	100	94	81	57	35	24	17	13	9	6.4	5.60
CO-4	100	100	89	56	36	27	20	NR	NR	6.5	5.30
CO-5	100	96	85	60	45	34	24	17	11	7.6	5.50
FL-1	100	100	97	65	40	29	23	14	9	5.3	5.70
GA-1	100	98	85	NR	38	NR	NR	NR	NR	5.0	4.80
IL-1	100	100	99	59	32	22	16	9	5	4.3	5.50
IL-2	100	98	90	57	34	22	14	9	7	5.5	5.50
IL-3	100	100	98	57	36	23	14	9	6	4.9	5.33
IN-1	100	100	91	59	39	NR	15	NR	NR	6.0	6.40
IN-2	100	100	95	58	43	NR	20	NR	NR	3.9	5.60
KS-1	100	100	90	54	38	25	17	11	7	5.0	5.70
KY-1	100	100	95	69	41	27	19	10	NR	5.0	5.80
KY-2	100	100	98	67	39	25	18	11	NR	4.5	5.80
KY-3	100	100	94	69	46	31	21	8	5	4.5	5.60
MI-1	NA	NA	NA	NA	NA	NA	NA	NA	NA	NA	NA
MI-2	100	100	100	83	63	40	28	19	10	5.7	6.80
MI-3	100	100	100	80	55	41	31	19	10	5.0	6.20
MO-1	100	97	85	49	29	17	10	6	4	3.1	5.50
MO-2	100	98	83	48	31	18	13	10	8	6.7	6.00
MO-3	100	98	89	52	28	18	12	9	7	5.7	6.00
NC-1	100	95	89	58	43	33	23	14	9	5.4	5.10
NE-1	100	95	90	78	49	30	23	12	NR	3.6	5.50
NE-2	99	90	81	62	41	27	19	11	6	3.4	5.00
NE-3	100	90	81	71	50	32	25	12	NR	3.5	5.30
NE-4	100	91	87	73	51	34	23	14	NR	6.1	4.80
TN-1	100	98	86	58	43	32	22	10	5	4.0	5.10
UT-1	100	100	89	70	62	45	31	15	NR	6.8	5.40
WI-1	100	98	90	62	39	26	17	9	5	3.5	5.10

NA = no data available.

NR = no measurement required.

agency by the design period and then multiplying the result by the elapsed time since construction. This method can produce varying degrees of error early in the life of the pavement depending on the growth rate used for the traffic. Traffic data were updated to reflect the actual traffic levels during the monitoring period. To obtain the best possible traffic estimates, the following procedure was used:

1. Determine average annual daily traffic (AADT) for the year the section was constructed.
2. Determine a growth rate. In some cases, the growth rate was provided by the agency. In other cases, it was fit from

historical AADT data using Equation 1. The growth rate was fit using a least squares approach and Microsoft Excel's Solver routine.

$$AADT_N = AADT_C \times (1+i)^N \quad (1)$$

where:

$AADT_N$  = Predicted AADT after N years,

N = number of years between when the project was constructed and the year of interest,

$AADT_C$  = AADT in the year the pavement was constructed (or repaved), and

i = growth rate.

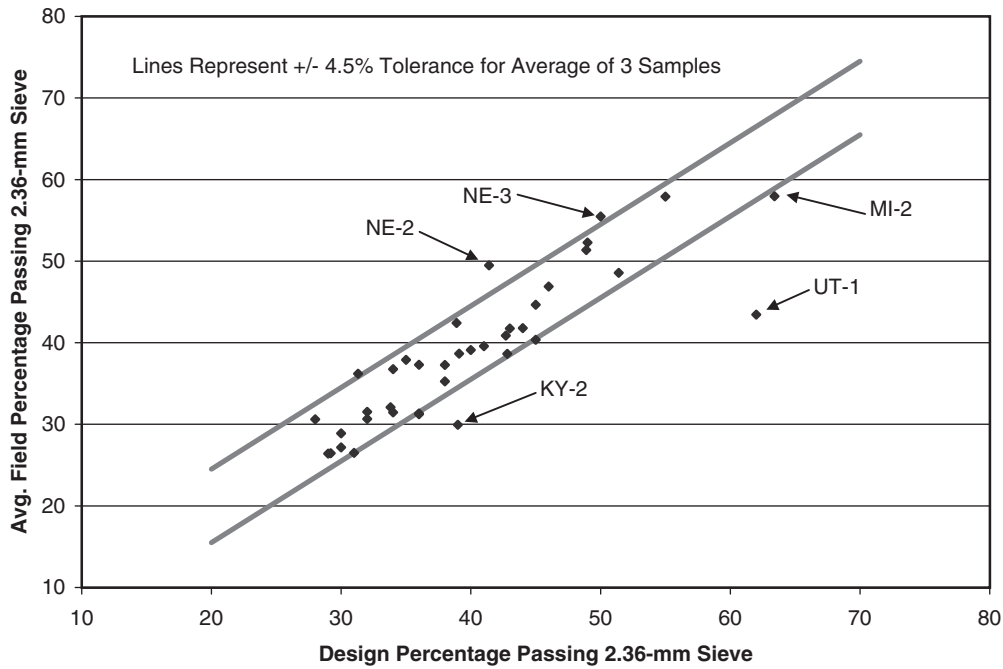


**Figure 4.2. Design versus average field percentage passing the 2.36-mm sieve.**

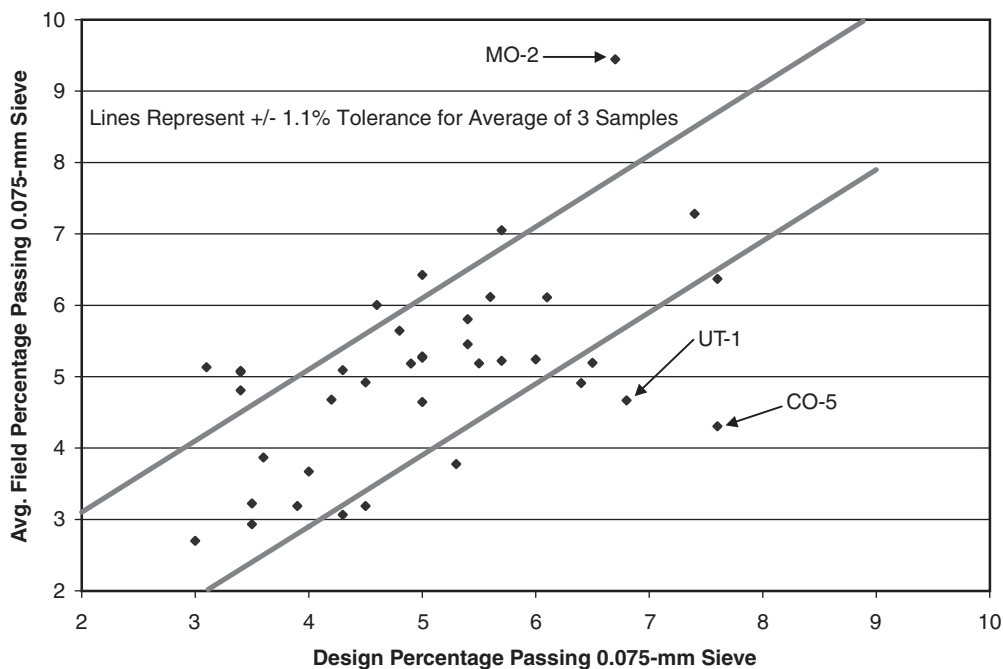


**Figure 4.3. Design versus average field percentage passing the 0.075-mm sieve.**

3. Determine the percentage of truck traffic. Some agencies measure a combined percentage of all trucks. Other agencies track separate percentages for single units (such as cube trucks) and multiple units (such as tractor trailers). Record the percentage of truck or heavy commercial vehicle traffic as either a single percentage or a percentage of single units and multiple units. Multiple units generally represent vehicles with predominantly tandem axles except for the steer axle.

4. Determine one or more truck factors to calculate ESALs from the percentage of heavy vehicles. In some cases, agencies used either a standard factor for all trucks or separate factors for single and multiple units. In other cases, agencies recorded the AASHTO vehicle classification or single and tandem axles load spectra. In the latter cases, a truck factor was calculated by multiplying the percentage of total repetitions in a load group by the corresponding equivalent axle load factor for that load

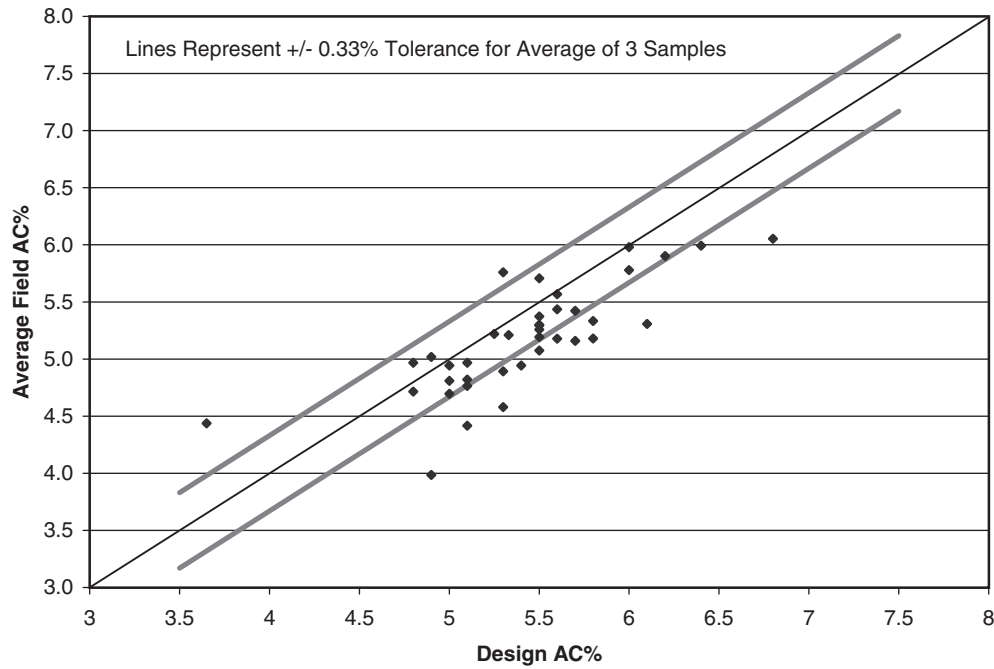


**Figure 4.4. Design versus average field asphalt content.**

group to determine a composite single-unit factor and multiple-unit factor.

5. Determine directional distribution and lane distribution factors. Directional distribution was generally assumed to be 0.5 unless AADT values were for a single direction or unless the agency recommended a specific value. Agency recommendations were used for the lane distribution factor. If no agency recommendations were provided, the recommendations from the AASHTO design guide (53) were used. Table 4.3 shows these recommendations.
6. The accumulated ESALs at each sampling period, as well as the ESALs for the specified design period, are calculated according to Equation 2 or Equation 3.

$$\text{ESAL} = (\text{AADT}_C + \text{AADT}_C \times (1+i)^N) / 2 \times \text{T}\% \times \text{TF} \times \text{D} \times \text{L} \times 365 \times \text{N} \quad (2)$$

$$\text{ESAL} = (\text{AADT}_C + \text{AADT}_C \times (1+i)^N) / 2 \times (\text{ST}\% \times \text{SF} + \text{MT}\% \times \text{MF} + (100 - \text{ST}\% - \text{MT}\%) \times \text{CF}) \times \text{D} \times \text{L} \times 365 \times \text{N} \quad (3)$$

**Table 4.3. Lane distribution factors.**

Number of Lanes in Each Direction	Percentage of 18-kip ESALs in Design Lane
1	100
2	80–100
3	60–80
4	50–75

where:

- AADT<sub>C</sub> = AADT in the year the pavement was constructed (or repaved),
- i = growth rate,
- N = number of years between construction and sampling time,
- T% = percentage trucks,
- TF = truck factor to convert trucks to ESALs,
- D = directional distribution factor,
- L = lane distribution factor,
- ST% = percentage single-unit trucks,
- SF = single-unit truck factor to convert to ESALs,
- MT% = percentage multiple-unit trucks,
- MF = multiple-unit truck factor to convert to ESALs, and
- CF = car factor to convert to ESALs.

Table 4.4 summarizes the factors used to calculate the traffic at various sampling periods. Using the data in Table 4.4, the design traffic at the design interval specified by the agency and the accumulated traffic at each coring interval were calculated. The accumulated traffic at each coring interval was calculated using the actual dates that the coring occurred and not the targeted intervals (e.g., 3 months, 6 months, 1 year, 2 years, and 4 years). The accumulated or design traffic for each of these intervals is shown in Table 4.5.

Figure 4.5 shows a distribution of the 20-year design traffic for the projects sampled. Although the original experimental

**Table 4.4. Factors used to calculate accumulated ESALs at various intervals.**

Project ID	Roadway	Number of Lanes Both Directions	AADT	Growth Rate	% Trucks	% Single Units	% Combo Units	Directional Distribution Factor	Lane Distribution Factor	Combined ESAL Factor	Single-Unit ESAL Factor	Combo-Unit ESAL Factor	Car ESAL Factor	Design Period (Yrs)
AL-1	Hwy 157	4	7,450	2.5%	20.0%			0.5	0.95	0.99				20
AL-2	Hwy 168	2	7,077	2.5%	10.7%			0.5	1.00	0.99				20
AL-3	Hwy 80	4	10,870	2.5%	19.0%			0.5	0.90	0.99				20
AL-4	Hwy 84	2	7,120	2.8%	14.0%			0.5	1.00	0.99				20
AL-5	Hwy 167	2	3,796	2.5%	10.0%			0.5	1.00	0.99				20
AL-6	Andrews Rd	2	1,066	3.5%	2.5%			0.5	1.00	0.99				20
AR-1	I-40	4	31,000	2.4%	27.6%	14.0%	5.3%	0.5	0.90		1.163	3.770	0.0002	20
AR-2	I-55	4	32,000	4.7%	33.7%	19.3%	7.2%	0.5	0.90		1.163	3.770	0.0002	20
AR-3	I-40	4	33,000	5.9%	51.8%	29.7%	11.0%	0.5	0.90		1.163	3.770	0.0002	20
AR-4	I-30	4	22,750	5.1%	47.8%	27.4%	10.2%	0.5	0.90		1.163	3.770	0.0002	20
CO-1	Hwy 9	4	22,193	1.9%		4.3%	0.5%	0.5	0.90		0.249	1.087	0.0030	10
CO-2	Hwy 82	4	15,893	2.0%		4.4%	2.0%	0.5	0.90		0.249	1.087	0.0030	10
CO-3	I-70 Bus.	6	12,581	1.5%		2.6%	0.8%	1.0	0.60		0.249	1.087	0.0030	10
CO-4	Hwy 13	2	2,279	1.8%		15.3%	10.8%	0.5	1.00		0.249	1.087	0.0030	10
CO-5	Hwy 82	4	15,893	2.0%		4.4%	2.0%	0.5	0.90		0.249	1.087	0.0030	10
FL-1	Davis Hwy	5	37,100	3.0%	2.0%			0.5	0.24	0.89				20
GA-1	Buford Hwy	4	13,924	1.6%	8.3%			1.0	0.90	0.97				20
IL-1	I-57	4	17,700	3.0%		2.3%	23.7%	0.5	0.90		0.360	1.320	0.0004	20
IL-2	I-64	4	23,100	3.0%		4.8%	31.6%	0.5	0.90		0.360	1.320	0.0004	20
IL-3	I-70	4	19,900	3.0%		9.1%	34.2%	0.5	0.90		0.360	1.320	0.0004	20
IN-1	US 136	2	14,080	2.5%	2.1%			0.5	1.00	1.30				20
IN-2	I-69	4	30,250	2.3%	27.3%			0.5	0.90	1.30				20
KS-1	I-70	4	5,461	3.5%	27.8%			1.0	0.88	0.69				20
KY-1	CR1796	2	211	5.2%	7.9%			0.5	1.00	0.47				20
KY-2	I-64	4	14,500	2.1%	18.7%			1.0	0.467	1.07				20
KY-3	CR1779	2	262	4.8%	7.7%			1.0	0.50	0.64				20
MI-1	I-75	8	60,500	2.2%	5.0%			1.0	0.80	0.72				20
MI-2	Hwy 50	2	5,500	1.5%	8.7%			0.5	1.00	0.61				20
MI-3	Hwy 52	2	7,900	1.5%	7.6%			0.5	1.00	0.59				20
MO-1	I-70	4	18,500	1.9%	34.9%			0.5	0.95	1.00				20
MO-2	Hwy 65	4	19,400	5.3%	9.8%			0.5	0.95	1.00				20
MO-3	I-44	4	32,750	2.5%	35.8%			0.5	0.95	1.00				20
NC-1	I-85	4	61,346	2.6%		11.0%	24.0%	0.5	0.80		0.300	1.150	0.0000	20
NE-1	Hwy 8	2	700	1.5%		7.7%	12.3%	0.5	1.00		0.250	0.890	0.0000	20
NE-2	Hwy 77	2	2,623	1.4%		4.9%	13.1%	0.5	1.00		0.230	0.910	0.0000	20
NE-3	Hwy 8	2	1,320	0.7%		4.2%	6.8%	0.5	1.00		0.250	0.890	0.0000	20
NE-4	I-80	4	7,506	3.6%		6.2%	52.8%	0.5	0.90		0.140	1.010	0.0000	20
TN-1	Hwy 171	2	8,800	4.87%		7.7%	2.3%	0.5	1.00		0.440	1.080	0.0020	20
UT-1	Hwy 150	2	1,013	3.0%	14.9%	9.5%	4.1%	1.0	1.00	0.55	0.360	0.560	0.0201	20
WI-1	US 45	6	81,428	2.0%	6.8%			1.0	0.40	0.72				20

Blank cells signify that the factor was not used to calculate traffic for the given project.

**Table 4.5. Accumulated ESALs at sampling intervals.**

Project ID	Roadway	3 months	6 months	1 year	2 years	4 years	20-Year Design ESALs
AL-1	Hwy 157	69,600	129,022	263,972	559,853	1,149,977	6,748,142
AL-2	Hwy 168	34,215	69,022	138,140	296,338	611,855	3,610,001
AL-3	Hwy 80	97,881	170,357	346,635	767,236		8,861,352
AL-4	Hwy 84	58,977	101,426	182,573	402,633		4,899,406
AL-5	Hwy 167	18,854	34,981	65,784	149,147		1,809,675
AL-6	Andrews Rd.	1,939	2,960	5,323	9,916	19,907	143,958
AR-1	I-40	690,394	1,131,450	2,110,407	4,619,146	8,120,222	48,726,562
AR-2	I-55	942,469	1,562,429	2,957,818	6,590,986	11,850,476	91,370,805
AR-3	I-40	956,294	1,936,956	4,141,677	9,974,122	18,576,489	170,842,507
AR-4	I-30	578,939	1,201,114	2,596,098	6,261,493	11,603,641	97,890,077
CO-1	Hwy 9	20,866	38,064	68,695	138,927	287,854	756,789
CO-2	Hwy 82	27,654	76,585	91,905	185,961	385,731	1,017,593
CO-3	I-70 Bus.	14,675	26,863	48,805	98,324	202,528	523,624
CO-4	Hwy 13	19,805	36,273	65,592	132,764	274,968	720,911
CO-5	Hwy 82	26,897	75,056	90,370	184,395	384,096	1,017,593
FL-1	Davis Hwy	8,117	16,784	30,420	62,813		811,658
GA-1	Buford Hwy	133,892	287,006	435,998	798,627	1,568,426	8,803,521
IL-1	I-57	252,510	449,723	948,145	1,963,241	3,970,500	26,285,917
IL-2	I-64	445,196	792,900	1,671,661	3,461,359	7,000,327	46,344,297
IL-3	I-70	365,925	699,160	1,541,346	3,256,535	6,648,086	44,466,336
IN-1	US 136	28,199	41,039	73,589	144,256	372,269	1,850,992
IN-2	I-69	688,995	957,471	1,827,656	3,586,718	9,265,105	45,150,555
KS-1	I-70	85,315	227,911	374,505	729,765	1,435,783	10,075,962
KY-1	CR1796	530	819	1,591	3,038	6,357	53,706
KY-2	I-64	181,101	278,340	539,117	1,016,831	2,061,494	12,438,605
KY-3	CR1779	857	1,334	2,608	4,988	10,412	84,028
MI-1	I-75	211,625	419,507	650,039	1,426,667	2,893,187	15,966,398
MI-2	Hwy 50	24,456	32,399	54,261	119,143	240,447	1,250,146
MI-3	Hwy 52	26,258	45,341		132,171	278,594	1,515,200
MO-1	I-70	493,003	884,139	1,306,076	2,541,928	4,778,697	27,546,007
MO-2	Hwy 65	107,389	224,065	349,533	734,786	1,462,700	12,517,675
MO-3	I-44	597,842	1,307,458	2,063,169	4,337,141	8,453,012	53,683,941
NC-1	I-85	692,210	1,427,287	2,889,164	6,040,907	12,565,156	73,918,507
NE-1	Hwy 8	4,441	10,481	16,872	37,057	67,176	383,385
NE-2	Hwy 77	16,728	39,363	63,672	140,411	255,199	1,450,960
NE-3	Hwy 8	4,183	10,424	17,010	37,683	68,179	365,719
NE-4	I-80	166,950	413,599	671,010	1,529,367	2,841,721	20,084,248
TN-1	Hwy 171	25,738	58,918	98,776	207,136	428,119	3,490,393
UT-1	Hwy 150	8,014	14,873	27,347	55,992	122,456	771,982
WI-1	US 45	345,088	494,711	597,614	1,316,468	2,557,478	14,614,748

Blank cells signify that the 4-year data were not collected for the given project.

matrix was not evenly filled because of the availability of projects, Figure 4.5 indicates a good distribution of 20-year design traffic. There are only three projects with fewer than 300,000 ESALs; however, it is expected that there is not a strong relationship between traffic and pavement densification at such low traffic levels. There are 14 projects with design traffic between 3 million and 30 million ESALs. Under AASHTO M 323, all projects with a design traffic level between 3 million and 30 million ESALs should be designed with an  $N_{\text{design}}$  of 100 gyrations (4). The maximum 20-year design traffic in the SHRP  $N_{\text{design}}$  experiment was 32.1 million ESALs (1). Nine projects in this study had 20-year design traffic in excess of 30 million ESALs.

### 4.2.3 Pavement Densification

The in-place density of HMA may be the single factor that most affects the performance of a properly designed mixture (54, 55). A mediocre mix that has been well constructed with good in-place air voids will often perform better than a good mix that has been poorly constructed (54). In-place density between 92 percent and 97 percent of  $G_{\text{mm}}$  for surface mixes passing through or above the Superpave-defined restricted zone will generally provide good performance (55). To limit permeability concerns, in-place density more than 93 to 95 percent of  $G_{\text{mm}}$  may be required for larger nominal maximum aggregate size mixtures, stone mastic asphalt, or coarse-

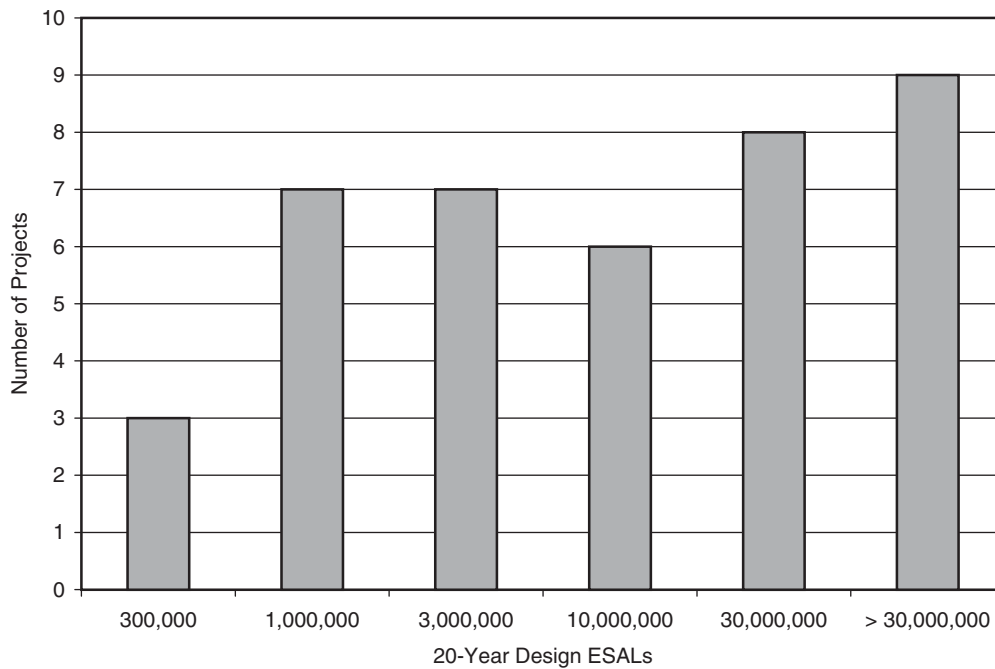


**Figure 4.5. Distribution of 20-year design traffic.**

graded Superpave mixtures (56). In-place air voids that are too high may result in permeability to water and excessive binder oxidization, resulting in moisture damage, cracking, or raveling (55, 57, 58). In-place density in excess of 97 percent of  $G_{mm}$  may result in permanent deformation or loss of skid resistance (59). Although the use of the ultimate pavement density has been questioned as a parameter to define  $N_{design}$  (44), it is clear for the reasons described above that the ultimate pavement density must be considered when determining the laboratory compaction effort. Table 4.6 summarizes the average in-place densities for the projects at each of the sampling intervals through 2-years; the complete data are presented in the Appendix Tables B.41 through B.80.

#### 4.2.3.1 As-Constructed Density

The average in-place, as-constructed density for the 40 projects was 91.6 percent. Figure 4.6 shows a cumulative frequency distribution of the average in-place density for the 40 projects at the time of construction. From Figure 4.6, it is evident that 55 percent of the projects had in-place densities that were less than 92 percent of  $G_{mm}$ , and 78 percent of the projects had in-place densities that were less than 93 percent of  $G_{mm}$ . This indicates that the in-place densities of the majority of the projects were less than desired. There may be a number of reasons for the as-constructed, in-place densities being less than desired, including:

- State agency specifications,
- The compactability of the mix,

- The compaction effort or method of compaction used by the contractor, or
- A combination of these factors.

An ANOVA was conducted using the General Linear Model (GLM) to examine factors that may have affected the as-constructed density. The two or three samples from each project were used as replicates, and each sample was represented by an average of three cores. Agency, gradation (coarse or fine), high-temperature PG, lift-thickness-to-NMAS ratio, and 2000  $N_{design}$  level were considered as factors. The 2000  $N_{design}$  level is the  $N_{design}$  rounded to the levels adopted in 2000 (50, 75, 100, and 125). The factor inputs are summarized in Table 4.1, presented previously. There were insufficient replicates to evaluate interactions, particularly considering the 16 levels of agency. Two factors were significant at the 95-percent confidence level: agency and  $N_{design}$ . The fitted means for the main effects indicated very low in-place density resulting from mixes with an  $N_{design}$  of 50 gyrations. Only project KY-1 was designed at 50 gyrations. The average as-constructed density for KY-1 was 85.5 percent. There were no in-place density requirements in the specifications for KY-1. Therefore, this project was eliminated from the data set. The ANOVA was re-run, thereby resulting in agency being the only significant factor ( $p = 0.000$ ). Examination of the main effects indicated that three agencies achieved particularly good as-constructed densities: Colorado, Missouri, and Georgia. As noted previously, Colorado DOT uses 100-mm diameter SGC molds, which tends to result in lower sample densities and therefore higher asphalt contents that may aid

**Table 4.6. Average in-place densities for field projects.**

Project ID	Roadway	Average In-Place Density, Percent $G_{mm}$				
		Construction	3 months	6 months	1 Year	2 Years
AL-1	Hwy 157	88.7	93.2	93.6	93.0	93.9
AL-2	Hwy 168	88.3	90.3	90.2	90.2	91.8
AL-3	Hwy 80	89.7	92.8	93.2	93.3	93.6
AL-4	Hwy 84	88.4	92.8	93.1	92.6	94.3
AL-5	Hwy 167	89.7	93.6	93.8	93.1	94.6
AL-6	Andrews Rd	91.8	93.1	92.7	93.1	93.3
AR-1	I-40	92.0	93.1	93.5	94.1	94.2
AR-2	I-55	89.4	90.9	91.4	91.8	91.8
AR-3	I-40	91.5	94.6	94.8	94.8	94.7
AR-4	I-30	90.9	94.2	93.5	94.5	94.5
CO-1	Hwy 9	93.8	96.9	96.5	97.2	98.1
CO-2	Hwy 82	94.7	96.6	96.6	96.9	97.1
CO-3	I-70	93.5	94.6	96.0	95.6	95.7
CO-4	Hwy 13	93.7	93.3	92.8	94.2	94.2
CO-5	Hwy 82	91.6	93.6	93.7	94.2	93.8
FL-1	Davis Hwy	91.8	94.2	94.8	94.3	95.2
GA-1	Buford Hwy	95.0	95.7	95.8	96.0	96.5
IL-1	I-57	91.0	93.9	93.8	94.2	94.4
IL-2	I-64	91.8	94.2	94.1	94.4	95.2
IL-3	I-70	92.2	94.3	93.9	94.4	94.5
IN-1	US 136	91.3	90.3	90.3	62.3	93.5
IN-2	I-69	91.4	90.7	91.7	94.7	94.1
KS-1	I-70	89.9	91.2	92.1	93.6	93.6
KY-1	CR1796	85.5	87.3	86.7	87.7	88.5
KY-2	I-64	92.2	93.2	93.3	93.9	94.1
KY-3	CR1779	92.6	93.1	93.7	94.3	94.2
MI-1	I-75	91.3	92.1	92.8	93.4	94.8
MI-2	Hwy 50	93.1	95.2	96.1	96.8	96.8
MI-3	Hwy 52	93.0	93.7	94.5	NR <sup>1</sup>	96.5
MO-1	I-70	93.4	96.4	95.6	95.8	96.5
MO-2	Hwy 65	92.6	94.2	92.7	94.4	95.1
MO-3	I-44	93.5	94.4	94.3	95.3	95.6
NC-1	I-85	90.1	92.8	91.7	93.0	93.4
NE-1	Hwy 8	92.6	95.4	95.5	95.3	95.7
NE-2	Hwy 77	93.0	95.2	95.0	95.3	95.7
NE-3	Hwy 8	91.0	94.8	95.1	95.0	95.4
NE-4	I-80	92.2	94.9	95.2	96.7	97.2
TN-1	Hwy 171	91.1	93.1	93.1	94.1	94.3
UT-1	Hwy 150	91.9	93.5	93.2	NR <sup>2</sup>	93.7
WI-1	US 45	92.4	93.8	93.8	94.4	94.3

<sup>1</sup>1-year cores not taken.

<sup>2</sup>Section overlaid with plant-mix seal coat, and NCAT research engineer elected not to take 1-year cores.

in field compaction (42). All of the Colorado DOT projects used crushed gravel for the coarse aggregate, which may be easier to compact than crushed stone aggregate. Although many agencies have switched (or switched back) to density specifications based on cores since the implementation of Superpave, Colorado DOT uses the nuclear gauge to determine in-place density. Gauges are calibrated to cores at the beginning of the project, and density is monitored with additional cores throughout the project. Both the contractor and the agency conduct nuclear density tests. Georgia DOT adjusts the asphalt content of a mixture in the field to ensure in-place density requirements are met.

The main effects for lift thickness to NMASS ratio indicated some unexpected trends when agency was included as a factor. It was believed that the unexpected trends may have

been due to interactions that could not be analyzed with the replicates available. Therefore, the ANOVA was rerun as described previously without using agency as a factor. Only high-temperature PG was significant ( $p = 0.000$ ); however, this significance is caused by the PG 67-22, which was only used by two agencies, one of which consistently had low as-constructed densities. The fitted model is poor ( $R^2 = 0.37$ ) without agency as a factor, but good ( $R^2 = 0.67$ ) with agency as a factor.

The main effects plot for the fitted means is shown in Figure 4.7. With the exception of PG 67, the trends are as expected: increasing density with increasing lift-thickness-to-NMASS ratio, decreasing density with increasing  $N_{design}$  level, and increasing density with fine-graded as compared to coarse-graded mixes. As noted previously, coarse-graded

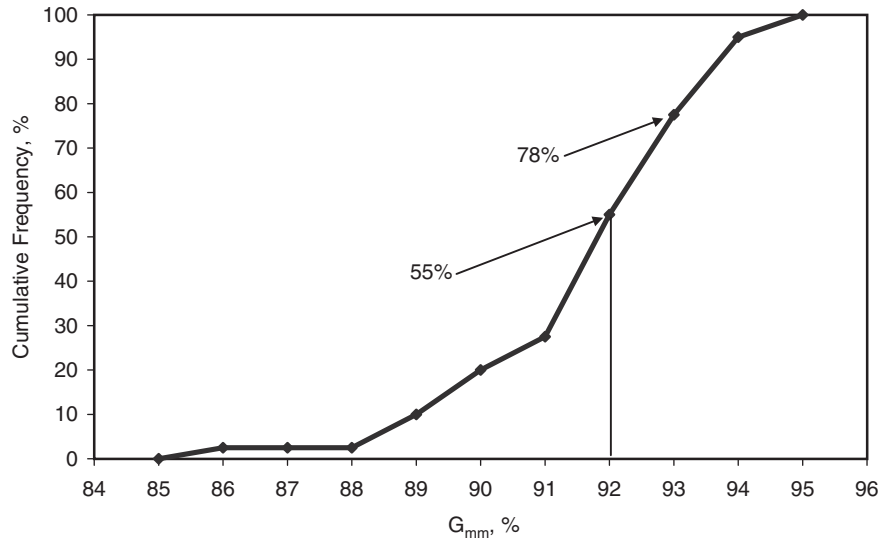


**Figure 4.6. Cumulative frequency distribution of as-constructed, in-place density.**

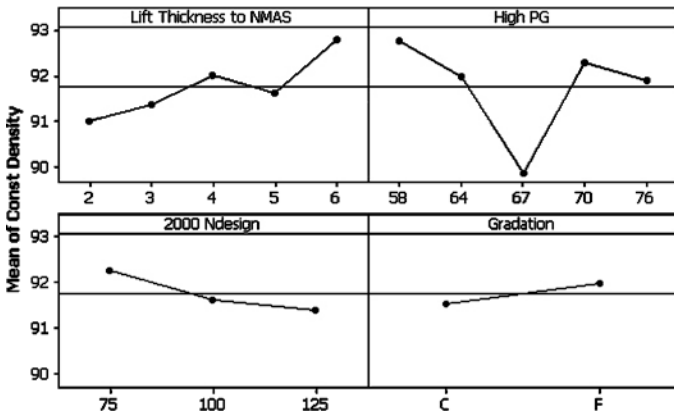


**Figure 4.7. Main effects plot for factors affecting as-constructed density.**

mixes tend to require higher in-place density to be impermeable to water (56).

**4.2.3.2 Densification with Time**

Figure 4.8 shows a cumulative frequency plot for in-place density for the sampling periods through 2 years. From Figure 4.8, it is apparent that the majority of the densification (63 percent) occurs in the first 3 months after construction. There is little if any difference between the 3-month and 6-month in-place densities, most likely because projects constructed during the summer would be experiencing cooler weather 3 to 6 months after construction. This finding matches the findings from the 2000 NCAT Test Track, which indicated that little densification occurred during the winter months (52). The in-place density representing the 50-percent frequency increased by

0.8 from 93.6 percent to 94.4 percent between 6 months and 1 year, and then only by 0.2 percent to 94.6 percent between 1 year and 2 years.

Since there was a slight increase in density between the 1-year and 2-year sampling intervals, it was impossible to know if the pavements had reached their ultimate density after 2 years. The literature suggests that pavements reach their ultimate density after 2 to 3 years of traffic (11, 17, 18, 24), but could densify for a longer period of time (23, 25). Since the goal of this project was to determine the N<sub>design</sub> gyrations that produced samples with the same density as the ultimate density on the roadway, it was decided to extend the monitoring of the in-place density and take an additional set of cores after 4 years of traffic. The pavement condition survey conducted at the 4-year interval would also provide a better indication of the long-term performance of the pavement. Table 4.7 compares the 2-year and 4-year pavement densities for each project.

**4.2.3.3 Determination of Ultimate Density**

The average in-place density for all of the projects after both 2 and 4 years was 94.6 percent. Two tests were conducted to compare the 2-year and 4-year pavement densities, Student’s t-test, and a paired Student’s t-test. In addition, an F-test was conducted to compare the sample variances prior to running the Student’s t-test to determine whether the model with equal or unequal sample variances should be used. The t-test was used to compare the population means:

- H<sub>0</sub>: average 2-year density = average 4-year density, and
- H<sub>1</sub>: average 2-year density ≠ average 4-year density.

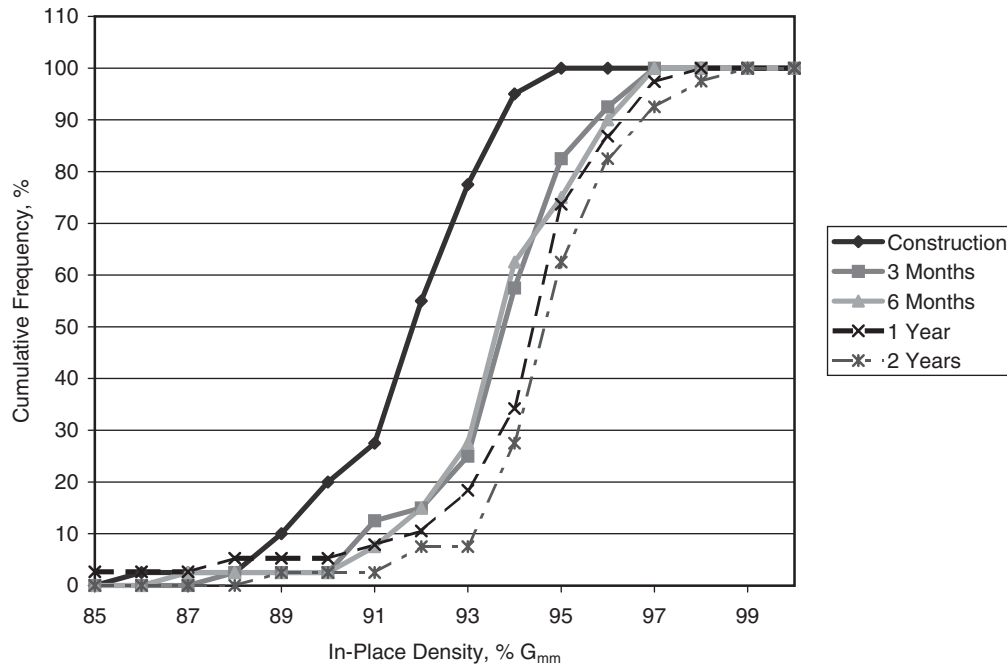


**Figure 4.8. Cumulative frequency plot for in-place density by sampling period.**

The paired t-test examined the difference between the 2-year and 4-year density at each core site. In three cases—KY-1, NE-2, and NE-3—the F-test indicated that the sample variances were different between the 2-year and 4-year densities. The Student's t-test for unequal sample variances was used for these sites. The two-tail p-value is reported in all sites.

The 4-year density was less than the 2-year density in 15 of 35 cases. If the 2-year and 4-year densities are not different (e.g., the 2-year density is the “ultimate” density), then lower values would be expected because of testing variability. The analyses indicate that the paired t-tests were significantly different ( $\alpha = 0.05$ ) in eight cases, and the average 4-year density was higher in six of those eight cases. However, the paired t-test could be subject to differences due to variances in the longitudinal density of the pavement, although generally pavement density is believed to be less variable in the longitudinal direction than in the transverse direction over short distances. The t-test to compare population means was only significantly different ( $\alpha = 0.05$ ) in one case, TN-1. The average 4-year in-place density (93.6 percent) for TN-1 was less than the average 2-year density (94.3 percent). One possible explanation for this could be the onset of moisture damage. Based on these analyses, it is concluded that the ultimate density was achieved after 2 years of traffic.

#### 4.2.3.4 Factors Affecting Pavement Densification

Factors affecting pavement densification are of interest in this study. Figures 4.9 through Figure 4.11 show typical

examples of the observed pavement densification with traffic. Figure 4.9 shows the densification of CO-4. CO-4 is a relatively low-volume pavement with 20-year design traffic less than 1 million ESALs and a posted speed limit of 55 mph. Figure 4.9 indicates that CO-4 shows little densification with traffic. It should be noted that CO-4 was compacted to a relatively high as-constructed density (93.7 percent).

Figure 4.10 shows the densification of AL-1. AL-1 had a significant increase in density in the first 3 months after construction, after which time the rate of densification levels off. The 20-year design traffic for AL-1 is 6.7 million ESALs. AL-1 was compacted to a low as-constructed density. AL-1 rapidly densified to an acceptable level in the first 3 months, and relatively little densification was observed after the first 3 months. This may be due to an increased rate of binder oxidation due to the low initial density.

Figure 4.11 shows the densification of MI-1. MI-1 is a high-volume Interstate with a 20-year design traffic level of 16.0 million ESALs. The higher traffic volume appears to cause a steady rate of densification up until the 2-year sampling interval. The as-constructed density of MI-1 was close to typical specifications.

The examples in Figures 4.9 through 4.11 demonstrate some of the apparent effects that initial density and traffic can have on densification. These effects will be investigated in greater detail in Section 4.2.4.

Since the largest percentage of pavement densification occurred in the first 3 months, the factors affecting the 3-month densification were investigated. The 3-month densification was calculated as the difference between the 3-month

**Table 4.7. Comparison of 2-year and 4-year densities.**

Project	Roadway	% G <sub>mm</sub>		Paired t-test		Population t-test	
		2-Year	4-Year	p-value	Significant? (α = 0.05)	p-value	Significant? (α = 0.05)
AL-1	Hwy 157	93.9	94.3	0.0886	No	0.2977	No
AL-2	Hwy 168	91.8	91.7	0.8968	No	0.9219	No
AL-3	Hwy 80	93.6					
AL-4	Hwy 84	94.3					
AL-5	Hwy 167	94.6					
AL-6	Andrews Rd	93.3	93.6	0.1202	No	0.4757	No
AR-1	I-40	94.2	94.2	0.2629	No	0.6918	No
AR-2	I-55	91.8	92.1	0.0941	No	0.4186	No
AR-3	I-40	94.7	94.6	0.7531	No	0.8442	No
AR-4	I-30	94.5	94.7	0.0894	No	0.3701	No
CO-1	Hwy 9	98.1	97.7	0.1063	No	0.3565	No
CO-2	Hwy 82	97.1	96.8	0.0196	Yes	0.4763	No
CO-3	I-70	95.7	95.7	0.6190	No	0.8492	No
CO-4	Hwy 13	94.2	94.4	0.4504	No	0.4613	No
CO-5	Hwy 82	93.8	93.3	0.0645	No	0.3068	No
FL-1	Davis Hwy	95.2					
GA-1	Buford Hwy	96.5	96.3	0.3201	No	0.6385	No
IL-1	I-57	94.4	94.6	0.2052	No	0.5548	No
IL-2	I-64	95.2	95.3	0.0265	Yes	0.4559	No
IL-3	I-70	94.5	94.6	0.2154	No	0.5249	No
IN-1	US 136	93.5	94.1	0.3286	No	0.3541	No
IN-2	I-69	94.1	94.8	0.0735	No	0.2087	No
KS-1	I-70	93.6	93.0	0.1085	No	0.2985	No
KY-1	CR1796	88.5	87.7	0.5281	No	0.4321	No
KY-2	I-64	94.1	94.4	0.0277	Yes	0.4279	No
KY-3	CR1779	94.2	94.4	0.4772	No	0.7774	No
MI-1	I-75	94.8	94.4	0.0944	No	0.1827	No
MI-2	Hwy 50	96.8	97.4	0.0091	Yes	0.3408	No
MI-3	Hwy 52	96.5	96.8	0.0279	Yes	0.1508	No
MO-1	I-70	96.5	NR <sup>1</sup>				
MO-2	Hwy 65	95.1	95.0	0.8276	No	0.8836	No
MO-3	I-44	95.6	95.5	0.6249	No	0.7958	No
NC-1	I-85	93.4	93.9	0.0062	Yes	0.0660	No
NE-1	Hwy 8	95.7	95.5	0.3002	No	0.6646	No
NE-2	Hwy 77	95.7	95.9	0.1870	No	0.3923	No
NE-3	Hwy 8	95.4	95.2	0.6303	No	0.6330	No
NE-4	I-80	97.2	97.4	0.0268	Yes	0.1964	No
TN-1	Hwy 171	94.3	93.6	0.0056	Yes	0.0427	Yes
UT-1	Hwy 150	93.7	93.6	0.7387	No	0.7850	No
WI-1	US 45	94.3	94.2	0.6521	No	0.8412	No

<sup>1</sup>Incorrect layer tested on 4-year cores (Novachip added between 2 and 4 years). Blank cells signify that the 4-year data were not collected for the given project.

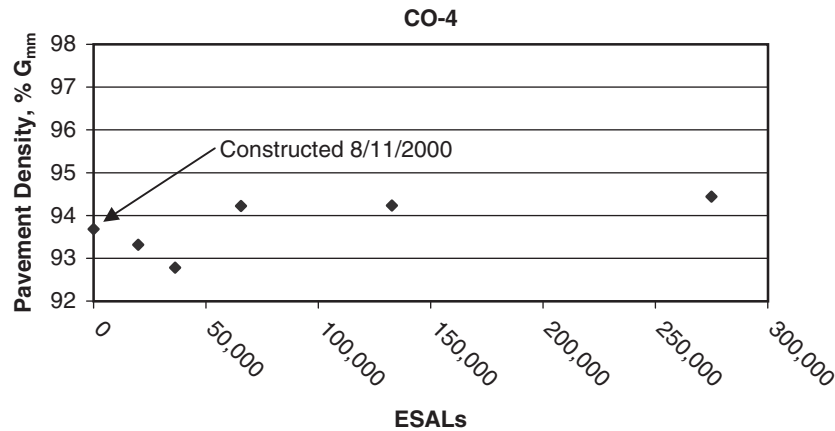


**Figure 4.9. Densification of CO-4 with traffic.**

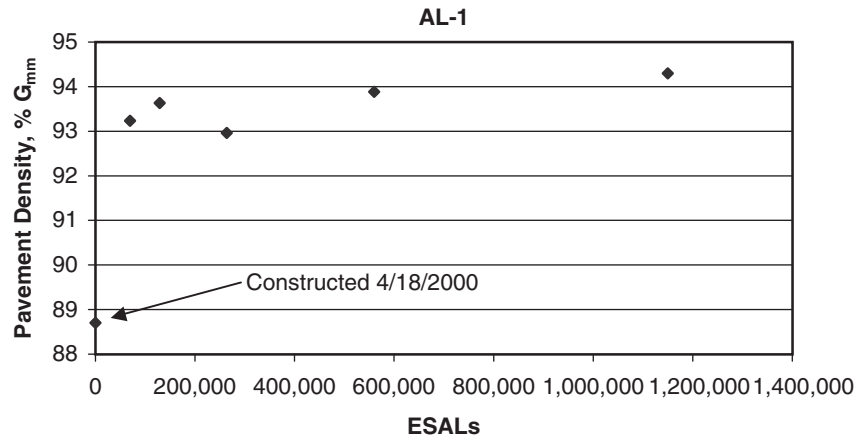


Figure 4.10. Densification of AL-1 with traffic.

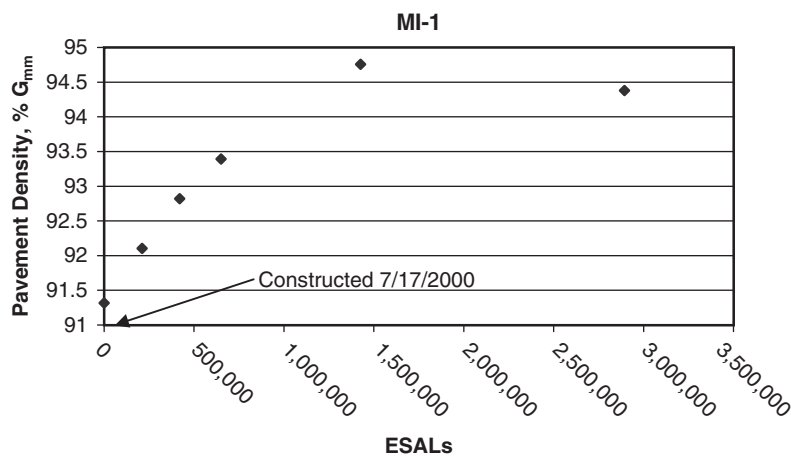


Figure 4.11. Densification of MI-1 with traffic.

and as-constructed in-place density. An ANOVA was conducted using the GLM to examine factors that may have affected the densification after 3 months. The two or three samples from each project were used as replicates, with each sample represented by the average of three cores. Gradation, either high-temperature PG or bump in high PG, lift-thickness-to-NMAS ratio, 2000  $N_{design}$  level, and month of construction were considered as factors. 2000  $N_{design}$  level is the  $N_{design}$  level rounded to the levels adopted in 2000 (50, 75, 100, and 125).

High-temperature PG bump was considered an alternative to high PG to better account for climatic differences between the sites. Month of construction was added based on speculation that pavements constructed in the fall would densify less than pavements constructed in the summer.

The factor inputs are summarized in Table 4.1, presented previously. The results of the analysis using high-temperature PG bump are shown in Table 4.8. High-temperature PG bump ( $p = 0.016$ ) and month of construction ( $p = 0.000$ )

Table 4.8. ANOVA (GLM) results for 3-month densification.

Source	Degrees of Freedom	Adjusted Sum of Squares	Adjusted Mean Squares	F-statistic	p-value	Significant? ( $\alpha = 0.05$ )
Lift Thickness to NMAS	4	4.910	1.227	0.86	0.490	No
High-Temperature PG Bump	3	16.491	5.497	3.86	0.012	Yes
2000 $N_{design}$	3	1.257	0.419	0.29	0.830	No
Month of Construction	6	59.405	9.901	6.95	0.000	Yes
Gradation	1	0.437	0.437	0.31	0.581	No
Error	92	131.141	1.425			
Total	109					

were identified as significant factors at  $\alpha = 0.05$ . A plot of the main effects is shown in Figure 4.12. The trends are generally as expected. There is a slight trend for increasing densification with increasing lift thickness to NMAS, except for the 6:1 ratio. Recall that there is only one project, MO-2, constructed at the 6:1 ratio. Densification decreases with high-PG bump (1 grade bump would correspond to a 6°C increase in high-temperature PG), except for the half-grade bump resulting from the use of PG 67-22. As discussed previously, PG 67-22 was used by only two agencies, one of which tended to have low as-constructed densities in the projects evaluated. Projects with low as-constructed densities would be expected to densify more under traffic.  $N_{design}$  is neutral except when it is 50. As noted previously, only one 50-yr project, KY-1, was sampled. It showed a very low as-constructed density. This finding suggests that the current tiered Superpave design system—with differing binder grades, aggregate properties, and  $N_{design}$  levels—generally accounts for the effect of varying traffic. Fine mixes appear to densify slightly more than coarse mixes. The most interesting effect may be that of month of construction. In Figure 4.12, the numerical month is shown on the x-axis (e.g., April = 4). It appears that projects constructed between April (4) and June (6) densified the most, approximately 1 percent more than projects constructed in July (7) and August (8). The fact that projects constructed in April (4) densified slightly less than the projects constructed in June (6) most likely illustrates the effect of binder aging because the projects constructed in April (4) would have aged slightly before the hottest summer weather. As expected, the projects constructed in September (9) and October (10) appear to have densified approximately 1 to 2 percent less than the projects constructed in mid-summer.

The ANOVA was rerun using the amount of densification after 2 years of traffic as the response variable. High-PG bump ( $p = 0.007$ ) was still significant at  $\alpha = 0.05$ . Month of construction ( $p = 0.068$ ) was not significant at  $\alpha = 0.05$ , but was significant at  $\alpha = 0.10$ . Figure 4.13 illustrates the fitted means of the effect. The figure indicates that month of construction has a strong influence on the long-term densification of a project, with approximately a 2-percent change in densification between pavements constructed in May (5) and pavements constructed in October (10). This finding emphasizes the need to obtain good compaction during late-season paving. Compaction requirements cannot be waived with the assumption that the pavement will densify to an acceptable level with the onset of hot weather the following year.

#### 4.2.3.5 Pavement Densification at the 2000 NCAT Test Track

Data from the 2000 NCAT Test Track was analyzed in addition to the data from the field projects. The NCAT Test Track offered a unique opportunity to study pavement densification and its relationship to the number of design gyrations, because all of the sections received the same traffic, had the same base and subgrade support, and were exposed to the same climatic conditions. Thirty-two of the test track sections were designed using Superpave and are included in the following analysis. The 32 sections represent a range of aggregate types, NMAAS, and gradations.

One of the objectives of the work at the track was to evaluate densification of HMA. Cores for evaluating densification were taken at various traffic levels from the left wheel path of the last 25 ft of each section. When the test track was constructed, paving was carried past the end of the section,

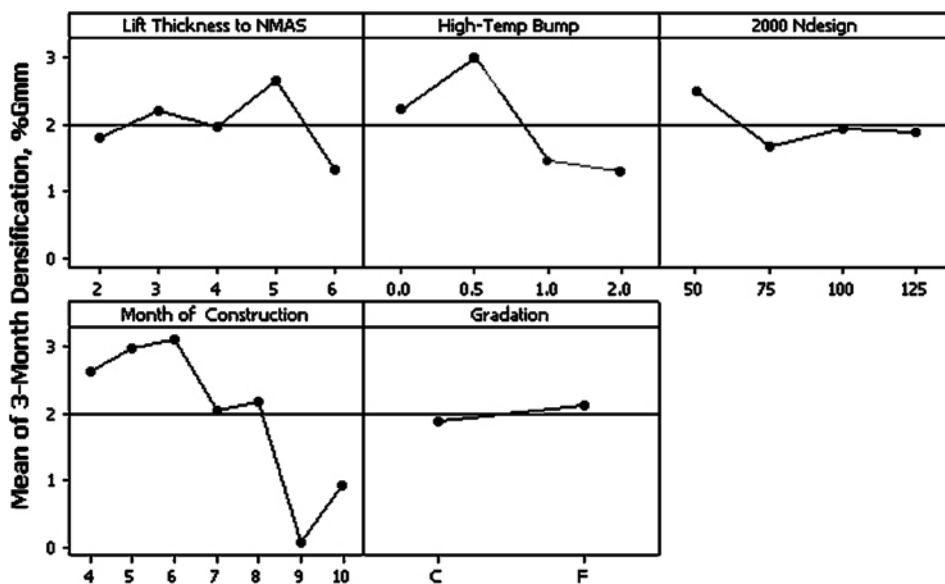
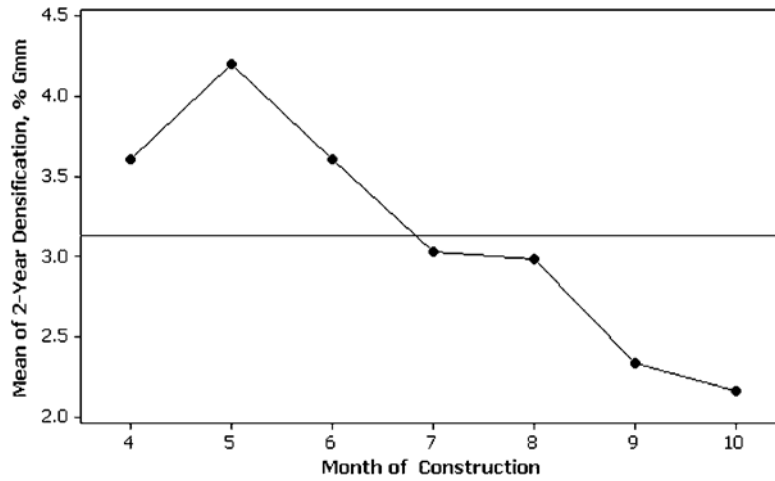


Figure 4.12. Main effects plot for factors affecting 3-month densification.



**Figure 4.13. Main effects plot for month of construction on 2-year densification.**

and the pavement was cut back prior to constructing the next section. In this manner, the last 25 ft of the section should be a representative mix. Initially, traffic began in September 2000 with only one truck in operation. Three trucks were operational in November 2000, and traffic was fully implemented (with four trucks) in February 2001. For the first 3 months, cores were taken on a monthly basis; later, cores were taken quarterly.

The cores are sawed into their respective layers, and the bulk-specific gravity of each layer is determined using AASHTO T166. Density of samples having more than 2-percent water absorption was determined using the Corelok device. In-place air voids were calculated using the

construction maximum specific gravity values. Figure 4.14 shows the average test track pavement density as a function of ESALs for the Superpave sections through the completion of 10 million ESALs in December 2002. The figure indicates that the initial construction densities were slightly lower for the PG 76-22 surface layers than for the other layers. In both the PG 67-22 and PG 76-22 sections, the construction densities were less for the upper lift than for the lower lift. A second-order polynomial was fit to the data for each binder grade/lift combination.

The data seem to indicate distinct rates of densification for each binder grade/lift combination related to time after construction and month. There appears to be an initial

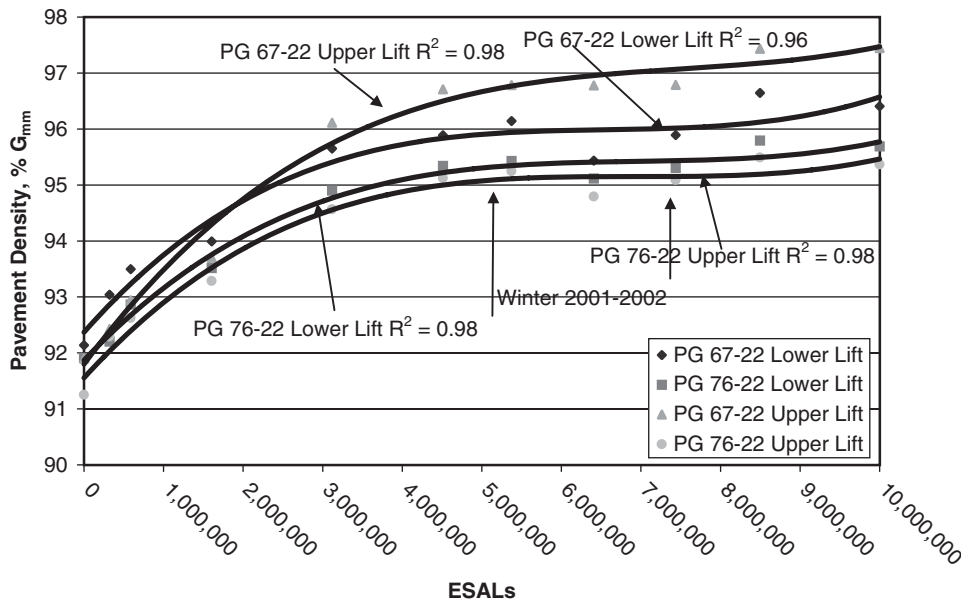


**Figure 4.14. Average test track pavement densification (52).**

seating of the mix between the first and third data points taken in September and December of 2000, respectively. The average pavement density appears to continue to increase from December 2000 (third data point) through October 2001 (data point at approximately 4.5 million ESALs). There is little increase in pavement density between October 2001 and June 2002 (data point at approximately 7.5 million ESALs). In fact, the average density for all but the PG 67-22 upper lift sections appears to decrease in March 2002 (data point at approximately 6.5 million ESALs). The change in density during the summer of 2002 (7.5 to 8.5 million ESALs) is similar to that which occurred during the summer of 2001 (3.0 to 4.5 million ESALs). A slight decrease in density was observed between September and December 2002, with the exception of the PG 67-22 upper lifts, which increased slightly.

There appears to be a significant difference in the rate of densification based on binder grade. As expected, the sections with the softer binder, PG 67-22, densified faster. This was true for both the upper and lower lifts. Further, it appears that for the PG 67-22 sections, the lower lift, which was 50 mm below the surface of the pavement, did not densify as fast as the surface lift did. The difference in density was approximately 1 percent from approximately 4 million ESALs through approximately 10 million ESALs. The difference was not apparent prior to 4 million ESALs because the lower lifts were constructed at a higher initial density. Blankenship (34) did not find a relationship between traffic and pavement densification for layers deeper than 100 mm from the pavement surface. Based on the reduced vertical pressure calculated using Boussinesq theory, Brown and Buchanan (2) recommended that  $N_{design}$  be reduced by 28 percent or approximately one gyration level for layers deeper than 100 mm from the pavement surface. Brown et al. (52) also note that permanent deformation (and densification) essentially stopped when the air temperature was less than 28°C. Important findings from the densification of the 2000 NCAT Test Track related to this study include the following (52):

- Modified binders (2 high-PG bumps) rutted approximately 60 percent less than unmodified (0.5 high-PG bump) based on an average rut depth after 10 million ESALs of 1.7 mm for the modified mixes and 4.1 mm for the unmodified mixes. Densification was reduced by 25 percent for the surface mixes containing modified binders, with an average reduction in air voids of 4.1 percent for the modified mixes and 5.6 percent for the unmodified mixes.
- The densification of pavement layers 50 mm from the pavement surface was approximately 1 percent less than the densification of surface layers.

#### 4.2.4 Determination of $N_{design}$ to Match Ultimate In-Place Density

Four different analyses were performed to relate  $N_{design}$  to the ultimate in-place density. First, regressions were performed between the accumulated traffic after 2 years and the predicted  $N_{design}$  values. The accumulated traffic after 2 years was selected because the pavements were determined to have reached their ultimate density after 2 years of traffic. The data were subdivided and potential outliers examined in an attempt to improve the relationship. Second, regressions were performed between the accumulated ESALs at each of the sampling intervals (3 months, 6 months, 1 year, 2 years, and 4 years) and the predicted gyrations to match the in-place density at each of those intervals. Third, models were developed to predict  $N_{design}$ , which accounted for as-constructed density, high-temperature PG, and traffic. Fourth, the ultimate in-place density was compared with the density at the agency-specified  $N_{design}$ . The results of these analyses are described in the following sections.

##### 4.2.4.1 Predicted $N_{design}$ Versus 2-Year Traffic

The number of gyrations necessary to obtain the in-place density after 2 years of traffic or ultimate density was determined by performing a linear regression between the estimated sample density at a given number of gyrations and the log gyrations. This regression was done both for (a) the average densities and specimen heights for a project as well as (b) the average density and sample height for each sample within a project. Each sample had measurements from three SGC specimens. The specimen heights and densities at 8, 25, 50, 75, 100, 125, and 160 gyrations were used for the regression to determine the slope and offset. The specimen heights and densities at 8, 25, 50, 75, and 100 gyrations were from the SGC specimens compacted to 100 gyrations, while the specimen heights and densities at 125 and 160 gyrations were from the SGC specimens compacted to 160 gyrations. It should be noted that the SGC specimen densities at 100 and 160 gyrations were measured, but the other specimen densities were estimated using Equation 4.

$$\text{Density at Gyration } n = \text{Density at } N_{\text{maximum}} \times \frac{\text{Height at } N_{\text{maximum}}}{\text{Height at Gyration } n} \quad (4)$$

Some of the literature (39, 40, 46) discusses the errors in backcalculation of sample density. Because of the scope of the project, backcalculation was unavoidable. Once the slope and offset were determined, the number of gyrations to match the ultimate density could be calculated. This was done for both

the Pine and Troxler SGCs. Figure 4.15 shows a plot of the average (for each project)  $N_{\text{design}}$  to match the 2-year in-place density for each SGC versus estimates of the accumulated traffic after 2 years. The figure is shown with an arithmetic scale to better show the difference in predicted gyrations between the Pine and Troxler SGCs. The best fit line in the figure is a power model that would produce a straight line on a log-log plot. The  $R^2$  values indicate a weak correlation between log 2-year ESALs and log-predicted gyrations. There appear to be numerous potential outliers. All of the potential outliers are 9.5-mm NMAS mixes that occurred with the Troxler compactor. It also appears that the predicted gyrations for the Troxler compactor are approximately 20 gyrations higher than the predicted gyrations for the Pine compactor.

Significant efforts have been made to study the differences in sample density produced by different models and units of gyratory compactors. One influencing factor that has been identified is the dynamic internal angle (DIA) of gyration. The internal angle of gyration can be measured using a device called the dynamic angle verification kit (DAVK). FHWA proposed a DIA of  $1.16 \pm 0.03$  degrees (60). In a study conducted for Alabama DOT, Prowell et al. (50) determined that a change of DIA of 0.1 degrees will result in a change of 0.01  $G_{\text{mb}}$  units. Dalton (61) found a similar relationship, with a change of DIA of 0.1 degrees resulting in a change of 0.014  $G_{\text{mb}}$  units. After the completion of this Alabama DOT study, the DIA of the Pine compactor was measured as 1.23 degrees. The DIA of the Troxler compactor was not measured at that time because of a problem with the electronics, but was

later measured as 1.02 degrees. Using the first relationship, the compacted sample densities from both compactors were adjusted to that which would have been produced if both compactors had been set to a DIA of 1.16 degrees. The predicted gyrations to match the in-place density after 2 years of traffic were then recalculated and are summarized in Figure 4.16. As shown in Figure 4.16, the best fit line for the predicted gyrations to match the in-place density from both compactors adjusted to an internal angle of 1.16 degrees falls along the line of equality. The best fit line for the original data is shown for comparison.

The data in Table 4.9 are sorted by the 20-year design traffic. In Figure 4.16 and Table 4.9, there appear to be a few potential outliers in the adjusted data, specifically the Pine results for IL-3 and the Troxler results for KY-2 and MI-1. The two Troxler points also appeared to be potential outliers in Figure 4.15. One tool for evaluating potential outliers in a relationship is to look at the standardized residual. The standardized residual is the difference between the observed and the fit values divided by the square root of the mean square error (MSE). Montgomery (62) states that standardized residuals that exceed  $\pm 3.0$  may be considered outliers. The standardized residuals for IL-3, KY-2, and MI-1 were -2.44, 2.45, and 2.57, respectively; this indicates that the residuals should not be removed as outliers. The other three potential outliers in Figure 4.15—FL-1, MI-2, and MI-3—have standardized residuals of 1.58, 1.09, and 1.33, respectively, when corrected to a DIA of 1.16 degrees in Figure 4.16. Research by Moseley et al. (63) indicates that the measured DIA is affected by the HMA mixture. In that

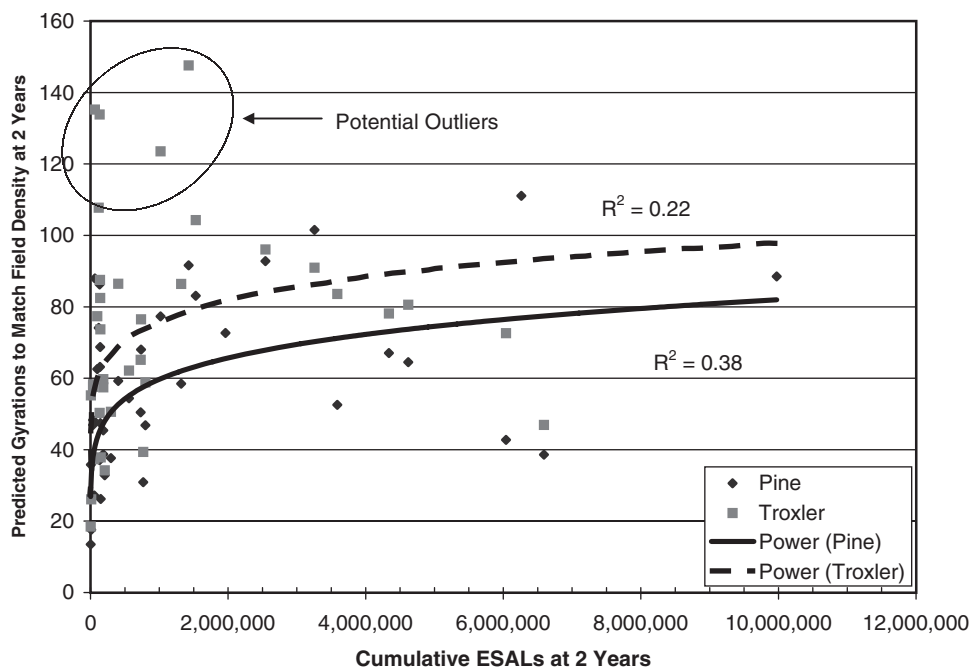
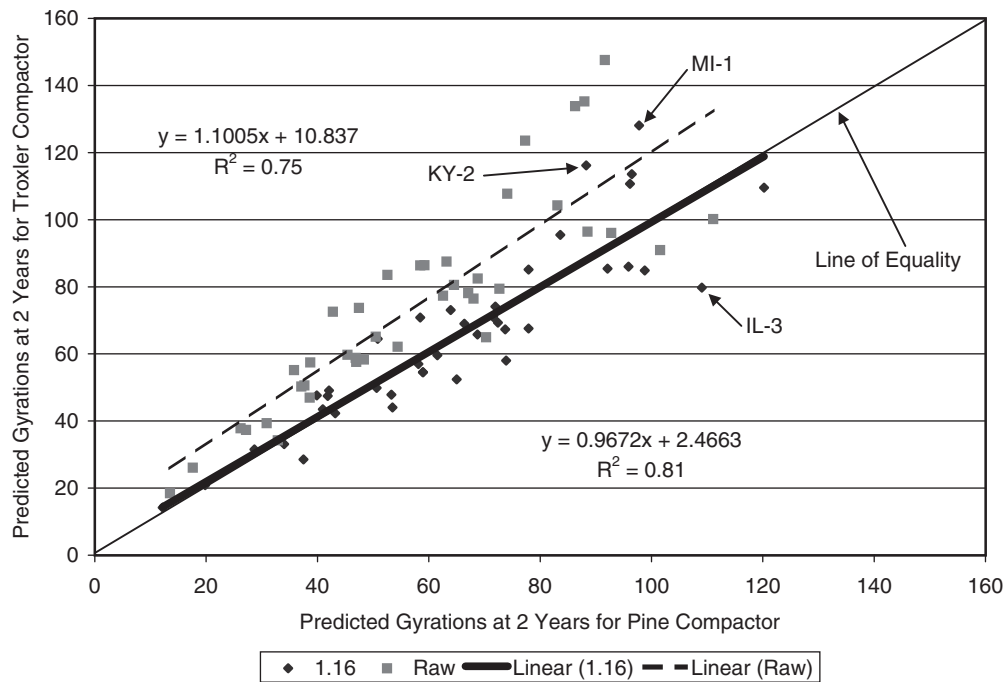


Figure 4.15. Predicted gyrations to match 2-year density.



**Figure 4.16. Comparison of predicted gyrations to match in-place density after 2 years with and without correction for DIA.**

research, of all the aggregates tested, Nova Scotia granite, the same as that used in project FL-1, produced the largest differences between compactors; of all the gradations tested, 9.5-mm NMA mixes showed the largest differences.

Table 4.9 indicates that very few of the predicted gyrations to match the in-place density after 2 years exceed the currently specified  $N_{\text{design}}$  values. The Pine and Troxler results for FL-1 (97 and 115, respectively) exceed 75 gyrations in the 0.3 million to 3 million ESALs category. The Troxler results for KY-2 (116) and MI-1 (126) exceed 100 gyrations in the 3 million to 30 million ESALs category. The higher numbers for the Troxler compactor may be partially attributed to error in the correction to a DIA of 1.16 degrees. It is expected that if the DIA of the Troxler compactor used in this study had been measured with the DAVK using these mixes, the measured DIA would be less than the DIA of 1.02 degrees measured in the Alabama DOT study.

Figure 4.17 shows the predicted gyrations to match the 2-year density, corrected to a DIA of 1.16 degrees, versus the 2-year ESALs. Comparison of Figure 4.17 with Figure 4.15 (showing the uncorrected gyration data) indicates that correction of the gyratory data to a common DIA produces similar relationships between 2-year ESALs and predicted gyrations for the two SGCs, but does not significantly improve the  $R^2$ . The same six projects discussed previously—IL-3, KY-2, MI-1, FL-1, MI-2, and MI-3—appear to be potential outliers. An additional point, AR-2, appears to be a potential outlier having a low number of predicted gyrations (43) for a high 2-year traffic level (6.6 million ESALs).

Figure 4.18 shows the predicted gyrations to match both the 2-year and 4-year in-place densities versus the 20-year design ESALs. Previously, it was shown that there was no statistical difference between the 2-year and 4-year in-place densities. Figure 4.18 shows a slight increase in predicted gyrations to match the 2-year and 4-year in-place densities for both the Pine and Troxler compactors. However, this appears to be somewhat driven by project AR-4. The in-place density for project AR-4 increased by 0.2 percent between 2 years and 4 years. This resulted in an increase of approximately 9 gyrations between 2 and 4 years. The slight increase in  $R^2$  for the 2- and 4-year relationships is most likely due to missing 4-year data, particularly for project FL-1.

#### 4.2.4.2 Comparison of Laboratory Density at $N_{\text{design}}$ and In-Place Density After 2 Years of Traffic

Another way to evaluate whether the current  $N_{\text{design}}$  values are correct is to compare the laboratory air voids at the  $N_{\text{design}}$  specified by the agency with the in-place density after 2 years of traffic or ultimate density. Colorado DOT conducted a similar study on 22 sites (42). The in-place air voids in the Colorado study after 3 years of traffic were 1.2 percent higher than the laboratory air voids at  $N_{\text{design}}$ . In the recommendations section of the study's report, Harmelink and Aschenbrener (42) state that the mixes are being designed at too low of an asphalt content for the environmental and traffic conditions in Colorado. Two suggestions for adjustment were

**Table 4.9. Original and adjusted gyrations to match in-place density at 2 years.**

Project	20-Tear Design Traffic, ESALs	Average Predicted Gyration to Match 2-Year Density					
		Pine 1.23 Degrees	Pine 1.16 Degrees	Pine Std. Dev.	Troxler 1.02 Degrees	Troxler 1.16 Degrees	Troxler Std. Dev.
KY-1	53,706	11	12	1.3	16	14	1.2
KY-3	84,028	34	40	17.4	54	47	22.9
AL-6	143,958	18	20	2.1	26	21	1.3
NE-3	365,719	46	53	10.6	56	44	13.6
NE-1	383,385	47	65	53.3	57	52	39.6
CO-3	523,624	63	69	11.0	77	66	7.4
CO-4	720,911	36	40	11.7	49	42	8.7
CO-1	756,789	62	72	21.7	88	75	18.9
UT-1	771,982	26	28	7.5	36	31	8.8
FL-1	811,658	87	97	14.7	138	115	19.4
CO-2	1,017,593	44	50	13.9	59	50	13.7
CO-5	1,017,593	37	42	13.5	56	49	15.4
MI-2	1,250,146	74	84	27.4	109	96	32.8
NE-2	1,450,960	69	78	15.1	82	68	13.2
MI-3	1,515,200	86	96	2.5	137	111	5.2
AL-5	1,809,675	25	59	9.2	36	55	9.1
IN-1	1,850,992	47	51	5.0	74	64	5.4
TN-1	3,490,393	33	37	10.1	34	29	10.2
AL-2	3,610,001	38	42	16.5	51	47	20.9
AL-4	4,899,406	59	66	3.0	86	69	4.9
AL-1	6,748,142	54	59	9.2	62	55	9.1
GA-1	8,803,521	47	53	10.7	59	48	5.4
AL-3	8,861,352	31	34	0.5	39	33	1.1
KS-1	10,075,962	50	58	21.6	65	57	20.4
KY-2	12,438,605	77	88	43.9	124	116	57.5
MO-2	12,517,675	68	74	3.6	77	67	6.9
WI-1	14,614,748	58	64	4.9	86	73	9.1
MI-1	15,966,398	91	97	8.9	145	126	15.6
NE-4	20,084,248	83	92	3.0	104	85	5.4
IL-1	26,285,917	73	78	7.2	79	85	10.6
MO-1	27,546,007	93	99	13.0	96	85	4.9
IL-3	44,466,336	102	109	10.6	91	80	6.6
IN-2	45,150,555	54	59	9.1	84	71	9.1
IL-2	46,344,297	70	74	17.6	65	53	15.0
AR-1	48,726,562	65	72	16.4	81	71	13.9
MO-3	53,683,941	68	72	4.8	78	69	4.4
NC-1	73,918,507	44	62	16.0	73	60	14.7
AR-2	91,370,805	40	43	5.6	48	42	7.3
AR-4	97,890,077	110	120	3.1	100	111	9.4
AR-3	170,842,507	88	96	14.3	94	86	11.0

lowering  $N_{design}$  and adjusting the mix design air void content to less than 4 percent.

Figure 4.19 shows the air voids at  $N_{design}$  (1.16 degrees) versus the 2-year in-place air voids for each of the samples within a project. As expected based on the data presented so far, there is a great deal of scatter in the data. However, the relationship is significant at  $\alpha = 0.05$ . Based on the regression line, at a void level at  $N_{design}$  of 4 percent, the average in-place air voids are 5.5 percent, or 1.5 percent higher than design. Only a few points fall below the line of equality. This indicates that the pavements have not densified to their design levels. It further suggests that the  $N_{design}$  levels may be too high.

The  $N_{design}$  II Experiment (3) provides a measure of the impact of the higher-than-expected air voids at the ultimate density of the pavement. As noted previously, the FSCH test was conducted using the Superpave Shear Tester to assess changes in mixture stiffness to changes in  $N_{design}$ . In Part 2 of

the experiment, samples of mixes designed at one gyration level (e.g., 130 gyrations) were compacted at other gyrations (e.g., 70 and 100 gyrations) and vice versa, resulting in changes in VMA and air voids (asphalt content and gradation were held constant). Relationships were developed between air voids and  $G^*$  at both 0.1 Hz and 10 Hz, at 50°C for the two aggregate types (gravel and limestone) used in the study. The authors note that the greatest change in shear stiffness occurs between 3- and 6-percent air voids (3). Using the relationships provided, an increase in air voids from 4 percent to 5.5 percent results in an average decrease in  $G^*$  of 23 percent.

#### 4.2.4.3 Predicted $N_{design}$ Versus Accumulated Traffic for 2000 NCAT Test Track

Similar to the 40 field projects, the numbers of gyrations to match field density were backcalculated for the 28 Superpave

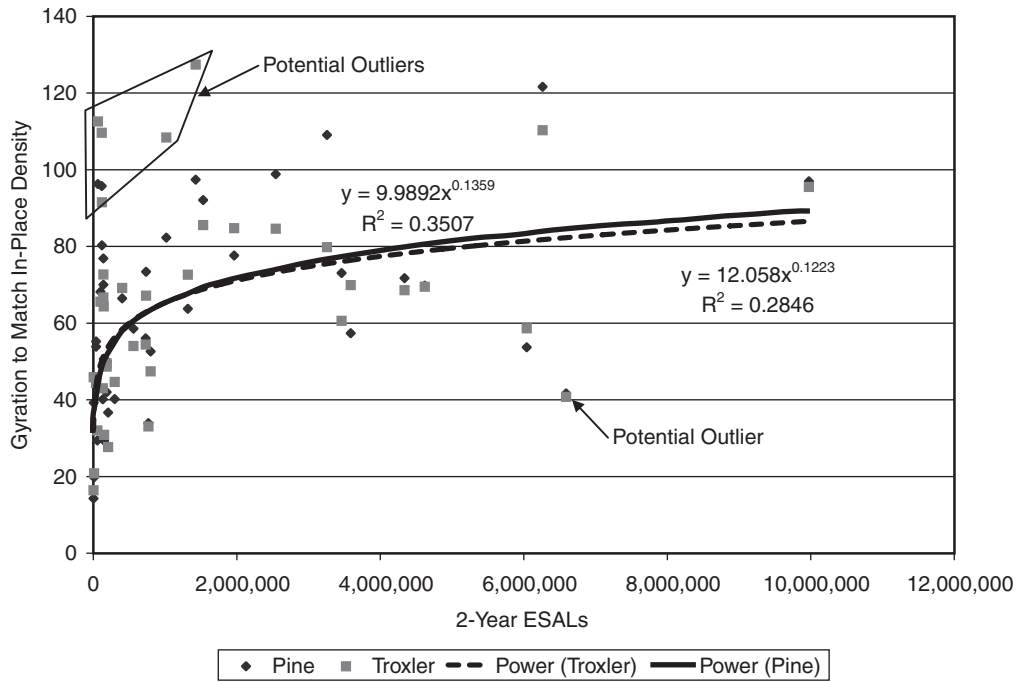


**Figure 4.17. Predicted gyrations to match 2-year density corrected to a DIA of 1.16 degrees.**

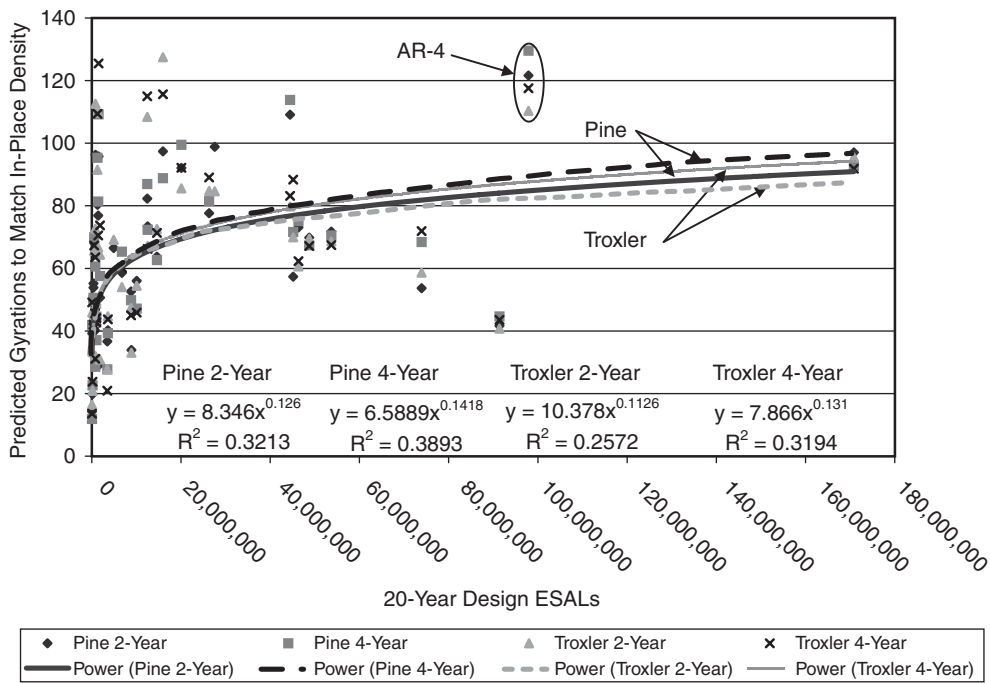


**Figure 4.18. Predicted gyrations to match in-place density corrected to a DIA of 1.16 degrees.**

sections at the 2000 NCAT Test Track. Two Troxler Model 4141 (the same Troxler model used in the field study) SGCs were used to compact the SGC samples at the 2000 NCAT Test Track. Three replicate samples were compacted for each subplot. The samples were compacted to the same  $N_{design}$  level used in the mix design, generally 100 gyrations.

The bulk-specific gravities of the samples were determined with AASHTO T166. All of the heights were digitally recorded and used in the backcalculation. The data have been adjusted to an internal angle of 1.16 degrees. The internal angles of gyration for the two compactors used during the construction of the 2000 NCAT Test Track were not

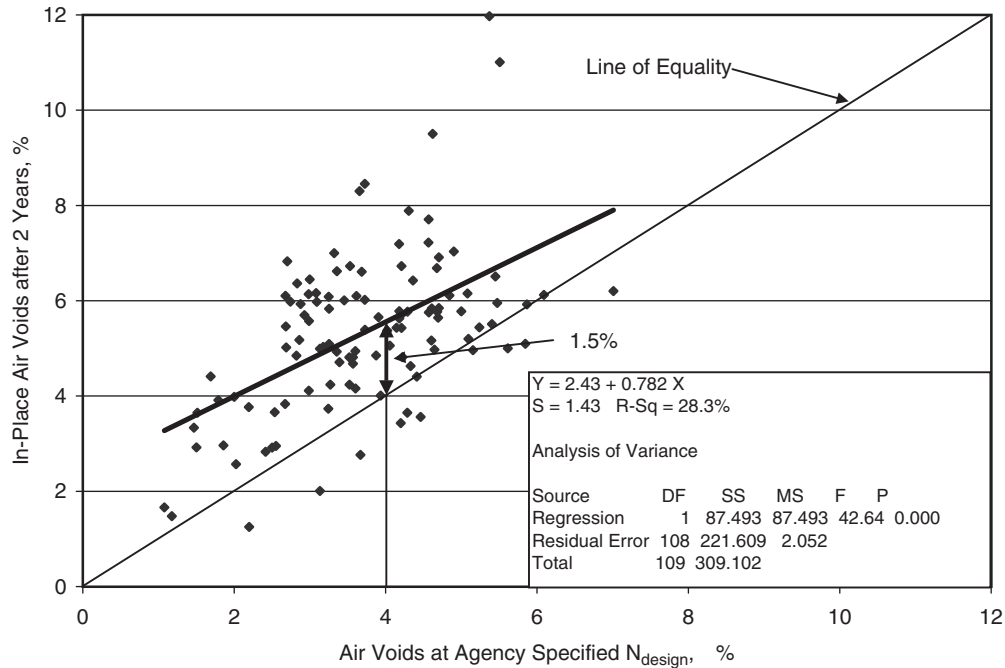


**Figure 4.19. In-place 2-year versus agency-specified  $N_{design}$  air voids.**

known and could not be measured because these compactors were no longer operational. Therefore, the average angle, 1.02 degrees, determined for that Troxler model in a previous study was used when adjusting the data to a DIA of 1.16 (50).

Figure 4.20 shows the average number of gyrations to match the in-place density versus ESALs for the Test Track Superpave sections. The data are subdivided by binder grade (PG 67-22 or PG 76-22) and lift (surface lift or lower lift 50 mm deep). Second-order polynomials provided good fits to the data. On average, there was a 25-gyration difference between predicted gyrations to match the upper (97 gyrations) and lower (72 gyrations) PG 67-22 lifts at 10 million ESALs, and there is a 37-gyration difference between the predicted gyrations to match the upper lifts of PG 67-22 (97 gyrations) and PG 76-22 (60 gyrations) at 10 million ESALs.

As noted previously, no densification occurred during the winter of 2001–2002. Although the relationship between the average predicted gyrations and applied traffic is strong, there is a great deal of scatter in the data. Figure 4.21 presents the actual data for the PG 67-22 and PG 76-22 upper lifts where each point represents the number of gyrations to match the in-place density for a given section at a given number of ESALs. It is apparent from Figure 4.21 that the scatter in the data is much larger for the PG 76-22 sections than for the PG 67-22 sections. This is evidenced by the  $R^2 = 0.63$  for the PG 67-22 mixes and  $R^2 = 0.18$  for the PG 76-22 mixes. It is possible that if the field data were similarly subdivided, a better relationship could be found from which to predict the appropriate  $N_{design}$  levels to match ultimate density.

#### 4.2.4.4 Predicted $N_{design}$ Versus 2-Year Traffic, Excluding Mixes Produced with PG 76-22

Figure 4.22 shows the predicted gyrations, corrected to an internal angle of gyration of 1.16 degrees, to match the 2-year in-place density from the NCHRP Project 9-9(1) field projects, excluding the nine projects that used PG 76-22. It is evident from the figure that there is still a great deal of scatter in the data. Three projects with a high number of predicted gyrations for a low design traffic level are CO-1, MI-2, and MI-3. All three of the projects were constructed with PG 58-28 binder and were constructed with crushed gravel aggregate. Project FL-1 was constructed to 91.8 percent  $G_{mm}$  and densified to 95.2 percent  $G_{mm}$  after 2 years. Nothing appears to be unusual about the densification; however, a high number of gyrations were predicted to match the 2-year density for a relatively low traffic volume. The laboratory voids for FL-1 were high, with air voids at the agency-specified  $N_{design}$  of 5.1 and 5.6 percent, respectively, for the Pine and Troxler compactors.

A regression was performed using log 20-year ESALs as a predictor for log gyrations. The average Pine and Troxler results at 1.16 degrees were combined, resulting in two data points for each project. The data for CO-1, MI-2, MI-3, and FL-1 were eliminated from the data set. The  $R^2 = 0.52$  indicates a weak correlation between log 20-year ESALs and log-predicted gyrations. However, the Troxler results for MI-1 were indicated as a possible outlier with a standardized residual of 3.41. The Troxler results for MI-1 were removed from the data set and the regression re-run. The

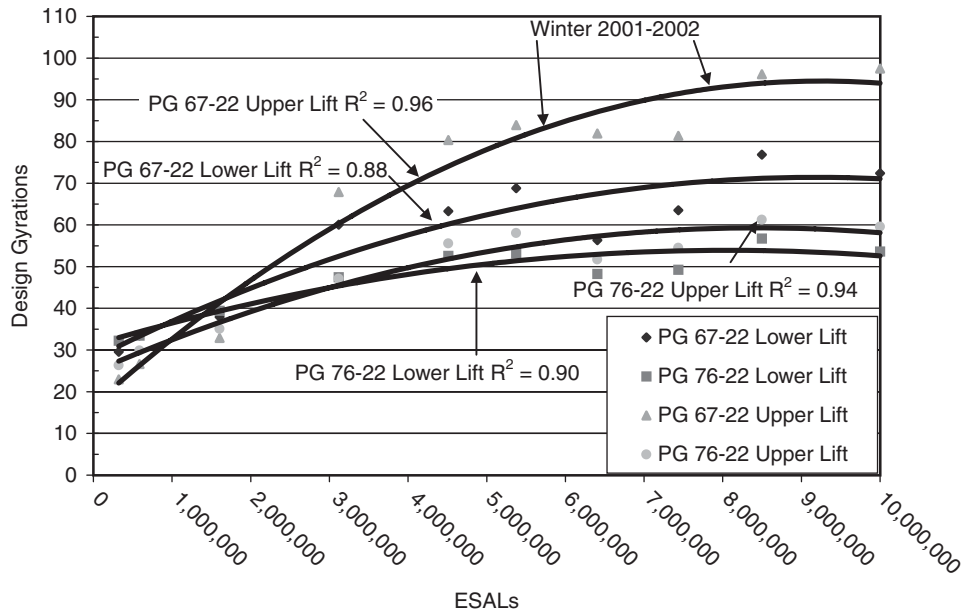


Figure 4.20. Average gyrations to match 2000 NCAT Test Track density.

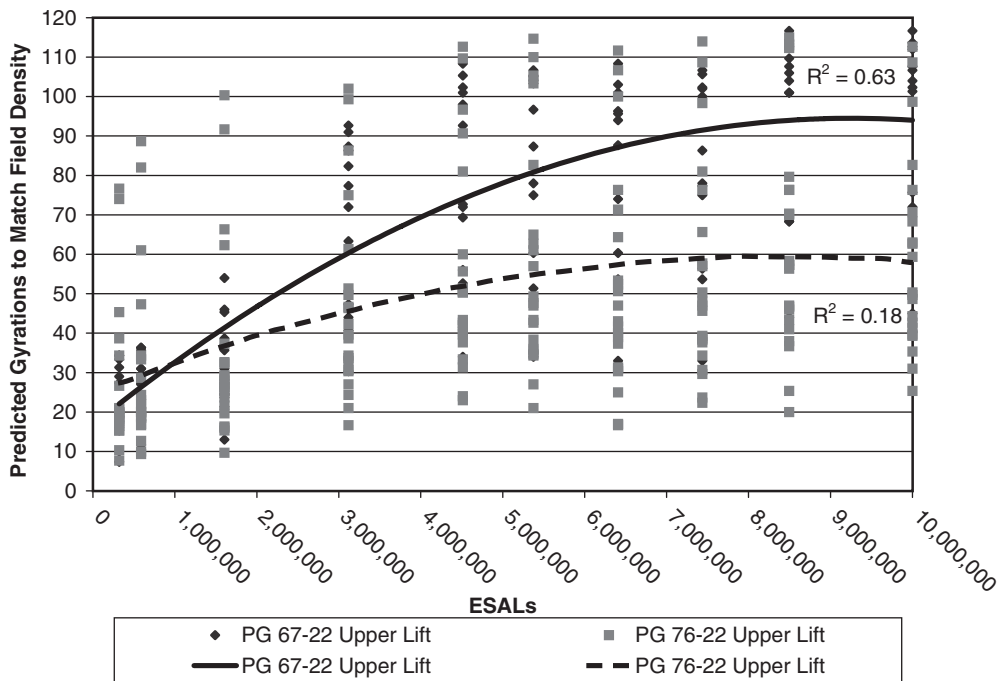


Figure 4.21. Predicted gyrations to match 2000 NCAT Test Track density.

resulting  $R^2$  (0.57) still indicates a weak correlation, but improved. Figure 4.23 shows the standardized residuals versus the fitted value for the regression. The residuals appear to be well distributed. Figure 4.24 shows a plot of the regression with the 80-percent confidence interval. The regression was used to predict fitted values for the currently specified traffic levels. The 80-percent prediction interval for the regression is also shown.

Using the regression shown in Figure 4.24, Table 4.10 shows the number of gyrations for each of the currently specified Superpave traffic levels, along with the 80-percent confidence prediction interval. The 80th percentile, calculated using the data in Table 4.9, is shown for comparison. The data for the 80th percentile includes the projects constructed with PG 76-22, while the predicted values from the regression does not include the projects constructed with

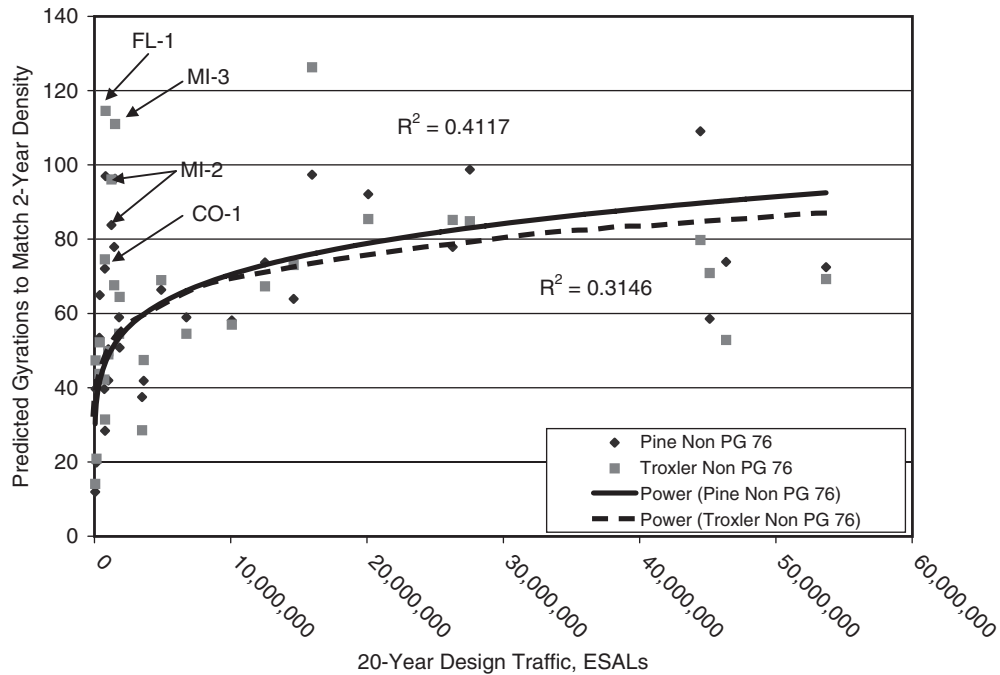


Figure 4.22. Predicted gyrations for Pine SGC, excluding projects using PG 76-22.

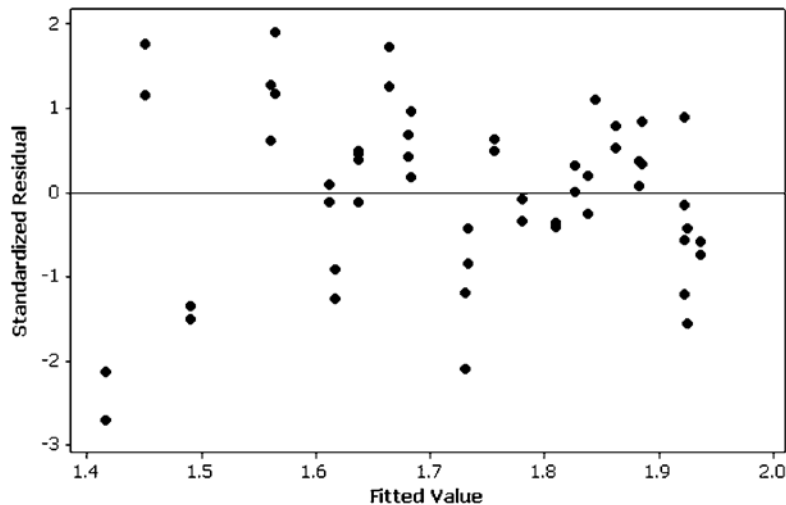


Figure 4.23. Standardized residuals versus fitted mean for log-predicted gyrations versus log 20-year ESALs.

PG 76-22. From Table 4.10, it can be seen that the high side of the interval for the 80-percent prediction interval approximately matches the currently specified gyration levels (4). However, the original  $N_{\text{design}}$  experiment used the predicted value with 50-percent confidence (34). As shown previously in Figure 4.20, the data from the 2000 NCAT Test Track and the 80th-percentile data reinforce that an  $N_{\text{design}}$  of 100 gyrations should be adequate for very high traffic levels. The 20-year design traffic for the 2000 NCAT Test Track would be in excess of 100 million ESALs. Further,

the  $N_{\text{design}}$  II Experiment indicated virtually no difference in shear stiffness between mixtures designed at 100 gyrations and 130 gyrations (3). These three facts combined suggest that  $N_{\text{design}}$  levels greater than 100 gyrations are unnecessary, even for the very highest traffic levels.

From Figure 4.24, it can be seen that the predicted gyrations change very rapidly at design traffic levels less than approximately 3 million ESALs. Caution is required when recommending  $N_{\text{design}}$  for between 0.3 million and 3 million design ESALs.

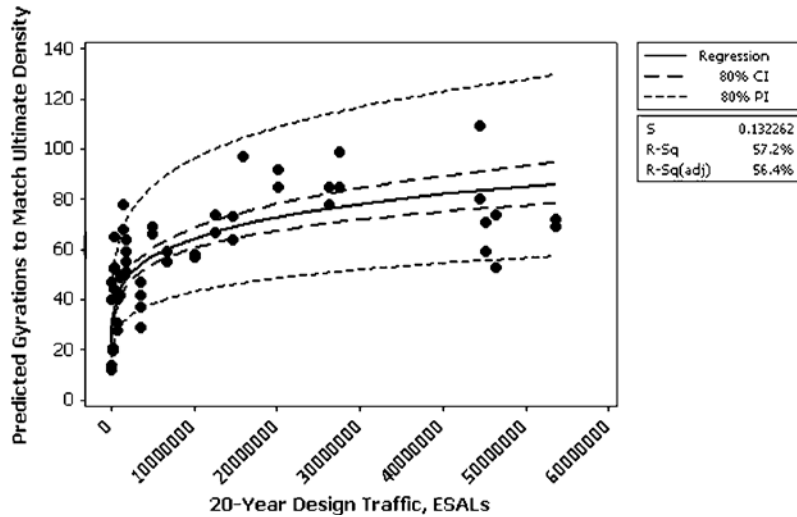


Figure 4.24. Predicted gyrations versus 20-year design traffic without PG 76-22 data.

Table 4.10. Predicted gyrations to match ultimate density.

20-Year Design ESAL	Current $N_{design}$	Predicted $N_{design}$	80% Prediction Interval		80th Percentile		
			Low	High	Pine	Troxler	Avg.
300,000	50	35	23	53	32	43	38
1,000,000	75	43	29	65	71	73	72
3,000,000	100	52	35	78	83	90	87
10,000,000	100	65	43	96	59	55	57
30,000,000	125	78	52	117	95	104	100
100,000,000	125	96	64	145	101	82	92

4.2.4.5 Predicted  $N_{design}$  Versus 2-Year Traffic for PG 76-22 Mixes

Figure 4.25 shows the relationship between 20-year design ESALs and the predicted gyrations to match the 2-year density for the projects constructed with PG 76-22. Although a best fit line is shown in the figure, there is no relationship between the 20-year design ESALs and the predicted gyrations for the projects constructed with PG 76-22. A poor relationship ( $R^2 = 0.18$ ) was also observed for the data from the 2000 NCAT Test Track (see Figure 4.21, shown previously). This indicates that, for the modified binders, there was no significant correlation between change in density and traffic.

4.2.4.6 Predicted  $N_{design}$  Versus Traffic for All Sampling Intervals

When the  $N_{design}$  table was originally developed, regression analysis was performed between gyrations determined to match the as-constructed density and the gyrations required to match the in-place pavement density after more than 12 years of traffic (34). The analyses for the NCHRP Project

9-9(1) field sections presented thus far have been based solely on the number of gyrations to match the ultimate pavement density (2-year or 4-year). Figures 4.20 and 4.21 presented the predicted gyrations to match in-place density for the 2000 NCAT Test Track as traffic accumulated. Figure 4.26 presents a log-log plot of predicted gyrations versus accumulated traffic for all of the NCHRP Project 9-9(1) field sections. The gyratory data corrected to a DIA of 1.16 degrees were used for the predictions. As expected, and as evidenced by the low  $R^2$  values, there is considerable scatter in the data. The regression lines for the Pine and Troxler data are approximately identical.

Table 4.11 uses the equations for the best fit line to predict gyration levels similar to Table 4.10. This method of analysis produces slightly higher predicted gyration levels, close to those currently specified.

4.2.4.7 Model Development to Account for Low As-Constructed Density

One concern about the predictions discussed to date, particularly those in Table 4.10, is the high percentage of projects with low as-constructed density. Figure 4.6 indicates that

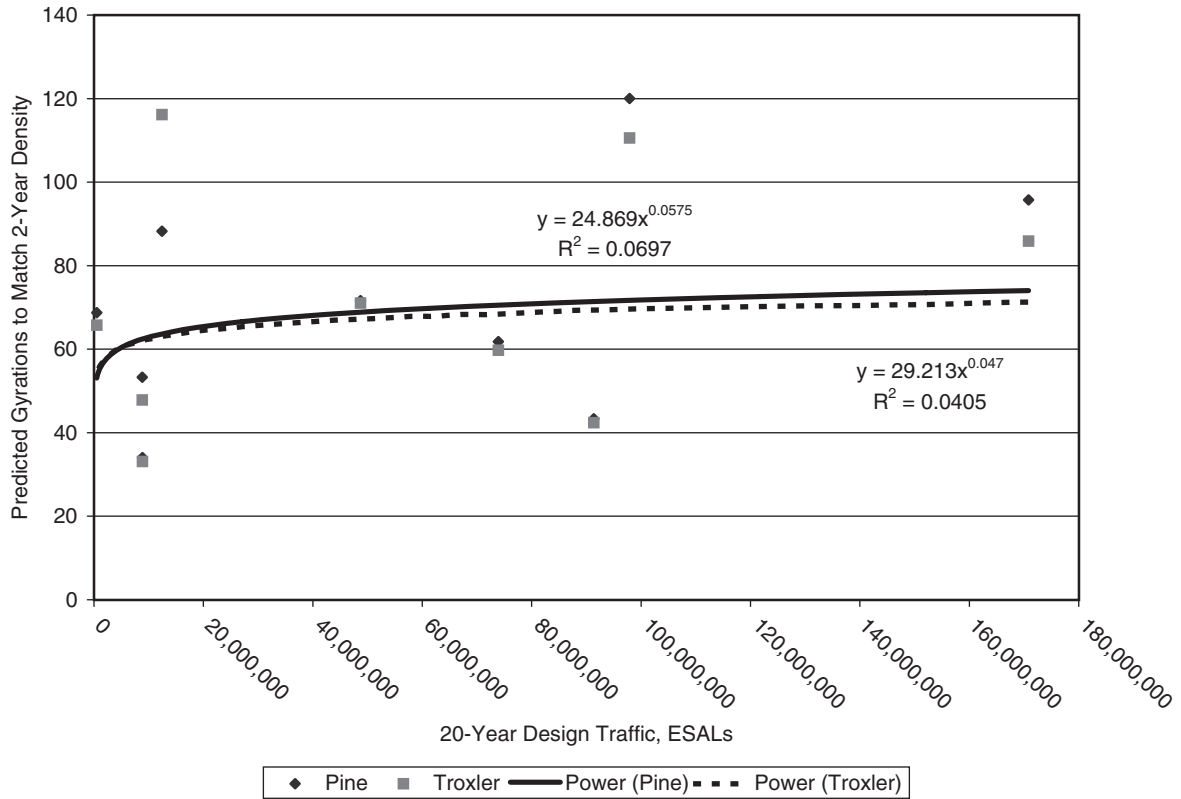


Figure 4.25. Predicted gyrations for projects with PG 76-22.

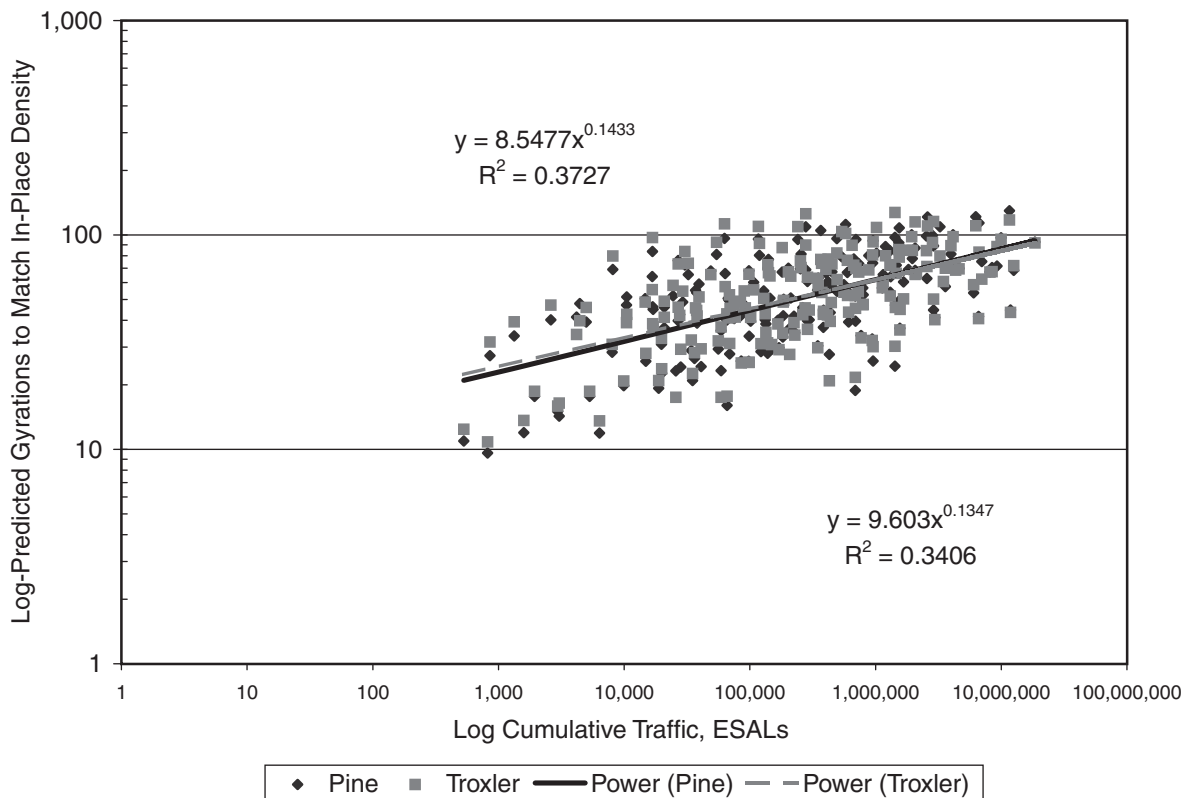


Figure 4.26. Predicted gyrations to match in-place density for all post-construction sampling periods.

**Table 4.11. Predicted gyrations to match in-place density.**

20-Year Design ESAL	Troxler	Pine
300,000	52	52
1,000,000	62	62
3,000,000	73	74
10,000,000	86	89
30,000,000	101	105
100,000,000	120	126

55 percent of the projects had as-constructed in-place densities less than 92 percent. Examination of the data suggested that there was a strong trend between as-constructed density and ultimate (2-year) density, as shown in Figure 4.27 for both the field projects and the 2000 NCAT Test Track. Regression analyses between the as-constructed and 2-year in-place densities indicated  $R^2 = 0.65$  and  $R^2 = 0.54$  for the NCHRP Project 9-9(1) field sections and 2000 NCAT Test Track, respectively. The shift in the regression lines between the field sections and the 2000 NCAT Test Track is somewhat expected because of the accelerated traffic loading at the 2000 NCAT Test Track. A higher as-constructed density would result in a higher ultimate density and, thus, could affect the predicted  $N_{\text{design}}$  levels. Therefore, an attempt was made to model pavement densification to predict in-place density. It was felt that this model could possibly be used to predict  $N_{\text{design}}$  with ideal

field conditions (e.g., 92-percent or 93-percent as-constructed density and 96-percent ultimate density).

Epps et al. (24) described factors expected to affect pavement densification. Previously, high-temperature PG bump and month of construction were shown to be significant factors that affect pavement densification. Brown and Cross (26) suggested that the log of accumulated ESALs divided by the log of the design compaction effort (in this case, gyrations) was a good predictor for in-place density. From the literature, it was suggested that pavements constructed to a low initial density would tend to densify more and eventually obtain the same ultimate density as pavements constructed to higher initial densities. Figure 4.28 indicates that there is a weak trend of increased densification for projects with lower as-constructed densities, but no trend for projects with acceptable construction densities. Therefore, the difference between the laboratory density at  $N_{\text{design}}$  and the as-constructed density was considered an alternative.

A number of techniques, such as best subsets and stepwise regression, and a number of iterations were attempted to develop a model to predict the 2-year pavement density. Variables used to predict 2-year density included degree days over 30°C, mean average annual air temperature, NMAS, high PG, agency-specified design gyrations, month of construction, 2-year ESALs, and as-constructed density. Initially, an attempt was made to model pavement densification, but not even a

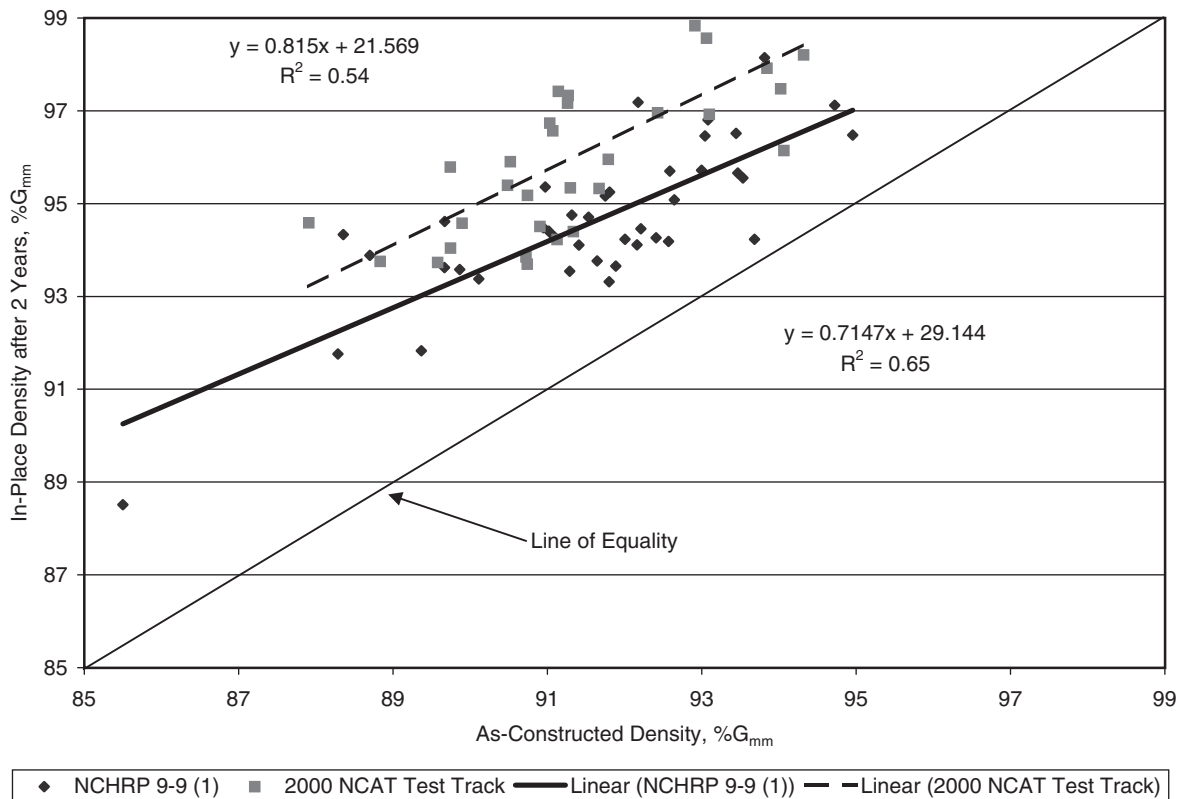


**Figure 4.27. Relationship between as-constructed and ultimate density.**

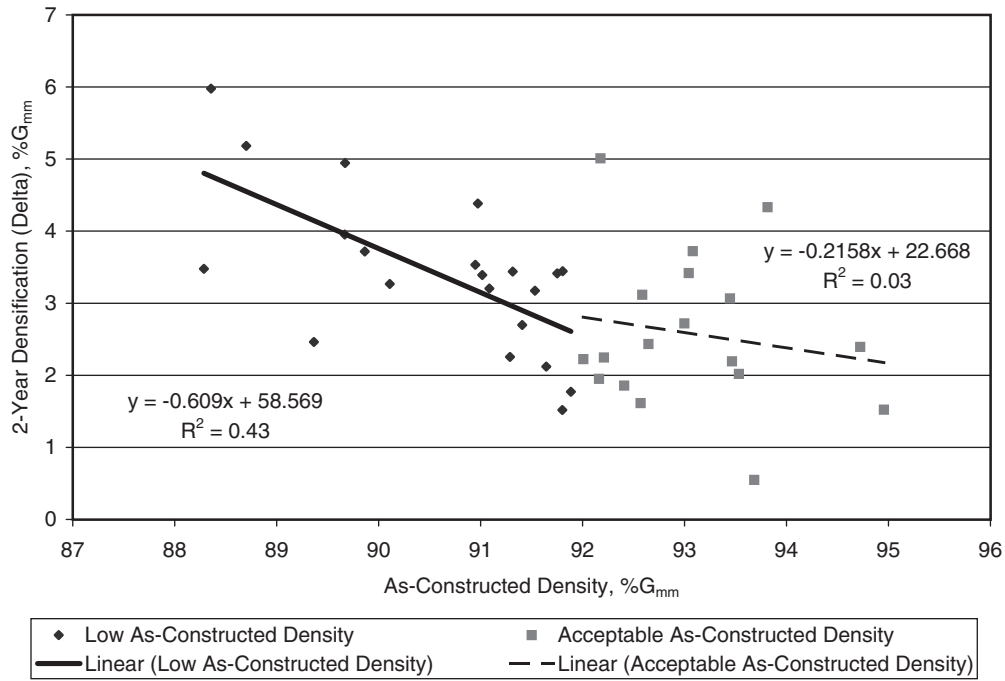


**Figure 4.28. Two-year densification versus as-constructed density.**

fair model could be found. Better results were obtained when predicting pavement density. One of the best models developed is Equation 5:

$$\begin{aligned} 2 \text{ Year Den.} = & 0.771 \times \text{Const. Den.} - 0.325 \\ & \times \text{Month of Const.} - 0.078 \times \text{High PG} \end{aligned} \quad (5)$$

Month of construction was entered as the numerical month of construction (e.g., July = 7). Data are included for projects constructed between April and October. Errors are expected for certain months outside this range (e.g., January through March). High PG is the high PG binder grade (e.g., 64, 67, 70, or 76). The model has an  $R^2$  of 0.71, a standard error of 0.91, and a Mallow's C-p statistic of 5.6. All of the variables in the model are significant ( $\alpha = 0.05$ ). It is generally desirable to have a Mallow's C-p statistic less than the number of variables in the model. This model only represents a slight improvement over the prediction made with as-constructed density, which was shown in Figure 4.27 with an  $R^2$  of 0.65.

Minitab's best subset analysis identified a five-variable model with a Mallow's C-p statistic of 4.5. In addition to as-constructed density, month of construction, and high-temperature PG, this model included degree days over 30°C and log of 2-year ESALs. Degree days over 30°C was determined for each project from LTPPBind Version 2.1 (51). If, on a given day, the temperature was 35°C, that day would account for 5 degree days. The reported value is the average yearly cumulative degree days. The data set contained projects with 0 to 444 degree days over 30°C. Regions in the southwestern United States have much higher values for degree days over

30°C. For example, Phoenix, Arizona, has approximately 1,400 degree days over 30°C. Equation 6 presents the second model developed for predicting 2-year (i.e., ultimate) density:

$$\begin{aligned} 2Y \text{ Density} = & 30.61 + 0.786 \times \text{ACD} - 0.132 \\ & \times \text{High PG} - 0.204 \times \text{MC} + 0.0041 \\ & \times 30\text{CDD} + 0.321 \times \text{Log}2Y \text{ ESALS} \end{aligned} \quad (6)$$

where:

- 2Y Density = in-place density after 2 years of traffic,
- ACD = as-constructed density,
- High PG = high-temperature PG,
- MC = month of construction (e.g., July = 7), including data from April through October,
- 30CDD = degree days over 30°C, and
- 2Y ESALs = accumulated ESALs at 2 years.

Equation 6 has an  $R^2$  of 0.76 and a standard error of 0.88. The number of degree days is not significant at the 5-percent level, but is significant at the 10-percent level. The p-value for log 2-year ESALs is 0.182, indicating that 2-year ESALs are not significant. The fact that accumulated traffic is not strongly related to densification is not completely surprising, since the projects were designed with a tiered system where projects with higher traffic levels tended to have more angular aggregates, stiffer binders, and higher design gyrations levels.

The models were then used to recalculate the 2-year density for each project assuming that the as-constructed density was 92 percent (the actual values were used for all of the other

variables). The number of gyrations to match the new 2-year density (based on a 92-percent as-constructed density) was calculated for each project. Unfortunately, the resulting predicted gyrations produced even poorer relationships with design traffic than those presented previously. This tends to indicate that the scatter in the predicted gyration versus ESAL data was not due to the range of as-constructed densities.

Another source for the scatter in the predicted gyration versus ESAL data might be the fact that the HMA for the different projects were not all produced at 4-percent air voids. A project constructed with higher laboratory air voids would be less likely to densify in the field, and a project constructed with low laboratory air voids would be more likely to densify in the field. One way to address this issue would be to look at the field densities as a percentage of laboratory density. A model was developed to predict  $N_{\text{design}}$  as a function of high-temperature PG and design ESALs. As-constructed density was normalized to 92-percent  $G_{\text{mm}}$  in the model development. The following steps were taken to develop the model:

1. The 2-year in-place density for each project was expressed as a percentage of  $G_{\text{mb}}$  (i.e., laboratory density) determined at 100 gyrations for both the Pine and Troxler SGCs normalized to a DIA of 1.16 degrees.
2. A model was developed to predict the 2-year percentage of laboratory density similar to Equations 5 and 6. Models were also developed to predict laboratory density (i.e., percentage of  $G_{\text{mb}}$ ) as a function of as-constructed density, high-temperature PG, and ESALs.
3. A matrix was developed consisting of twelve 2-year in-place densities based on as-constructed densities of 92 percent, two high-temperature PGs (64 and 76), and a range of design traffic (Table 4.12).
4. The in-place density (i.e., the percentage of  $G_{\text{mm}}$ ) corresponding to each of the predicted laboratory densities

**Table 4.12. Matrix of predicted percentage of laboratory density.**

As-Constructed Density	2-Year ESALs	Log 2-Year ESALs	Approximate 20-Year ESALs	High PG	Pine Predicted 2-Year % $G_{\text{mb}}$ (Lab Density)	Troxler Predicted 2-Year % $G_{\text{mb}}$ (Lab Density)
92	30,000	4.48	300,000	64	97.2	97.3
92	90,000	4.95	1,000,000	64	97.8	97.8
92	230,501	5.36	3,000,000	64	98.3	98.2
92	920,577	5.96	10,000,000	64	99.0	98.9
92	2,583,607	6.41	30,000,000	64	99.5	99.3
92	6,773,140	6.83	100,000,000	64	100.0	99.8
92	30,000	4.48	300,000	76	96.5	96.4
92	90,000	4.95	1,000,000	76	97.1	96.9
92	230,501	5.36	3,000,000	76	97.6	97.3
92	920,577	5.96	10,000,000	76	98.3	98.0
92	2,583,607	6.41	30,000,000	76	98.8	98.4
92	6,773,140	6.83	100,000,000	76	99.3	98.9

(i.e., the percentage of  $G_{\text{mb}}$ ) was determined for each project. (Table 4.12 shows these densities.)

5. The number of gyrations needed to match each of the in-place densities determined in Step 4 was determined. The range of gyrations for each percentage of laboratory density determined in Step 3 is relatively small. In other words, the SGC compacted all of the mixes in this study at approximately the same rate. This makes sense because the SGC is a constant strain compaction device. The average number of gyrations to match each of the percentages of laboratory density in Table 4.12 was determined for both the Pine and Troxler SGCs.
6. Finally, a model was developed to relate  $N_{\text{design}}$  back to high-temperature PG and log ESALs. As-constructed density dropped out of the model because it was set to 92 percent  $G_{\text{mm}}$  in all cases. This was accomplished through the percentage of laboratory ( $G_{\text{mb}}$ ) density described in Steps 1–5.

The 2-year in-place density, expressed as a percentage of the laboratory density determined at 100 gyrations, was regressed against the same set of predictors used previously (Step 2). Equations 7 and 8 present the models developed for the Pine and Troxler compactors, respectively:

$$\begin{aligned} 2 \text{ Year\% Pine Lab Density} = & 53.95 + 0.452 \times \text{ACD} - 0.58 \\ & \times \text{HPG} + 1.19 \times \text{Log 2Y ESALs} \end{aligned} \quad (7)$$

$$\begin{aligned} 2 \text{ Year\% Troxler Lab Density} = & 62.34 + 0.381 \times \text{ACD} \\ & - 0.08 \times \text{HPG} + 1.06 \\ & \times \text{Log 2Y ESALs} \end{aligned} \quad (8)$$

where:

ACD = as-constructed density,  
 HPG = high-temperature PG, and  
 2Y ESALs = accumulated ESALs at 2 years.

The  $R^2$  is 0.53 for the Pine model and 0.45 for the Troxler model. Standard errors are 1.27 and 1.28 for the Pine model and Troxler model, respectively. The high PG was not significant in either model, with p-values of 0.235 and 0.129 for the Pine and Troxler data, respectively. These variables were selected because they produced reasonable  $R^2$  values for both compactors. Better models were identified for one or the other compactor, but they did not share the same variables.

A matrix of variables was developed to examine the effect of determining the predicted gyrations to match a given percentage of laboratory density (Step 3 above). Table 4.12 presents the matrix of variables and the resulting percentages of laboratory density. The in-place density corresponding to each of the percentages of laboratory density shown in

Table 4.12 was calculated for each project (Step 4). Then the number of gyrations to match that in-place density was calculated for each project (Step 5). The predicted gyrations to match each of the percentages of laboratory density are shown in Tables 4.13 and 4.14 for the Pine and Troxler compactors, respectively. For the Pine compactor, the predicted gyrations for a given percentage of laboratory density had a low variability, with standard deviations ranging from 3.44 to 8.99. The predicted gyrations to match a given percentage of laboratory density for the Troxler compactor also had low variability, with standard deviations ranging from 4.83 to 8.98. Thus, regardless of the mix, a given percentage of laboratory density (determined at an  $N_{\text{design}}$  of 100) can be achieved with a similar number of gyrations.

Because the gyrations were related to the percentage of laboratory density at 100 gyrations, and because the percentage of laboratory density was related to as-constructed density, high PG, and ESALs, the data were analyzed to see if a relationship existed among the average predicted gyration, high PG, and ESALs (Step 6). Because a single target as-constructed density (92 percent) was desired, this variable should drop out of the relationship. Higher as-constructed densities would (using Equations 7 or 8) result in higher-predicted gyrations. Although this result seems counterintuitive from a field compaction standpoint, if a mix were constructed to a higher level of density initially, then one would want the mix to be more resistant to additional densification. Likewise, a pavement constructed

**Table 4.13. Pine-predicted gyrations to match percentage of lab density.**

Project	Percentage of Lab Density, %G <sub>mb</sub>											
	97.2	97.8	98.4	99.0	99.6	100.2	96.5	97.1	97.7	98.3	98.9	99.5
	Predicted Gyrations											
AL-1	50	58	68	79	91	107	42	49	57	66	77	90
AL-2	55	64	72	83	94	108	47	55	62	71	81	93
AL-3	42	51	62	75	91	111	33	41	49	60	72	89
AL-4	34	43	54	69	86	109	26	33	41	53	66	83
AL-5	33	42	53	67	84	108	25	32	40	51	64	82
FL-1	43	52	61	73	86	104	35	42	50	60	70	84
MI-1	52	60	69	80	91	105	44	51	59	68	77	89
MI-2	48	57	66	78	91	107	40	47	55	65	75	89
WI-1	44	53	63	76	90	108	36	43	51	62	73	88
CO-1	38	47	57	71	86	107	30	37	45	56	68	84
CO-2	38	47	57	71	86	106	30	37	45	56	68	84
CO-3	44	53	62	74	87	103	36	43	51	61	71	85
CO-4	47	55	65	77	90	107	38	46	53	63	74	88
CO-5	46	55	64	76	89	106	38	45	53	63	73	87
IN-1	54	62	71	81	92	106	47	53	61	70	79	91
IN-2	40	49	58	71	85	103	32	39	47	57	68	83
KY-1	58	66	75	85	96	109	50	57	64	73	83	94
KY-2	58	66	74	84	94	107	50	57	64	73	82	93
KY-3	42	51	61	74	89	108	34	41	49	60	71	87
AL-6	33	42	54	70	89	115	24	32	40	52	66	86
AR-1	52	61	71	83	96	113	43	51	59	69	80	94
AR-2	52	61	71	83	96	112	44	51	59	69	80	94
AR-3	47	56	67	80	95	114	38	46	54	65	77	93
AR-4	42	50	60	72	85	102	34	41	48	58	69	83
GA-1	34	44	55	71	89	115	26	33	41	53	67	87
IL-1	56	64	72	82	93	107	48	55	62	71	80	92
IL-2	56	64	73	84	96	111	47	55	62	72	82	94
IL-3	54	62	71	82	93	107	46	53	60	69	79	91
KS-1	43	52	62	75	89	107	35	42	50	60	72	87
MI-3	40	49	59	72	87	107	32	39	47	57	69	85
MO-1	58	67	76	87	98	113	50	57	65	74	84	97
MO-2	54	63	71	82	93	107	47	54	61	70	79	91
MO-3	55	64	73	84	96	110	47	55	62	72	81	94
NC-1	29	39	51	68	88	117	21	28	37	49	64	85
NE-1	30	39	50	65	84	110	22	29	37	48	62	81
NE-2	36	45	56	70	86	108	28	35	43	54	67	83
NE-3	27	36	46	61	78	103	20	26	34	45	57	76
NE-4	37	46	56	70	86	107	29	36	44	55	67	83
TN-1	36	46	57	71	88	111	28	36	44	55	68	86
UT-1	47	56	66	78	91	108	39	46	54	64	75	89
Minimum	27.1	35.7	46.0	60.6	78.0	102.4	19.9	26.2	33.8	44.5	57.3	75.5
Average	44.6	53.4	63.1	75.8	89.8	108.3	36.5	43.7	51.5	61.7	73.0	87.8
Maximum	58.0	66.5	75.5	86.7	98.4	116.6	50.2	57.2	64.7	74.3	84.3	96.8
Std. Dev.	8.97	8.61	7.82	6.30	4.33	3.44	8.95	8.99	8.72	7.95	6.67	4.60

**Table 4.14. Troxler-predicted gyrations to match percentage of lab density.**

Project	Percentage of Lab Density, %G <sub>mb</sub>											
	97.2	97.8	98.4	99.0	99.6	100.2	96.5	97.1	97.7	98.3	98.9	99.5
	Predicted Gyrations											
AL-1	52	60	68	78	89	102	41	48	54	62	71	81
AL-2	58	66	73	83	92	104	48	54	60	68	76	85
AL-3	43	52	60	72	84	99	33	39	46	54	63	75
AL-4	36	44	54	67	81	101	25	31	38	47	57	71
AL-5	35	42	51	62	75	91	25	31	37	45	54	66
FL-1	46	54	63	75	87	103	35	41	48	57	66	78
MI-1	53	61	69	79	89	102	43	49	55	63	71	82
MI-2	49	57	65	76	88	103	38	44	51	59	68	80
WI-1	45	54	63	74	87	102	34	41	48	56	66	78
CO-1	42	51	60	72	85	101	32	38	45	53	63	75
CO-2	44	53	62	75	88	106	32	39	46	55	66	79
CO-3	46	54	63	73	84	99	36	42	49	57	65	77
CO-4	48	56	65	76	87	102	37	44	50	59	68	79
CO-5	47	55	63	74	86	100	36	42	49	57	66	78
IN-1	54	62	69	79	89	101	44	50	56	64	72	82
IN-2	41	50	59	71	83	100	31	37	44	52	62	74
KY-1	58	66	73	83	92	104	48	54	60	68	76	85
KY-2	59	66	74	84	93	105	48	55	61	69	77	87
KY-3	42	51	60	71	84	101	32	38	45	53	63	75
AL-6	34	42	52	65	81	101	23	29	36	45	56	70
AR-1	54	63	71	82	93	106	43	50	57	65	74	85
AR-2	56	64	72	83	94	108	44	51	58	66	75	86
AR-3	56	65	74	86	98	113	45	51	59	68	77	89
AR-4	50	59	69	81	95	112	38	45	52	62	72	85
GA-1	36	45	55	68	83	103	26	32	39	48	58	73
IL-1	56	63	71	80	89	101	46	52	58	65	73	83
IL-2	59	66	74	84	94	107	48	54	61	69	77	87
IL-3	57	64	72	82	92	104	46	52	59	67	75	85
KS-1	46	55	64	76	88	104	35	42	49	57	67	79
MI-3	41	49	58	70	83	100	30	36	43	51	61	74
MO-1	60	68	76	86	96	109	49	56	62	71	79	89
MO-2	57	65	72	81	91	103	47	53	59	67	75	84
MO-3	58	65	73	83	93	105	47	53	60	67	76	86
NC-1	30	38	46	57	69	85	22	27	32	40	49	60
NE-1	33	41	51	64	79	99	22	28	35	44	54	68
NE-2	39	47	57	70	84	102	28	34	41	50	60	74
NE-3	30	38	47	60	75	95	20	25	32	40	50	64
NE-4	40	48	57	68	81	98	29	35	42	50	60	72
TN-1	37	46	56	68	83	102	27	33	40	49	59	73
UT-1	48	56	65	75	86	100	38	44	50	59	67	78
Minimum	29.5	37.6	45.7	56.6	68.7	85.0	19.9	25.3	31.6	40.0	48.6	60.1
Average	46.9	55.0	63.6	74.7	86.7	102.1	36.3	42.4	49.0	57.5	66.6	78.3
Maximum	60.3	68.2	76.2	86.2	97.7	112.9	49.3	55.8	62.4	70.6	79.0	89.3
Std. Dev.	8.98	8.78	8.30	7.39	6.19	4.83	8.81	8.98	8.96	8.66	8.08	7.05

to a lower as-constructed density would tend to age faster, thereby producing a stiffer mix. Therefore, one would need a mix that would densify more readily to achieve the same ultimate density.

Table 4.15 shows the data used to develop the models to predict  $N_{\text{design}}$  gyration levels from high PG and 2-year ESALs. The average gyrations to match a percentage of laboratory density are those shown in Tables 4.13 and 4.14 to meet the percentage of lab density determined for the matrix in Table 4.12. Since the Pine and Troxler numbers of gyrations to match a percentage of laboratory density at a DIA of 1.16 degrees were so close to each other, they were averaged. Two models were then developed using ESALs, high PG, and gyrations. One model uses the 2-year ESALs (Equation 9), and the other model uses the 20-year ESALs (Equation 10).

Equation 10 was determined following the same steps as Equation 9 using the 20-year ESALs.

$$N_{\text{design}} = 33.0 - 1.25 \times \text{HPG} + 20.9 \times \text{Log 2 Year ESALs} \quad (9)$$

$$N_{\text{design}} = 16.8 - 1.27 \times \text{HPG} + 20.1 \times \text{Log 20 Year ESALs} \quad (10)$$

where:

$N_{\text{design}}$  = the number of design gyrations,

HPG = high PG, and

2-Year or 20-Year ESALs = the 2-year or 20-year design ESALs for the project.

The  $R^2$  for both Equation 9 and Equation 10 is 0.97, with standard errors of 3.66 and 3.54, respectively. Note that the

**Table 4.15. Matrix of gyrations.**

2-Year ESALs	20-Year ESALs	High PG	Avg. Pine Gyrations to a Percentage of Lab Density*	Avg. Troxler Gyrations to a Percentage of Lab Density*	Average Gyrations to a Percentage of Lab Density	Predicted Gyrations to a Percentage of Lab Density	
						Eq. 9	Eq. 10
30,000	300,000	64	45	47	46	46	46
90,000	1,000,000	64	53	55	54	56	56
230,501	3,000,000	64	63	64	64	64	66
920,577	10,000,000	64	76	75	76	77	76
2,583,607	30,000,000	64	90	87	89	86	86
6,773,140	100,000,000	64	108	102	105	95	96
30,000	300,000	76	37	36	37	31	30
90,000	1,000,000	76	44	42	43	41	41
230,501	3,000,000	76	51	49	50	49	50
920,577	10,000,000	76	62	58	60	62	61
2,583,607	30,000,000	76	73	67	70	71	71
6,773,140	100,000,000	76	88	78	83	80	81

\*Percentages of lab density shown in Table 4.12

model reduces  $N_{design}$  by approximately 15 gyrations for a two-grade bump in high PG (e.g., 64 to 72). The lowest traffic level is approximately equal to the 50 gyrations currently specified in AASHTO R 35 for less than 300,000 ESALs. The predicted  $N_{design}$  for unmodified binders for the highest traffic level is approximately 25 gyrations less than the 125 gyrations currently specified in AASHTO R 35. Further, the predicted gyrations for the unmodified binder (PG 64) approximately match those determined in Table 4.10 (presented previously), but are slightly higher in the 10 million to 30 million, 20-year ESAL range.

**4.2.5 Evaluation of Locking Point**

The locking point concept was first developed for Illinois DOT (45, 46). The Illinois definition of the locking point is the first instance of three consecutive gyrations having the same sample height immediately preceded by two instances of two consecutive gyrations resulting in the same sample height (locking point 3-2-2), as shown in Figure 4.29. Other agencies have used different definitions of the locking point: (1) the first instance of two consecutive gyrations resulting in the same sample height (locking point 2), as shown in Figure 4.30; (2) the second instance of two consecutive gyrations resulting in the same sample height (locking point 2-2), as shown in Figure 4.31; and (3) the third instance of two consecutive gyrations resulting in the same sample height (locking point 2-2-2), as shown in Figure 4.32. One general criticism of the locking point concept is that there is little research to tie the results to a physical quantity in the field.

Table 4.16 shows the locking point for each of the cases described above. One encouraging aspect of the locking point calculations was that the locking point was approximately the

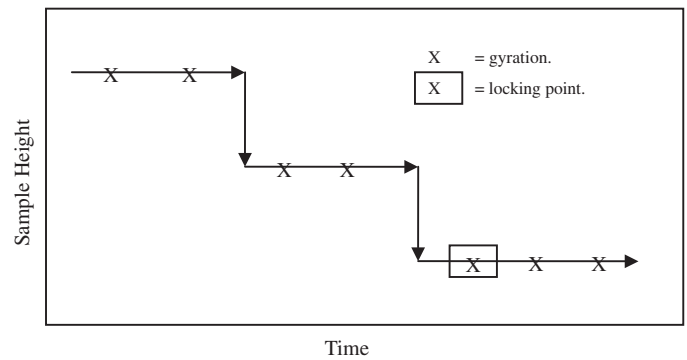


**Figure 4.29. Illinois definition of locking point—locking point 3-2-2.**

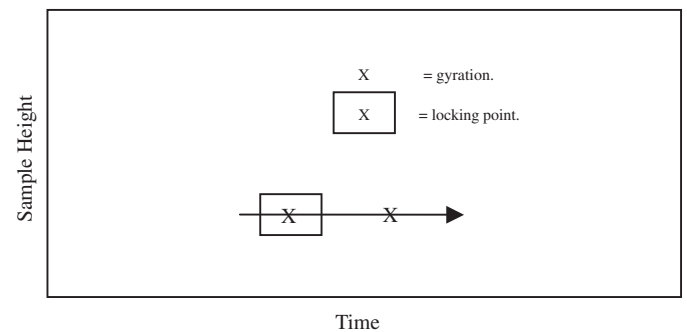


**Figure 4.30. Different locking point definition—locking point 2.**

same number of gyrations for both the Pine and Troxler SGCs without any adjustments, as shown in Figure 4.33. However, as shown in Figure 4.34, the density at a given definition of the locking point was higher for the Pine compactor if the data are not corrected to a DIA of 1.16 degrees. There was almost no relationship ( $R^2 = 0.14$ ) between the agency-specified

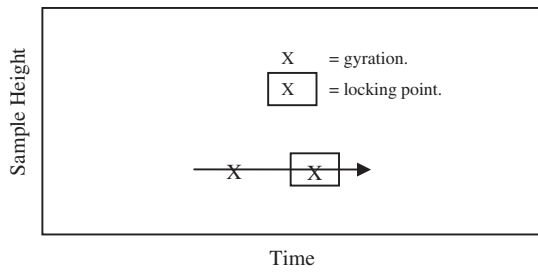


Figure 4.31. Different locking point definition—locking point 2-2.

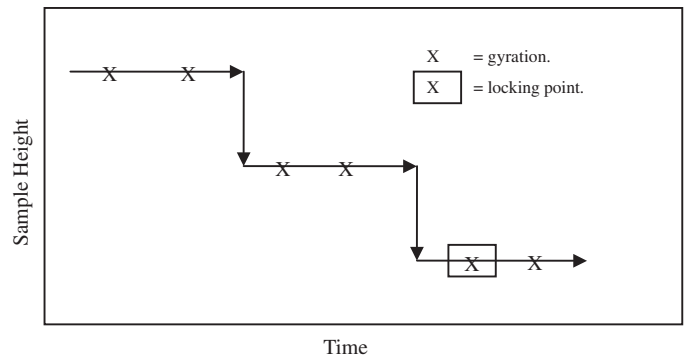
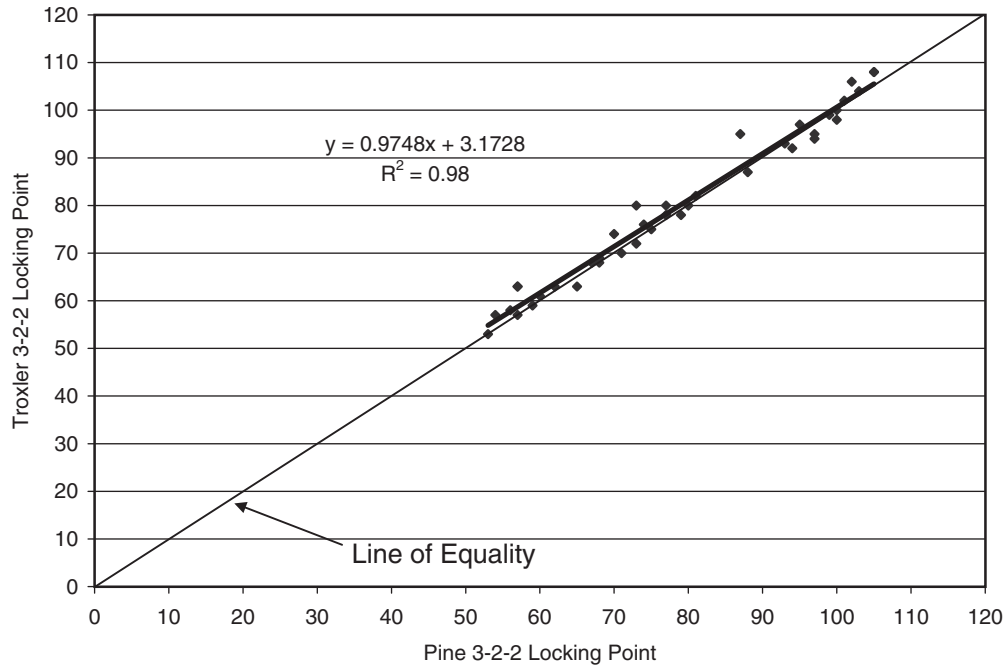


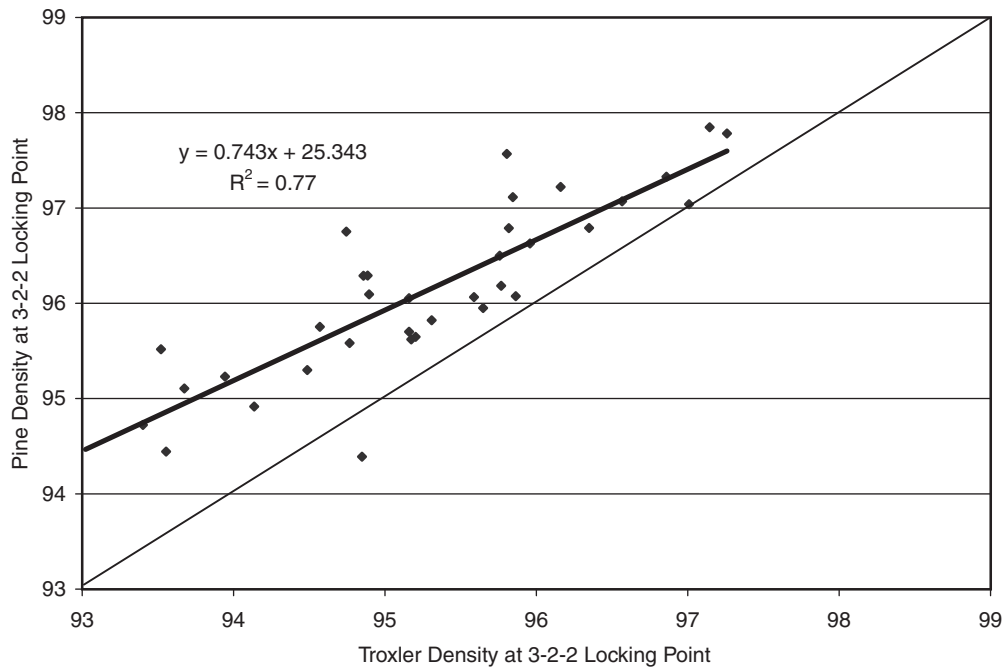
Figure 4.32. Different definition of locking point—locking point 2-2-2.

Table 4.16. Locking point (LP) values.

Project	20-Year ESALs	Agency N <sub>design</sub>	Pine LP 2	Troxler LP 2	Pine LP 2-2	Troxler LP 2-2	Pine LP 2-2-2	Troxler LP 2-2-2	Pine LP 3-2-2	Troxler LP 3-2-2
KY-1	53,706	50	60	61	65	66	69	70	95	97
KY-3	84,028	75	42	42	47	47	50	50	71	70
AL-6	143,958	95	35	34	39	39	42	42	57	57
NE-3	365,719	76	31	31	35	36	38	39	53	53
NE-1	383,385	68	34	34	38	38	40	41	54	57
CO-3	523,624	109	47	49	51	53	55	57	73	80
CO-4	720,911	86	45	46	49	53	54	56	77	80
CO-1	756,789	68	37	39	41	44	44	47	57	63
UT-1	771,982	75	47	48	52	53	55	56	74	76
FL-1	811,658	86	45	46	50	51	54	55	75	75
CO-2	1,017,593	86	39	41	43	45	46	49	57	63
CO-5	1,017,593	86	47	46	53	52	56	56	80	80
MI-2	1,250,146	75	49	48	54	53	58	58	81	82
NE-2	1,450,960	96	38	39	42	44	46	47	67	68
MI-3	1,515,200	75	40	39	45	45	49	48	68	69
AL-5	1,809,675	75	35	37	39	41	42	44	56	58
IN-1	1,850,992	100	58	58	63	64	68	69	99	99
TN-1	3,490,393	100	37	35	41	39	45	43	65	63
AL-2	3,610,001	100	60	63	65	67	69	71	103	104
AL-4	4,899,406	100	36	37	41	42	44	44	62	63
AL-1	6,748,142	106	52	53	58	56	61	62	88	87
GA-1	8,803,521	100	37	37	41	42	44	45	60	61
AL-3	8,861,352	100	42	44	46	49	50	53	70	74
KS-1	10,075,962	100	46	46	51	52	55	56	77	78
KY-2	12,438,605	100	63	62	69	69	73	73	105	108
MO-2	12,517,675	100	61	60	66	66	71	71	101	102
WI-1	14,614,748	100	45	44	49	49	53	53	79	78
MI-1	15,966,398	125	58	58	63	64	68	68	94	92
NE-4	20,084,248	109	41	41	45	46	49	49	68	68
IL-1	26,285,917	90	61	62	65	65	70	69	100	98
MO-1	27,546,007	125	62	60	68	65	73	71	105	108
IL-3	44,466,336	105	55	62	60	67	66	71	100	100
IN-2	45,150,555	125	41	41	46	47	50	51	73	72
IL-2	46,344,297	90	59	58	64	64	69	69	97	95
AR-1	48,726,562	125	55	58	60	64	64	67	93	93
MO-3	53,683,941	125	60	60	66	66	70	71	102	106
NC-1	73,918,507	125	35	36	39	39	42	43	59	59
AR-2	91,370,805	125	60	60	65	66	69	70	97	94
AR-4	97,890,077	125	47		52		56		84	
AR-3	170,842,507	125	49	57	54	62	59	66	87	95



**Figure 4.33. Comparison between 3-2-2 Pine and Troxler locking points.**



**Figure 4.34. Comparison of average Pine and Troxler densities at 3-2-2 locking points.**

$N_{\text{design}}$  and the 3-2-2 locking point. Inspection of Table 4.16 shows that the 3-2-2 locking point was closest to  $N_{\text{design}}$  for the Illinois projects, where the locking point concept was developed.

Comparisons were made between the calculated density at the four different definitions of the locking point and the as-constructed and 2-year in-place densities. The 2 locking point

overestimated the as-constructed density, as seen in Figure 4.35. The 3-2-2 locking point appears to provide the best relationship with ultimate density, as shown in Figure 4.36. However, the relationship is weaker than that determined using design traffic. Various subdivisions of unmodified and modified binder were attempted, since binder stiffness should not affect the results during compaction. The best relationship

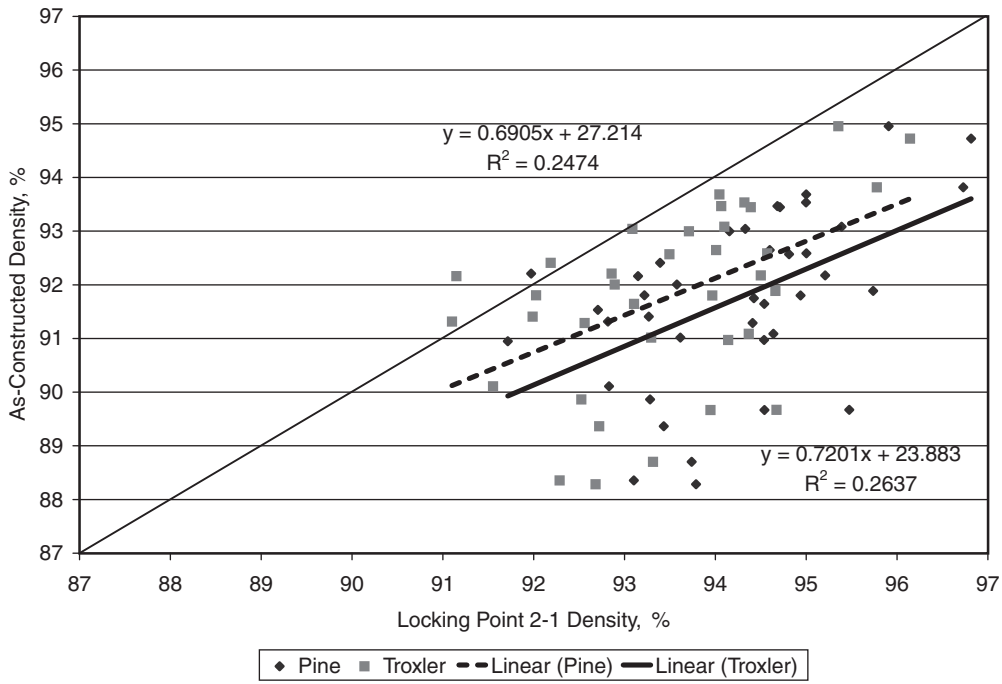


Figure 4.35. 2 locking point density versus as-constructed density.

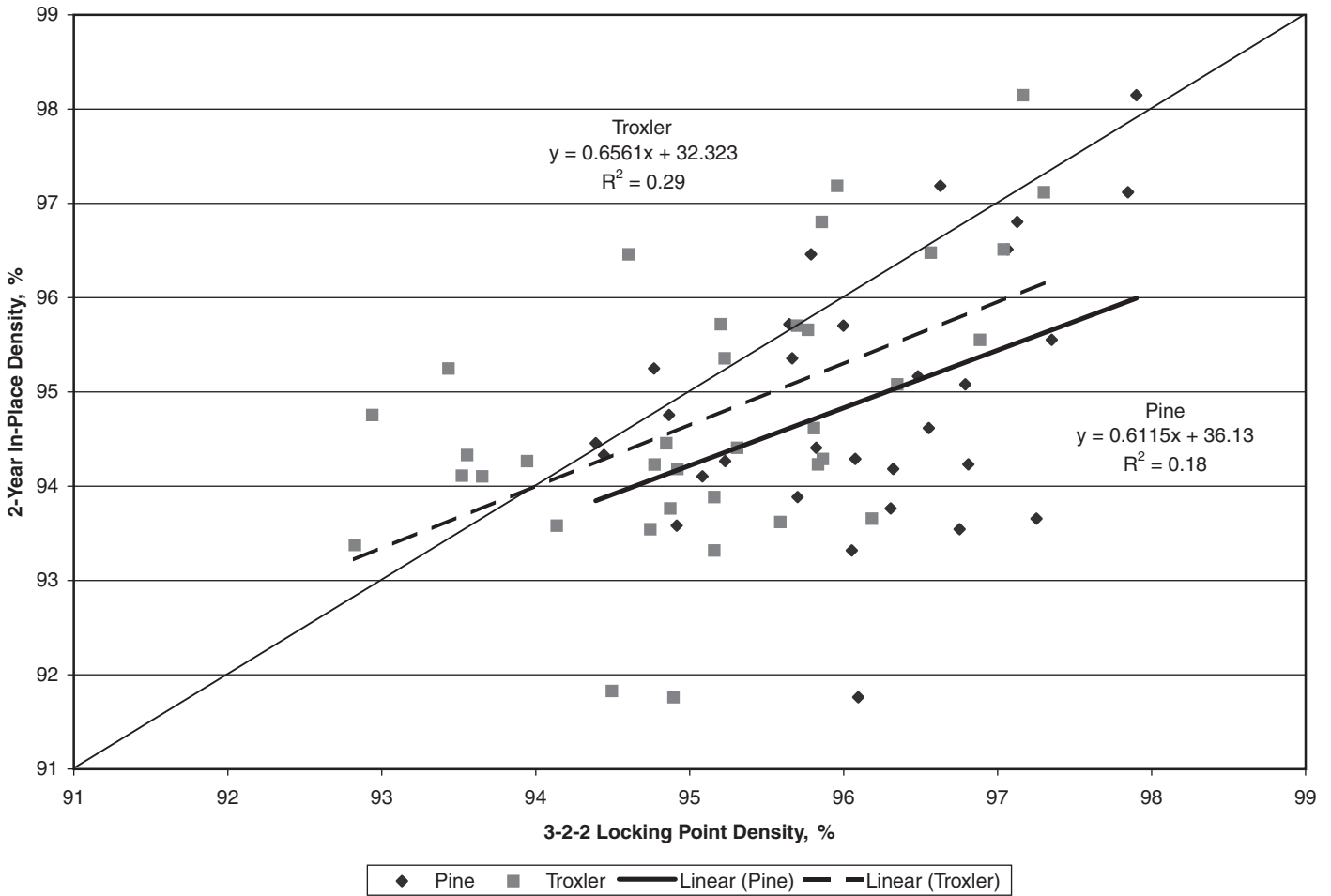


Figure 4.36. 3-2-2 locking point density versus 2-year density.

( $R^2 = 0.47$ ) was determined for the projects with modified binders based on the Troxler densities for the 3-2-2 locking point. However, 3 of the 20 projects—AR-3, AR-4, and IL-2—had missing data, which prevented their inclusion.

The use of the 3-2-2 locking point appears to be a conservative way to estimate the ultimate density of the pavement. However, one potential concern about the use of the locking point is the lubricating effect of binder content on the number of gyrations determined for the locking point. If the asphalt content selected for the locking point determination is on the dry portion of the VMA curve, then the locking point may be higher, whereas if it is on the wet side, then the locking point may be lower than or close to the locking point at the optimum asphalt content. An evaluation of the locking point over a range of binder contents is beyond the scope of this study. Also, the locking point appears to be a function of the aggregate type, angularity, and gradation and is not related to the design traffic. Table 4.17 summarizes the 3-2-2 locking point values by primary aggregate type. Harder aggregates, such as granite, produce lower locking points than softer or more friable aggregates, such as limestone or sandstone. Obviously, a wide range of materials meet the description of gravel or limestone.

**4.2.6 Pavement Condition After 4 Years**

Visual assessments were conducted along with the pavement coring at each coring interval (see Appendix C). Rut depths were measured with a 6-ft string line. Table 4.18 presents the 4-year rut depth measurements. The maximum observed rutting averaged 6.4 mm. The average rutting observed for all of the projects was 1.7 mm. The Superpave mixes were all very rut resistant. Fourteen projects showed noticeable raveling; 13 projects showed cracking; 13 projects had popouts; and 7 projects showed moisture damage in either the test layer or the underlying layer.

The rut depths from the field projects match the findings of the 2000 NCAT Test Track. Brown et al. (52) reported an average rut depth after 10 million ESALs in 2 years of 2.7 mm, with a maximum rut depth of 7.4 mm. The two sections with

**Table 4.18. Four-year rut depth measurements, mm.**

Project	Sublot 1			Sublot 2			Sublot 3			Avg., mm	Std. Dev., mm
	Core Location										
	1	2	3	1	2	3	1	2	3		
AL-1	2	2	2	2	1	3	-	-	-	2.0	0.83
AL-2	3	2	2	0	0	2	5	5	6	2.7	2.03
AL-3											
AL-4											
AL-5											
FL-1											
MI-1	10	9	9	6	7	7	3	2	4	6.4	2.60
MI-2	2	2	2	1	0	2	-	-	-	1.3	0.82
WI-1	0	0	0	0	0	0	0	0	0	0.0	0.00
CO-1	3	2	4	5	5	3	7	6	7	4.8	1.77
CO-2	1	2	2	2	3	3	3	3	3	2.6	0.79
CO-3	0	0	0	0	0	0	-	-	-	0.0	0.00
CO-4	2	1	1	2	2	1	2	2	2	1.5	0.62
CO-5	3	2	2	5	5	5	4	3	3	3.6	0.98
IN-1	2	3	2	0	0	2	3	5	2	2.2	1.53
IN-2	3	2	2	5	3	4	3	2	2	3.0	0.95
KY-1	0	0	0	0	0	0	-	-	-	0.0	0.00
KY-2	1	2	0	0	0	0	-	-	-	0.4	0.66
KY-3	1	0	0	0	0	1	0	0	0	0.2	0.37
AL-6	0	0	0	0	0	0	-	-	-	0.0	0.00
AR-1	2	2	2	2	2	2	2	2	2	1.9	0.40
AR-2	3	2	3	3	3	2	-	-	-	2.8	0.66
AR-3	3	3	2	2	1	3	-	-	-	2.2	1.06
AR-4	2	2	2	2	2	2	2	2	2	2.1	0.40
GA-1	1	1	1	1	1	0	2	1	0	0.7	0.48
IL-1	0	1	0	1	1	1	0	0	1	0.4	0.42
IL-2	1	3	2	3	3	3	3	2	2	2.6	0.79
IL-3	0	0	0	0	0	1	1	2	2	0.5	0.69
KS-1	1	0	1	1	2	2	2	1	1	1.0	0.53
MI-3	0	0	0	0	0	0	0	0	0	0.0	0.00
MO-1	1	2	1	2	1	3	4	1	2	1.9	1.19
MO-2	2	2	2	1	1	2	3	2	2	1.7	0.74
MO-3	0	0	0	1	0	0	0	0	0	0.1	0.26
NC-1	6	2	2	1	2	2	1	2	1	2.0	1.73
NE-1	2	5	4	2	2	2	-	-	-	2.5	1.46
NE-2	1	1	1	2	2	2	2	2	2	1.5	0.62
NE-3	2	2	2	2	2	2	2	2	2	2.2	0.35
NE-4	1	1	2	2	2	4	2	2		1.8	1.02
TN-1	2	2	2	3	2	3	2	2	1	2.0	0.80
UT-1	0	0	0	0	0	0	0	0	0	0.0	0.00

Blank cells signify that the 4-year data were not collected. Dashes signify that only two samples were taken at the time of construction.

the most rutting, N3 (7.4 mm) and N5 (7.1 mm), were both placed with asphalt contents approximately 0.5 percent above optimum. Brown et al. also noted that sections containing PG 76-22 rutted 60 percent less than sections constructed with unmodified PG 67-22. The majority of the observed rutting was attributed to pavement densification under traffic.

**4.2.7 Evaluation of  $N_{initial}$**

Table 4.19 shows the densities at  $N_{initial}$  corrected to a DIA of 1.16 degrees. The table is sorted by 20-year traffic. AASHTO M 323-04 specifies that the density at  $N_{initial}$  be less than 91.5 percent for 20-year traffic levels less than 0.3 million ESALs, less than 90.5 percent for traffic levels between 0.3 million and 3 million ESALs, and less than 89.0 percent

**Table 4.17. 3-2-2 Locking point by aggregate type.**

Aggregate Type	N	Average	Standard Deviation
Granite	4	63	7.6
Gravel	18	72	12.8
Dolomite	2	87	13.9
Limestone	9	93	15.4
Sandstone	3	96	6.5
Slag	1	99	NR

NR = no measurement required.

**Table 4.19. Summary of densities, %G<sub>mm</sub>, at N<sub>initial</sub>.**

Project	20-Year ESALs	Gradation	N <sub>initial</sub>	Pine			Troxler		
				1	2	3	1	2	3
KY-1	53,706	C	6.0	85.3	84.9	-	85.1	84.5	-
KY-3	84,028	F	7.0	88.8	89.1	88.9	88.8	88.6	88.6
AL-6	143,958	F	8.0	90.8	91.0	-	90.6	91.0	-
NE-3	365,719	F	7.0	90.5	91.7	90.8	90.5	92.1	91.3
NE-1	383,385	F	7.0	90.4	91.9	-	90.7	91.9	-
CO-3	523,624	C	8.0	87.8	88.3	-	88.1	88.3	-
CO-4	720,911	F	7.0	88.4	88.9	87.3	88.3	88.4	87.6
CO-1	756,789	F	7.0	90.6	92.3	91.5	90.4	91.9	91.2
UT-1	771,982	F	7.0	87.9	88.8	88.9	87.7	88.5	88.8
FL-1	811,658	C	7.0	85.8	87.9	-	86.1	87.1	-
CO-2	1,017,593	F	7.0	91.9	90.8	90.9	91.8	91.0	90.8
CO-5	1,017,593	F	7.0	87.5	87.9	87.6	87.3	87.5	87.4
MI-2	1,250,146	F	7.0	87.8	88.4	87.9	87.9	88.1	87.9
NE-2	1,450,960	F	8.0	89.4	89.6	89.7	89.6	90.1	89.8
MI-3	1,515,200	F	7.0	88.8	89.0	-	88.5	88.8	-
AL-5	1,809,675	C	7.0	91.2	91.1	90.9	90.9	90.4	91.0
IN-1	1,850,992	C	8.0	84.3	85.8	85.8	84.3	85.2	85.2
TN-1	3,490,393	F	8.0	89.9	90.2	90.0	91.3	90.8	90.4
AL-2	3,610,001	C	8.0	85.5	84.3	83.9	84.9	83.7	83.4
AL-4	4,899,406	C	8.0	88.6	88.9	89.2	88.7	88.7	89.0
AL-1	6,748,142	C	8.0	86.9	85.9	86.0	87.1	86.1	86.2
GA-1	8,803,521	F	8.0	91.1	91.9	91.8	91.6	92.1	91.4
AL-3	8,861,352	C	8.0	88.9	89.1	-	88.8	89.1	-
KS-1	10,075,962	F	8.0	86.4	88.1	87.3	86.7	87.9	87.1
KY-2	12,438,605	C	8.0	81.3	84.8	-	80.9	84.4	-
MO-2	12,517,675	C	8.0	NA	86.2	84.5	85.6	86.5	84.1
WI-1	14,614,748	C	8.0	87.0	87.5	87.6	86.4	87.5	87.6
MI-1	15,966,398	C	9.0	84.3	85.0	84.2	83.7	84.3	84.0
NE-4	20,084,248	F	8.0	90.1	90.6	90.0	89.7	90.6	90.2
IL-1	26,285,917	C	8.0	83.8	84.5	84.2	84.0	83.9	84.0
MO-1	27,546,007	C	9.0	84.6	85.9	86.1	86.0	86.4	85.7
IL-3	44,466,336	C	8.0	83.6	84.0	83.3	84.7	84.7	84.2
IN-2	45,150,555	C	9.0	88.7	88.5	87.1	88.1	88.4	86.9
IL-2	46,344,297	C	8.0	84.5	86.2	86.1	85.3	87.0	86.8
AR-1	48,726,562	C	9.0	85.0	86.8	86.1	85.0	86.5	86.0
MO-3	53,683,941	C	9.0	85.5	86.5	86.4	85.6	86.4	86.4
NC-1	73,918,507	F	9.0	89.7	89.3	89.2	89.2	87.7	88.8
AR-2	91,370,805	C	9.0	85.7	85.3	-	85.3	85.5	-
AR-4	97,890,077	C	9.0	85.5	86.3	86.2	85.7	85.9	86.3
AR-3	170,842,507	C	9.0	87.5	85.5	-	84.7	86.0	-

Dashes signify that only two samples were taken at the time of construction. NA signifies that results were not available.

for traffic levels greater than 3 million ESALs. As shown in Table 4.19, none of the samples from projects with design traffic less than 0.3 million ESALs fail N<sub>initial</sub>, 36 percent of the samples with design traffic levels between 0.3 million and 3 million ESALs fail N<sub>initial</sub>, and 26 percent of the samples with design traffic levels greater than 3 million ESALs fail N<sub>initial</sub>. Failures occur in 11 of the 40 projects. The mixes are fine-graded for 9 of the 11 projects that fail N<sub>initial</sub>. Both of the coarse-grade projects, AL-3 and AL-5, had lower laboratory air voids at the agency-specified N<sub>initial</sub> level. Both projects averaged 3.0 percent air voids. Project GA-1 also had low air voids (1.9 percent) at the agency-specified N<sub>initial</sub> gyrations.

The field notes taken at the time of construction indicate tender mix problems for only one project, NE-4 (which fails

the N<sub>initial</sub> requirements). However, construction issues were not commented on at all for many of the projects, so it is possible that there were tender mix problems on other projects. Historically, contractors have found ways to deal with tender mixes in the field.

When the Superpave system was first introduced, the N<sub>initial</sub> requirements worked in conjunction with the restricted zone requirements and the fine aggregate angularity requirements to limit the amount of natural sand or rounded fine aggregate particles in HMA. The restricted zone requirement has been eliminated because it was demonstrated that well-performing mixes frequently passed through the restricted zone. N<sub>initial</sub> is sensitive to gradation and the presence of rounded fine aggregate particles.

**Table 4.20. Summary of densities, %G<sub>mm</sub>, at N<sub>maximum</sub>.**

Project	N <sub>maximum</sub>	Pine			Troxler		
		1	2	3	1	2	3
AL-1	169	98.5	97.5	97.6	98.9	98.0	97.8
AL-2	160	97.7	97.0	97.2	98.3	96.3	96.4
AL-3	160	97.9	97.7	-	98.0	98.7	-
AL-4	160	95.5	96.2	97.0	95.3	96.0	97.1
AL-5	115	98.1	98.0	97.8	98.4	97.8	98.2
FL-1	134	95.6	97.0	-	95.0	96.5	-
MI-1	205	97.4	98.5	97.4	96.1	97.4	96.3
MI-2	115	97.9	98.4	98.0	97.3	97.9	97.5
WI-1	160	96.2	97.2	97.3	95.9	96.5	97.0
CO-1	104	98.8	99.9	98.8	98.5	100.0	99.0
CO-2	134	99.4	99.5	99.4	99.5	99.4	99.4
CO-3	174	98.8	98.9	-	98.7	99.2	-
CO-4	134	98.7	98.7	97.9	98.3	98.3	97.8
CO-5	134	97.5	97.9	97.8	96.8	97.3	97.1
IN-1	160	97.4	98.7	98.6	96.2	97.6	97.4
IN-2	205	98.2	98.8	97.2	97.5	97.9	96.5
KY-1	75	96.7	96.8	-	95.8	95.5	-
KY-2	160	94.9	98.4	-	93.5	97.2	-
KY-3	115	97.0	97.5	97.8	96.7	96.8	97.2
AL-6	150	97.2	97.8	-	97.4	98.0	-
AR-1	205	97.3	99.5	98.4	97.5	99.0	98.9
AR-2	205	97.5	98.4	-	97.8	98.5	-
AR-3	205	96.8	97.8	-	97.3	99.2	-
AR-4	205	95.8	96.5	96.3	95.8	96.5	96.9
GA-1	160	98.3	99.1	98.3	98.1	100.0	99.1
IL-1	140	96.5	97.4	97.3	96.3	96.7	96.8
IL-2	140	96.7	98.7	98.5	98.1	99.7	99.4
IL-3	165	95.7	96.6	96.3	97.1	97.6	97.7
KS-1	160	96.9	96.2	96.5	96.2	96.8	96.6
MI-3	115	97.0	97.0	-	96.6	96.5	-
MO-1	205	99.0	100.0	100.0	100.0	100.0	100.0
MO-2	160	NA	98.5	97.6	98.6	99.3	97.8
MO-3	205	99.5	100.0	100.0	99.9	100.0	100.0
NC-1	205	97.1	96.5	95.9	96.5	96.3	96.9
NE-1	104	96.5	97.8	-	97.0	98.4	-
NE-2	152	97.0	97.6	97.4	97.3	97.9	97.7
NE-3	117	96.6	97.6	96.9	96.9	98.2	97.3
NE-4	174	98.5	98.9	98.4	99.0	99.4	98.5
TN-1	160	97.9	97.7	97.7	98.6	98.5	98.4
UT-1	115	97.9	99.0	98.7	97.4	98.7	98.6

Dashes signify that only two samples were taken at the time of construction. NA signifies that results were not available.

#### 4.2.8 Evaluation of N<sub>maximum</sub>

Table 4.20 shows the densities at N<sub>maximum</sub> corrected to a DIA of 1.16 degrees. AASHTO M 323 specifies that the density at N<sub>maximum</sub> be less than 98 percent. At the agency-specified N<sub>maximum</sub>, 36 percent of the Pine samples and 40 percent of the Troxler samples failed the N<sub>maximum</sub> density criterion. One or more samples exceeded the maximum density at N<sub>maximum</sub> for 25 of the 40 projects. When NCAT collected the field data, samples were compacted to both 100 and 160 gyrations. Therefore, sample densities for N<sub>maximum</sub> gyrations greater than 160 are extrapolated. Although there is a very good relationship between sample density and log of gyrations, at high gyration levels (above the mixture's locking point and N<sub>design</sub>) this relationship tends to break down with additional gyra-

tions, thereby producing little increase in sample density. The sample densities at N<sub>maximum</sub> are extrapolated above N<sub>maximum</sub> for 10 of the 25 projects that failed the density requirements at N<sub>maximum</sub>. These extrapolations may be erroneous. However, this still leaves 15 of 40 projects that failed N<sub>maximum</sub>. The maximum rutting for a sample that failed density at N<sub>maximum</sub> occurred for project MI-1, subplot 2, with an average rut depth of 7 mm after 4 years of traffic. Subplot 1 of MI-1 actually had a slightly higher average rut depth (9 mm), but the sample did not fail the N<sub>maximum</sub> density criterion. Further, as evidenced by Table 4.18, all of the mixes have been extremely rut resistant. Based on the data, the N<sub>maximum</sub> criterion should be eliminated.

#### 4.2.9 Summary and Discussion of Test Results

The asphalt content of HMA mixture, as-constructed density, and ultimate density are all critical to the performance of an HMA pavement. These values are all interrelated because mixes with higher asphalt contents, for a given aggregate structure, are generally easier to compact initially and will tend to densify more under traffic. The determination of an HMA mixture's optimum asphalt content has changed significantly since the first asphalt pavements were introduced in the 1870s. Optimum asphalt contents were initially selected by experience. As the popularity of HMA grew, there were not enough experienced individuals to determine the optimum asphalt content for all of the HMA mixtures being placed. In the late 1930s and 1940s, asphalt technologists began to develop laboratory compaction methods, with the goal of matching the ultimate pavement density. It had been observed that an HMA pavement densified under traffic from its as-constructed density to an ultimate density, typically within 2 to 3 years after construction. Initially, only one laboratory compaction level was used for a given system, but as tire pressures and traffic volumes grew, the concept of a tiered design system was developed where laboratory compaction increased with increasing tire pressures or traffic volumes. The concept of a tiered laboratory compaction was to address the tendency for increased tire pressure or traffic volumes to produce a denser aggregate skeleton. However, if the laboratory compaction effort was too high, it could be difficult for the contractor to achieve the required as-constructed density in the field. A general summary of the historical HMA mix design philosophy would be to put as much asphalt in a mix as possible without compromising rut resistance. Hveem (5) suggested using just enough asphalt to allow adequate compaction in the field with the equipment available. Marshall was quoted as emphasizing the importance of designing the densest (i.e., minimum VMA) possible aggregate structure (6).

A tiered system was adopted for the Superpave mix design system. In the Superpave mix design system, minimum required aggregate properties, such as angularity, recommen-

dations for high-temperature binder grade, volumetric properties, and laboratory compaction effort, all change with design traffic levels.

Brown and Buchanan (2, 39) demonstrated that, for a given gradation, VMA was reduced approximately 1 percent when the  $N_{\text{design}}$  level was increased by 30. Thus, a mixture designed for minimum VMA at an  $N_{\text{design}}$  level of 125 would be expected to have a measured VMA of approximately 2 percent above the value at 125 gyrations when compacted to 75 gyrations. Thus, higher  $N_{\text{design}}$  levels tend to force the aggregate gradation away from the maximum density line. If traffic does not densify these mixtures to as dense of an aggregate structure as the SGC, then the mix gradation may be coarser or finer than is needed. Cooley et al. (56) discussed the influence of gradation on pavement permeability. Coarser mixes tend to be more permeable at a given pavement density than finer mixes. It is also expected that as the  $N_{\text{design}}$  level is increased, more compaction effort is required to achieve acceptable density in the field, though this has been difficult to quantify.

It should be noted that asphalt content is generally considered to be independent of  $N_{\text{design}}$  (although dependent for a given mix) and dependent on the design (i.e., minimum) VMA and air void content. However, Watson et al. (43) indicated that the average design VMA for Georgia DOT mixes, using similar aggregates, was higher for Marshall-designed mixes than for Superpave mixes, even though the minimum VMA requirements were the same in both cases. If  $N_{\text{design}}$  levels are too high, the designer is forced to design closer to the minimum VMA requirement and cannot allow a cushion for production variability.

The field data from this study indicated that the as-constructed density, based on cores, for 55 percent of the projects tested was less than 92 percent of  $G_{\text{mm}}$ . Statistical analyses indicated that the agency specifications or practices significantly affected the as-constructed density. Two of the agencies with the best as-constructed densities, Colorado DOT and Georgia DOT, have specifications that tend to increase the asphalt content of the mixture. Colorado DOT designs with 100-mm-diameter SGC molds. Samples compacted in 100-mm-diameter molds tend to result in lower sample densities than samples compacted in 150-mm-diameter molds for the same number of gyrations. Georgia DOT will field-adjust a mixture's asphalt content in order to ensure specified levels of as-constructed density.

The field projects reached their ultimate density after 2 years of traffic, as indicated by the fact that the in-place densities did not change between 2 years and 4 years of trafficking. The majority of the densification occurred in the first 3 months. The month in which the project was constructed significantly affected the amount of densification that occurred. Projects constructed in the month of May

tended to densify the most (approximately 4.0 percent). Projects constructed in April or June on average densified approximately 0.5 percent less than those constructed in May. Projects constructed in July or August densified slightly less than the average of all of the projects, approximately 3.0 percent. Projects constructed in September or October densified the least, an average of approximately 2.3 percent. High-temperature PG or the number of high-temperature PG bumps as compared with the climatic PG significantly affected pavement densification. Mixes containing PG 76-22 or with two high-temperature PG bumps densified less than softer binders.

The majority of the samples from the field projects did not achieve the laboratory air void content at the agency-specified  $N_{\text{design}}$  level (Figure 4.19). At a laboratory air void content of 4 percent, the average in-place air void content was 5.5 percent after 2 years of traffic. This indicates that the laboratory compaction effort is higher than the combined compaction during construction and from traffic. Brown et al. (52) showed that mixtures designed to 100 gyrations at the 2000 NCAT Test Track compacted to their ultimate density when 10 million ESALs were applied in 2 years. This equates to more than 100 million ESALs for a 20-year design life, indicating that the mixes should have been designed at 125 gyrations using the AASHTO R35-04  $N_{\text{design}}$  table. Further, the mixes were designed using an SGC with a low (approximately 1.02) DIA, which would provide less laboratory compaction than an SGC set to a DIA of  $1.16 \pm 0.02$  degrees.

Three different analyses were used to try and determine where the  $N_{\text{design}}$  levels should be set. In the first analysis, the numbers of gyrations to match the 2-year (i.e., ultimate) in-place densities were related to the accumulated traffic. The two different compactors used in the study produced backcalculated  $N_{\text{design}}$  values that differed by approximately 20 gyrations. These differences were attributed to differences in the DIA for the two compactors. AASHTO (4) has adopted a DIA of  $1.16 \pm 0.02$  degrees as an alternative to an external angle of gyration of  $1.25 \pm 0.02$  degrees. The data were adjusted to a DIA of 1.16 degrees, and the resulting backcalculated  $N_{\text{design}}$  values for the two SGCs compared well (Figure 4.16).

A relationship was developed between log of design traffic (ESALs) and the log of  $N_{\text{design}}$ . There was a good deal of scatter in the data, but this was expected based on the literature review. The exclusion of projects constructed with PG 76-22 improved the relationship. Using this relationship, the  $N_{\text{design}}$  values for the currently specified traffic levels could be calculated. The best fit line ( $R^2 = 0.57$ ) indicated reduced gyration levels at all traffic levels (Figure 4.24). The high side of the 80-percent prediction interval approximated the currently specified  $N_{\text{design}}$  levels (Table 4.10). The 80th percentiles for the projects within each category were also calculated; these percentiles also indicated reduced  $N_{\text{design}}$  levels, though the

reduction in the 0.3 million to 1 million ESAL category was minimal. The original  $N_{\text{design}}$  levels were determined using the best fit of the data, without any adjustment for the confidence or prediction interval (34). Several projects that could not clearly be identified as outliers were excluded from this analysis, as was the use of modified binders.

The second analysis looked at the predicted gyrations to match the in-place density at each of the sampling periods (3 months, 6 months, 1 year, 2 years, and 4 years). The original  $N_{\text{design}}$  table was determined by a log-log regression analysis between the gyrations to match the as-constructed density and the density after 12 or more years of traffic and accumulated ESALs (Figure 4.26). This second analysis is then closer to what was originally done to determine the  $N_{\text{design}}$  levels. This second analysis indicated design gyration levels (Table 4.11) close to those currently specified by AASHTO R 35. However, there is a tremendous amount of scatter in the data ( $R^2 = 0.37$  for Pine compactor and  $R^2 = 0.34$  for Troxler compactor).

The third analysis attempted to reduce the scatter in the data and to adjust the data for the effect of as-constructed density. As noted previously, 55 percent of the projects had as-constructed densities less than 92 percent. It was demonstrated that the as-constructed density affected the 2-year, or ultimate, density. Models were developed to relate the 2-year percentage of laboratory density at 100 gyrations to as-constructed density, high PG, and accumulated ESALs. It was found that the predicted gyrations to match a given percentage of laboratory density represented a small range, with a standard deviation between 3.44 and 8.99 gyrations. A matrix of expected percentages of laboratory density was developed based on high PG and traffic (Table 4.12). The as-constructed density was set to 92 percent in all cases. The number of gyrations to match the percentage of laboratory density determined in the matrix was calculated for each of the projects. Equations 9 and 10 were then developed to relate the average gyrations determined to match the in-place densities to high PG and traffic, assuming an as-constructed density of 92 percent. Table 4.15 summarizes these results, which are similar to the results determined using the first analysis (Table 4.10).

Rut depth measurements were taken in the field at the 2-year and 4-year sampling intervals. A maximum average rut depth for a project after 4 years of traffic was 7.4 mm, with an overall average of 2.7 mm. The rut depth measurements alone support lowering the  $N_{\text{design}}$  levels because, even at 95-percent reliability, 2 of 40 pavements would be expected to have unacceptable levels of rutting. Similar findings were reported for the 2000 NCAT Test Track. It was also noted that sections constructed with PG 76-22 at the 2000 NCAT Test Track rutted 60 percent less than sections constructed with PG 67-22. Most of the rutting at the 2000 NCAT Test Track was attributed to pavement densification.

Combined, these data indicate that the  $N_{\text{design}}$  levels can be reduced. As noted previously, the predicted  $N_{\text{design}}$  levels change very rapidly at 20-year design traffic levels less than 3 million ESALs; therefore, caution must be used at this traffic level. Though lower  $N_{\text{design}}$  values than currently specified are recommended based on the first analysis for the lowest traffic levels (Table 4.10), there is little or no experience with these levels. Further, density and, therefore, optimum asphalt content can change very rapidly at lower gyration levels. If the levels are too low, the compacted samples are not stable immediately after compaction. Therefore, it is recommended that 50 gyrations be maintained for the lowest traffic levels.

The combined data from the field projects and the 2000 NCAT Test Track indicate that a maximum  $N_{\text{design}}$  level of 100 gyrations will provide good performance for very high traffic levels. This is a 25-gyration decrease from the currently specified levels. This reduction is also supported by the  $N_{\text{design}}$  II Experiment (3), which suggested that there was virtually no difference in shear stiffness for mixes designed at 100 and 130 gyrations.

Of the various approaches considered to evaluate  $N_{\text{design}}$ , two approaches were considered to recommend new  $N_{\text{design}}$  levels. Both of these approaches were summarized above. The first approach used the relationship between accumulated ESALs and the number of gyrations to match the in-place density after 2 years of traffic, or ultimate density, for the unmodified projects (shown in Figure 4.24 and summarized in Table 4.10). The second approach used regression analysis to predict the in-place density after 2 years of traffic as a percentage of laboratory density based on as-constructed density, high PG, and log of accumulated ESALs after 2 years. A second analysis related the percentages of laboratory density to gyration levels (Equations 9 and 10 and Table 4.15). The second approach was selected to recommend new  $N_{\text{design}}$  levels. The second approach allowed the data to be corrected for the low as-constructed densities observed for 55 percent of the projects. The second approach could also be used to account for the effect of PG 76-XX or stiffer binders.

Table 4.21 summarizes the recommended  $N_{\text{design}}$  levels for all traffic levels. The values in Table 4.21 are based on Equations 9 and 10. The predicted values from Equation 9, which are presented in Table 4.15, were rounded in Table 4.21 to produce four levels. The largest rounding occurred at 30 million ESALs, where the predicted value was 88 and 86 based on Equations 9 and 10, respectively. The recommended  $N_{\text{design}}$  levels determined from Table 4.15 are slightly more conservative than the  $N_{\text{design}}$  levels recommended in Table 4.10. Values are presented for two ranges of binder stiffness: high-temperature PG less stiff than PG 76-XX and high-temperature PG of PG 76-XX or stiffer. The NCHRP Project 9-9(1) field studies did not indicate a clear differentiation in performance for the limited number of modified binders that did not meet PG 76-22.

**Table 4.21. Proposed  $N_{\text{design}}$  levels for an SGC DIA of  $1.16 \pm 0.02$  degrees.**

20-Year Design Traffic, ESALs	2-Year Design Traffic, ESALs	$N_{\text{design}}$ for binder < PG 76-XX	$N_{\text{design}}$ for binders $\geq$ PG 76-XX or mixes placed > 100 mm from surface
< 300,000	< 30,000	50	NR
300,000 to 3,000,000	30,000 to 230,000	65	50
3,000,000 to 10,000,000	230,000 to 925,000	80	65
10,000,000 to 30,000,000	925,000 to 2,500,000	80	65
> 30,000,000	> 2,500,000	100	80

The NCAT Test Track data (52) support the NCHRP Project 9-9 (2) recommendation to lower  $N_{\text{design}}$  when the layer is deeper than 100 mm from the surface. The 2000 NCAT Test Track data suggested a reduction in  $N_{\text{design}}$  of 37 gyrations between the surface lift and a lift 50 mm from the pavement surface.

In addition to the 20-year design traffic, a 2-year design traffic level is shown as an alternative for consideration. The 2-year ESALs were used to develop most of the relationships in this study. A 20-year design for a surface course is most likely unreasonably long. Further, the specified traffic growth rate has a large effect on the 20-year design traffic. The WesTrack experiment noted that rate of loading was important, especially for temporary pavements designed for short periods (64).

The 3-2-2 locking point values, determined from the field projects, are generally of the same magnitude, though not necessarily for the same mixes, as the unmodified  $N_{\text{design}}$  values proposed in Table 4.20. The minimum 3-2-2 locking point was 53 gyrations for project NE-3 with a gravel coarse aggregate, and the maximum 3-2-2 locking point was 108 gyrations for project KY-2 with a limestone coarse aggregate. The locking point values were distributed throughout the proposed gyration levels for unmodified binders. Ten projects

had a 3-2-2 locking point between 50 and 65 gyrations, 13 projects between 65 and 80 gyrations, 12 projects between 80 and 100 gyrations, and 5 projects more than 100 gyrations (108 maximum).

Huber and Anderson (44) provided an overview of the expected consequences of changing  $N_{\text{design}}$ , as shown in Table 4.22. The changes in aggregate properties would occur within the checks and balances provided by the consensus aggregate properties. The use of lower  $N_{\text{design}}$  levels will tend to allow mixtures to be designed with gradations closer to the maximum density line and still meet minimum VMA requirements. The use of lower  $N_{\text{design}}$  levels will tend to increase optimum asphalt contents slightly because contractors will most likely design with a slightly larger cushion above the minimum specified VMA. However, to ensure that the optimum asphalt contents increased, the minimum VMA requirements would also need to be increased. An increase in the minimum VMA requirements of 0.5 percent would result in an increase of approximately 0.2 percent in optimum asphalt content. Thus, the adoption of the recommended  $N_{\text{design}}$  levels in Table 4.21, along with an increase in minimum VMA of 0.5 percent, would have a combined effect of allowing somewhat denser gradations and increasing the optimum asphalt content slightly. Probably the most important outcome resulting from

**Table 4.22. Effect of design compaction on mixture properties (44).**

Property	Increased $N_{\text{design}}$	Decreased $N_{\text{design}}$
Coarse aggregate angularity	Increased demand for crushed aggregate	Reduced demand for crushed aggregate or no change
Fine aggregate angularity	Reduced natural sand	Reduced need for manufactured sand or no change
Gradation	Changed to increase VMA	Changed to reduce VMA or no change
Air voids	No effect	No effect
VMA	No effect after mix adjustment	No effect after mix adjustment
Voids filled with asphalt	Little or no change	Little or no change
Compaction on road	More difficult	Less difficult
Mixture stiffness	Increased stiffness	Decreased stiffness

a reduction in the  $N_{\text{design}}$  levels would be the fact that mixtures designed with lower  $N_{\text{design}}$  values would tend to be more compactable in the field. The reduction in mixture stiffness may be overstated. In the  $N_{\text{design}}$  II Experiment (3), for mixes designed at their respective gyration levels (70, 100, and 130 gyrations), there was essentially no difference in  $G^*_{(10 \text{ Hz}, 50 \text{ C})}$  between 130 and 100 gyrations and a 18- and 3-percent reduction in shear

stiffness between 100 and 70 gyrations for the limestone and gravel mixes, respectively. However, the shear stiffness of the gravel mixes averaged 34 percent less than the shear stiffness of the limestone mixes. The use of the locking point would tend to exacerbate this difference because the locking point values for limestone aggregates tended to be higher than for gravel aggregates.

---

## CHAPTER 5

# Conclusions and Recommendations

The three objectives of this research were (1) to evaluate the field densification of pavements designed using the Superpave mix design system, (2) to verify or determine the correct  $N_{\text{design}}$  levels, and (3) to evaluate the locking point concept. A wide range of climates, design traffic levels, PGs, lift-thickness-to-NMAS ratios, gradations, and aggregate types was included in this study.

The general goal of previous studies has been to determine the laboratory compaction effort that matches the ultimate density of the pavement after the application of traffic. Previous studies to determine or confirm laboratory compaction efforts have indicated a great deal of variability between field and laboratory compaction; therefore, variability was expected in this study. The variability in this study may have been exacerbated by three factors:

1. Field and traffic compaction are generally constant stress, while the SGC is a constant strain device.
2. The mixes sampled in this study contained a wide range of binder grades, which was not typical of previous studies.
3. The mixes in this study were designed under a tiered system of aggregate properties and  $N_{\text{design}}$  levels.

## 5.1 Conclusions

Based on the results from this research study, the following conclusions can be made.

1. Pavements appear to reach their ultimate density after 2 years of traffic. The average in-place density for all of the projects was the same at 2 and 4 years (94.6 percent of  $G_{\text{mm}}$ ). A fair relationship was determined between the as-constructed density and the density after 2 years of traffic. The majority of pavement densification, approximately 66 percent, occurs during the first 3 months after construction. Both the high PG and the high-temperature

bumps between the climatic and specified PG were found to significantly affect pavement densification, with stiffer binders resulting in less densification. The ultimate in-place densities of the pavements evaluated in this study were approximately 1.5 percent less than the densities of the laboratory-compacted samples at the agency-specified  $N_{\text{design}}$ .

2. The number of gyrations to match the ultimate in-place density was calculated for each project in this study. The calculated values for the two compactors used in this study differed by approximately 20 gyrations. This was attributed to differences in their DIA. The predicted gyrations adjusted to a DIA of 1.16 degrees showed good agreement between the two machines.
3. Several analyses were conducted to evaluate the  $N_{\text{design}}$  levels. Combined, these analyses indicated that the  $N_{\text{design}}$  levels could be reduced.
4. A relationship was also developed to relate the 2-year percentage of laboratory density at 100 gyrations to as-constructed density, high PG, and accumulated ESALs. It was found that the predicted gyrations to match a given percentage of laboratory density represented a small range, with a standard deviation of 3.44 to 8.99 gyrations. A matrix of expected percentages of laboratory density was developed based on high PG, traffic, and an as-constructed density of 92 percent. The numbers of gyrations to match the percentages of laboratory density determined in the matrix were calculated for all of the projects. An equation was then developed to relate the average gyrations determined to match the in-place densities to high PG and traffic. The predicted gyrations were very similar to those determined using the first analysis. However, this analysis accounted for the low as-constructed densities of some of the projects and the use of PG 76-XX or stiffer binders. It was found that  $N_{\text{design}}$  could be reduced by approximately 15 gyrations when PG 76-XX was specified. This methodology was used to recommend new  $N_{\text{design}}$  levels.

5. The locking point concept was evaluated as an alternative to  $N_{\text{design}}$ . The locking point values determined for the Pine and Troxler compactors were almost identical; however, densities at the locking point value (without adjustment to account for differing DIAs) were different. The density at the 3-2-2 locking point is weakly correlated to the ultimate density of the pavement. The locking point appears to be related to aggregate type, with softer aggregate producing higher locking point values.
6. All of the projects in this study were very rut resistant. The maximum observed rutting for the field projects was 7.4 mm, with an average rut depth for all of the projects of 2.7 mm after 4 years of traffic. Indications of durability problems suggested that increased asphalt contents would be beneficial.
7. The requirements for  $N_{\text{initial}}$  were evaluated based on the field project data. AASHTO M 35 specifies a tiered density requirement at  $N_{\text{initial}}$  depending on traffic level. In the 300,000 to 3,000,000 ESAL range, 32 percent of the samples failed the  $N_{\text{initial}}$  requirement. In the greater than 3,000,000 million ESAL range, 20 percent of samples failed the  $N_{\text{initial}}$  requirement. The majority of the projects that failed the  $N_{\text{initial}}$  requirement were fine-graded. All of the projects are performing well in terms of rutting resistance. Only one project failed the  $N_{\text{initial}}$  and was tender in the

field. There is no strong evidence to keep the requirements for  $N_{\text{initial}}$ .

8. The requirement for  $N_{\text{maximum}}$  was evaluated based on the field project data. AASHTO M 35 specifies a density requirement of less than 98 percent at  $N_{\text{maximum}}$  to guard against the potential for rutting. Thirty-six percent of the samples tested with the Pine compactor and 40 percent of the samples tested with the Troxler compactor failed the density requirement at  $N_{\text{maximum}}$ . However, the projects have all been extremely rut resistant. Therefore, the density requirement at  $N_{\text{maximum}}$  does not appear to be a good indicator of rutting potential and should be eliminated.

## 5.2 Recommendations

Based on the research conducted in this study, the following recommendations are made: The specification for angle of gyration should be revised to allow a DIA of only  $1.16 \pm 0.02$  degrees. The  $N_{\text{design}}$  levels shown in Table 5.1 should be adopted for the design of Superpave HMA. Consideration should be given to using the 2-year design traffic volume, as opposed to the 20-year design traffic volume or another method of specifying rate of loading, to determine  $N_{\text{design}}$ . The criteria for  $N_{\text{initial}}$  and  $N_{\text{maximum}}$  should be eliminated.

**Table 5.1. Recommended  $N_{\text{design}}$  levels for an SGC DIA of  $1.16 \pm 0.02$  degrees.**

20-Year Design Traffic, ESALs	2-Year Design Traffic, ESALs	$N_{\text{design}}$ for binders < PG 76-XX	$N_{\text{design}}$ for binders $\geq$ PG 76-XX or mixes placed > 100 mm from surface
< 300,000	< 30,000	50	NA
300,000 to 3,000,000	30,000 to 230,000	65	50
3,000,000 to 10,000,000	230,000 to 925,000	80	65
10,000,000 to 30,000,000	925,000 to 2,500,000	80	65
> 30,000,000	> 2,500,000	100	80

# References

1. Cominsky, R., "The Superpave Mix Design Manual for New Construction and Overlays," SHRP-A-407, Strategic Highway Research Program, National Research Council, 1994.
2. Brown, E. R., and M. S. Buchanan, *NCHRP Research Results Digest 237: Superpave Gyratory Compaction Guidelines*, Transportation Research Board, National Research Council, 1999. [http://www.trb.org/news/blurb\\_detail.asp?id=3052](http://www.trb.org/news/blurb_detail.asp?id=3052)
3. Anderson, R. M., R. B. McGennis, W. On Tam, and T. W. Kennedy, "Sensitivity of Mixture Performance Properties to Changes in Laboratory Compaction Using the Superpave Gyratory Compactor," *Journal of the Association of Asphalt Paving Technologists*, Vol. 69, 2000.
4. American Association of State Highway and Transportation Officials, *Standard Specifications for Transportation Materials and Methods of Sampling and Testing*, Part 1B: Specifications, 25th Ed., 2005.
5. Hveem, F. N., "Asphalt Pavements from the Ancient East to the Modern West," Fifth Annual Nevada Street and Highway Conference, 1970.
6. Leahy, R. B., and R. B. McGennis, "Asphalt Mixes: Materials, Design and Characterization," *Journal of the Association of Asphalt Paving Technologists*, Vol. 68A, 1999.
7. Crawford, C., "The Rocky Road of Mix Design," *Hot Mix Asphalt Technology*, Winter 1989, National Asphalt Pavement Association.
8. Vallegra, B. A., and W. R. Lovering, "Evolution of the Hveem Stabilometer Method of Designing Asphalt Paving Mixtures," *Proceedings of the Association of Asphalt Paving Technologists*, Vol. 54, 1985.
9. War Department, U.S. Army Corps of Engineers, Mississippi River Commission, "Investigation of the Design and Control of Asphalt Paving Mixtures," Technical Memorandum No. 3-254, Vol. 1, *U.S. Waterways Experiment Station*, Vicksburg, MS, May 1948.
10. White, T. D., "Marshall Procedures for Design and Quality Control of Asphalt Mixtures," *Proceedings of the Association of Asphalt Paving Technologists*, Vol. 54, 1985.
11. Ortolani, L., and H. A. Sandberg, Jr., "The Gyratory-Shear Method of Molding Asphaltic Concrete Test Specimens; Its Development and Correlation with Field Compaction Methods. A Texas Highway Department Standard Procedure," *Proceedings of the Association of Asphalt Paving Technologists*, Vol. 21, 1951.
12. Philippi, O. A., "Compaction of Bituminous Concrete," *Proceedings of the Association of Asphalt Paving Technologists*, Vol. 26, 1957.
13. McRae, J. L., "Compaction of Bituminous Concrete," *Proceedings of the Association of Asphalt Paving Technologists*, Vol. 26, 1957.
14. McRae, J. L., and A. R. McDaniel, "Progress Report on the Corps of Engineers' Kneading Compactor for Bituminous Mixtures," *Proceedings of the Association of Asphalt Paving Technologists*, Vol. 27, 1958.
15. Von Quintus, H. L., J. A. Scherocman, C. S. Hughes, and T. W. Kennedy, *NCHRP Report 338: Asphalt-Aggregate Mixture Analysis System AAMAS*, Transportation Research Board, National Research Council, 1991.
16. War Department, U.S. Army Corps of Engineers, Mississippi River Commission, "Investigation of the Design and Control of Asphalt Paving Mixtures," Technical Memorandum No. 3-254, Vol. 3, *U.S. Waterways Experiment Station*, Vicksburg, MS, May 1948.
17. Dillard, J. H., "Comparison of Density of Marshall Specimens and Pavement Cores," *Proceeding of the Association of Asphalt Paving Technologists*, Vol. 24, 1955.
18. Campen, W. H., J. R. Smith, L. G. Erickson, and L. R. Mertz, "The Effect of Traffic on the Density of Bituminous Paving Mixtures," *Proceedings of the Association of Asphalt Paving Technologists*, Vol. 30, 1960.
19. Graham, M. D., W. C. Burnett, J. J. Thomas, and W. C. Dixon, "Pavement Density—What Influences It," *Proceedings of the Association of Asphalt Paving Technologists*, Vol. 34, 1965.
20. Woodward, E. J., Jr., and J. L. Vicelja, "Aviation Boulevard—Evaluation of Materials, Equipment and Construction Procedures," *Proceedings of the Association of Asphalt Paving Technologists*, Vol. 34, 1965.
21. Bright, R., B. Steed, J. Steele, and A. Justice, "The Effect of Viscosity of Asphalt on Properties of Bituminous Wearing Surface Mixtures," *Proceedings of the Association of Asphalt Paving Technologists*, Vol. 35, 1966.
22. Serafin, P. J., L. L. Kole, and A. P. Chritz, "Michigan Bituminous Experimental Road: Final Report," *Proceedings of the Association of Asphalt Paving Technologists*, Vol. 36, 1967.
23. Palmer, R. K., and J. J. Thomas, "Pavement Density—How It Changes," *Proceedings of the Association of Asphalt Paving Technologists*, Vol. 37, 1968.
24. Epps, J. A., B. M. Gallaway and W. W. Scott, Jr., "Long-Term Compaction of Asphalt Concrete Pavements," *Highway Research Record 313*, Highway Research Board, National Research Council, 1970.
25. Kandahl, P. S., and M. E. Wenger, "Asphalt Properties in Relation to Pavement Performance," *Transportation Research Record 544*, Transportation Research Board, National Research Council, 1975.
26. Brown, E. R., and S. A. Cross, "Comparison of Laboratory and Field Density of Asphalt Mixtures," *Transportation Research Record 1300: Asphalt Pavement and Surface Treatments: Construction and*

- Performance 1991*, Transportation Research Board, National Research Council, 1991.
27. Hanson, D. I., R. B. Mallick, and E. R. Brown, "Five-Year Evaluation of HMA Properties at the AAMAS Test Projects," *Transportation Research Record 1454: Asphalt Concrete Mixture Design and Performance*, Transportation Research Board, National Research Council, 1994.
  28. Stroup-Gardiner, M., D. E. Newcomb, R. Olson, and J. Teig, "Traffic Densification of Asphalt Concrete Pavements," *Transportation Research Record 1575: Construction: Flexible Pavements, Bridges, Quality, and Management*, Transportation Research Board, National Research Council, 1997.
  29. Brown, E. R., and R. B. Mallick, "An Initial Evaluation for  $N_{\text{design}}$  Superpave Gyratory Compactor," *Journal of the Association of Asphalt Paving Technologists*, Vol. 67, 1998.
  30. Cominsky, R., R. B. Leahy, and E. T. Harrigan, "Level One Mix Design: Materials Selection, Compaction, and Conditioning," SHRP-A-408, Strategic Highway Research Program, National Research Council, 1994.
  31. Consuegra, A., D. N. Little, H. Von Quintus, and J. Burati, "Comparative Evaluation of Laboratory Compaction Devices Based on Their Ability to Produce Mixtures with Engineering Properties Similar to Those Produced in the Field," *Transportation Research Record 1228: Asphalt Mixtures and Asphalt Chemistry*, Transportation Research Board, National Research Council, 1989.
  32. Button, J. W., D. N. Little, V. Jagadam, and O. J. Pendleton, "Correlation of Selected Laboratory Compaction Methods with Field Compaction," *Transportation Research Record 1454: Asphalt Mixture Design and Performance*, Transportation Research Board, National Research Council, 1994.
  33. Bonnot, J., "Asphalt Aggregate Mixtures," *Transportation Research Record 1096: Asphalt Analysis, Sulfur, Mixes, and Seal Coats*, Transportation Research Board, National Research Council, 1986.
  34. Blankenship, P. B., "Gyratory Compaction Characteristics: Relation to Service Densities of Asphalt Mixtures," Master's Thesis, University of Kentucky, Lexington, 1993.
  35. Harman, T. P., J. D'Angelo, and J. R. Bukowski, "Evaluation of SUPERPAVE Gyratory Compactor in the Field Management of Asphalt Mixes: Four Simulation Studies," *Transportation Research Record 1513: Flexible Pavement Construction*, Transportation Research Board, National Research Council, 1995.
  36. Habib, A., M. Hossain, R. Kaldate, and G. A. Fager, "Comparison of Superpave and Marshall Mixtures for Low-Volume Roads and Shoulders," *Transportation Research Record 1609: Superpave: Binder Specifications, Mixture Design, and Construction*, Transportation Research Board, National Research Council, 1998.
  37. Forstie, D. A., and D. K. Corum, "Determination of Key Gyratory Compaction Points for Superpave Mix Design in Arizona," in *Progress of Superpave (Superior Performing Asphalt Pavement): Evaluation and Implementation*, ASTM STP 1322, R. N. Jester, Ed., American Society for Testing and Materials, 1997.
  38. Gowda, G., K. Hall, R. Elliot, and A. Meadors, "Critical Evaluation of Superpave Volumetric Mix Design Using Arkansas Surface Coarse Mixes," *Journal of the Association of Asphalt Paving Technologists*, Vol. 66, 1997.
  39. Buchanan, M. S., "Evaluation of the Superpave Compaction Procedure," Doctoral Dissertation, Auburn University, Auburn, AL, 1999.
  40. Mallick, R. B., S. Buchanan, E. R. Brown, and M. Huner, "Evaluation of Superpave Gyratory Compaction of Hot Mix Asphalt," *Transportation Research Record 1638: Asphalt Mixture Components*, Transportation Research Board, National Research Council, 1998.
  41. American Association of State Highway and Transportation Officials, *AASHTO Provisional Standards*, 2001.
  42. Harmelink, D., and T. Aschenbrener, *In-Place Voids Monitoring of Hot Mix Asphalt Pavements*, Report No. CDOT-DTD-R-2002-11, Colorado Department of Transportation, 2002.
  43. Watson, D. E., J. Moore, and E. R. Brown, *Verification of Superpave  $N_{\text{design}}$  Compaction Levels*, Phase I Final Report, Georgia Department of Transportation, 2005.
  44. Huber, G., and R. M. Anderson, "Superpave Design Compaction Effort: Validity of using Density at the End of Service Life as Parameter to Define N-Design," *Journal of the Association of Asphalt Paving Technologists*, Vol. 73, 2004.
  45. Pine, W. J., "Superpave Gyratory Compaction and the  $N_{\text{design}}$  Table," internal report to Illinois Department of Transportation, 1997.
  46. Vavrik, W. R., and S. H. Carpenter, "Calculating Air Voids at Specified Numbers of Gyration in Superpave Gyratory Compactor," *Transportation Research Record 1630: Asphalt Mixtures: Stiffness Characterization, Variables, and Performance*, Transportation Research Board, National Research Council, 1998.
  47. Virginia Department of Transportation, Special Provision for Section 211 Asphalt Concrete Mixtures (Superpave), Richmond, VA, September 2001.
  48. Ohio Department of Transportation, Road and Bridge Specifications, Columbus, OH, 2005.
  49. Hinrichsen, J., "Comparison of Four Brands of Superpave Gyratory Compactors," *Transportation Research Record 1767: Asphalt Mixtures 2001*, Transportation Research Board, National Research Council, 2001.
  50. Prowell, B. D., E. R. Brown, and M. Huner, *Evaluation of the Internal Angle of Gyration of Superpave Gyratory Compactors in Alabama*, NCAT 03-04, National Center for Asphalt Technology, 2003.
  51. Federal Highway Administration, *LTPPBind*, Version 2.1, 1999.
  52. Brown, E. R., B. D. Prowell, L. A. Cooley, Jr., J. Zhang, and R. B. Powell, "Evaluation of Rutting Performance on 2000 NCAT Test Track," *Journal of Association of Asphalt Paving Technologists*, Vol. 73, 2004.
  53. American Association of State Highway and Transportation Officials, *AASHTO Guide for Design of Pavement Structures 1992*, 1992.
  54. Hughes, C. S., *NCHRP Synthesis of Highway Practice 152: Compaction of Asphalt Pavement*, Transportation Research Board, National Research Council, 1989.
  55. Brown, E. R., "Density of Asphalt Concrete—How Much Is Needed?" *Transportation Research Record 1282: Transportation Construction 1990*, Transportation Research Board, National Research Council, 1990.
  56. Cooley, Jr., L. A., E. R. Brown, and S. Maghsoodloo, "Developing Critical Field Permeability and Pavement Density Values for Coarse-Graded Superpave Pavements," *Transportation Research Record 1761: Construction 2001*, Transportation Research Board of the National Academies, 2001.
  57. Linden, R. N., J. P. Mahoney, and N. C. Jackson, "Effect of Compaction on Asphalt Concrete Performance," *Transportation Research Record 1217: Asphalt Construction, Premature Rutting, and Surface Friction Courses*, Transportation Research Board, National Research Council, 1989.
  58. Harvey, J. T., T. Hoover, N. F. Coetzee, W. A. Nokes, and F. C. Rust, "CALTRANS Accelerated Pavement Test (CAL/APT) Program-Test Results: 1994-1997," *Journal of the Association of Asphalt Paving Technologists*, Vol. 67, 1998.

59. Brown, E. R., and S. A. Cross, "A National Study of Rutting in Hot Mix Asphalt (HMA) Pavements," *Journal of the Association of Asphalt Paving Technologists*, Vol. 61, 1992.
  60. Al-Khaateeb, G., C. Paugh, K. Stuart, T. Harman, and J. D'Angelo, "Target and Tolerance Study for Angle of Gyration Used in Superpave Gyrotory Compactor," *Transportation Research Record 1789: Bituminous Paving Mixtures 2002*, Transportation Research Board of the National Academies, 2002.
  61. Dalton, F., "Observations of SGC End Plate Deflection Using the FHWA Angle Validation Kit," Report 2000-02, Revision C, Pine Instrument Company, PA, 2000.
  62. Montgomery, D. C., *Design and Analysis of Experiments*, Fifth Ed., John Wiley & Sons, 2001.
  63. Moseley, H. L., G. C. Page, J. A. Musselman, G. A. Sholar, and P. B. Upshaw, "Evaluation of Dynamic Angle Validator," *Transportation Research Record 1891: Bituminous Paving Mixtures 2004*, Transportation Research Board of the National Academies, 2004.
  64. Federal Highway Administration, "Performance of Coarse-Graded Mixes at WesTrack–Premature Rutting," Final Report. Washington, D.C. 1998. <http://www.tfrc.gov/pavement/pubs/westrack/westrack.htm>
-

# List of Acronyms

AADT: average annual daily traffic  
AASHTO: American Association of State Highway and  
Transportation Officials  
AC: asphalt content  
ANOVA: analysis of variance  
DAVK: dynamic angle verification kit  
DIA: dynamic internal angle  
ESAL: equivalent single-axle load  
FHWA: Federal Highway Administration  
FSCH: frequency sweep at constant height  
GLM: General Linear Model  
GTM: Gyratory Testing Machine  
HMA: hot mix asphalt

JMF: job mix formula  
LTPP: long-term pavement performance  
MSE: mean square error  
NCAT: National Center for Asphalt Technology  
NMAS: nominal maximum aggregate size  
PG: performance grade  
RSCH: repeated shear at constant height  
SGC: Superpave gyratory compactor  
SHRP: Strategic Highway Research Program  
SST: Superpave Shear Tester  
VFA: voids filled with asphalt  
VMA: voids in mineral aggregate

---

## APPENDIXES

The following appendixes are not published herein, but are available online as *NCHRP Web-Only Document 96* at [www.TRB.org/news/blurbs\\_detail.asp?id=7270](http://www.TRB.org/news/blurbs_detail.asp?id=7270):

- Appendix A: Literature Review
  - Appendix B: Field Project Data
  - Appendix C: Roadway Condition Surveys
-

*Abbreviations and acronyms used without definitions in TRB publications:*

AAAE	American Association of Airport Executives
AASHO	American Association of State Highway Officials
AASHTO	American Association of State Highway and Transportation Officials
ACI-NA	Airports Council International-North America
ACRP	Airport Cooperative Research Program
ADA	Americans with Disabilities Act
APTA	American Public Transportation Association
ASCE	American Society of Civil Engineers
ASME	American Society of Mechanical Engineers
ASTM	American Society for Testing and Materials
ATA	Air Transport Association
ATA	American Trucking Associations
CTAA	Community Transportation Association of America
CTBSSP	Commercial Truck and Bus Safety Synthesis Program
DHS	Department of Homeland Security
DOE	Department of Energy
EPA	Environmental Protection Agency
FAA	Federal Aviation Administration
FHWA	Federal Highway Administration
FMCSA	Federal Motor Carrier Safety Administration
FRA	Federal Railroad Administration
FTA	Federal Transit Administration
IEEE	Institute of Electrical and Electronics Engineers
ISTEA	Intermodal Surface Transportation Efficiency Act of 1991
ITE	Institute of Transportation Engineers
NASA	National Aeronautics and Space Administration
NASAO	National Association of State Aviation Officials
NCFRP	National Cooperative Freight Research Program
NCHRP	National Cooperative Highway Research Program
NHTSA	National Highway Traffic Safety Administration
NTSB	National Transportation Safety Board
SAE	Society of Automotive Engineers
SAFETEA-LU	Safe, Accountable, Flexible, Efficient Transportation Equity Act: A Legacy for Users (2005)
TCRP	Transit Cooperative Research Program
TEA-21	Transportation Equity Act for the 21st Century (1998)
TRB	Transportation Research Board
TSA	Transportation Security Administration
U.S.DOT	United States Department of Transportation